2006

Pathological Upregulation of a Calcium-Stimulated Phosphatase, Calcineurin, in Two Models of Neuronal Injury

Jonathan Elledge Kurz
Virginia Commonwealth University

Pathological upregulation of the calcium-stimulated phosphatase, calcineurin, in two models of neuronal injury.

A dissertation submitted in partial fulfillment of the requirements for the degree of Doctor of Philosophy at Virginia Commonwealth University.

By

Jonathan Elledge Kurz
Bachelor of Science
Virginia Commonwealth University
May, 2001

Director: Severn B. Churn, Ph.D.
Associate Professor, Departments of Neurology;
Anatomy and Neurobiology;
Pharmacology and Toxicology; and Physiology

Virginia Commonwealth University
Richmond, Virginia
November, 2006

ACKNOWLEDGMENT

I would like to thank my advisor, Dr. Churn, for mentoring me over the past few years. Dr. Churn has given me the freedom to pursue my own research interests while also teaching me a great deal, and I am profoundly grateful.

I would also like to thank Dr. DeLorenzo and the members of his laboratory for graciously allowing me to use equipment and space when needed throughout this project, Dr. Hamm for helping with the brain injury studies, Dr. Povlishock and the members of his laboratory for help with histochemical studies and the use of their microscope, and Dr. Travis Parsons for his valuable insights and discussion. Additionally, I am grateful to the members of my committee for their assistance

Finally, I would never have gotten this far without the support of my friends and family, especially my parents, who have always been there when I needed help. Thank you all.

TABLE OF CONTENTS

LIST OF FIGURES

ABSTRACT

PATHOLOGICAL UPREGULATION OF THE CALCIUM STIMULATED PHOSPHATASE, CALCINEURIN, IN TWO MODELS OF NEURONAL INJURY

A dissertation submitted in partial fulfillment of the requirements for the degree of Doctor of Philosophy at Virginia Commonwealth University.

Virginia Commonwealth University, 2006

Director: Severn B. Churn, Ph.D.
Associate Professor, Departments of Neurology;
Anatomy and Neurobiology; Pharmacology and Toxicology;
and Physiology

Excitotoxic calcium influx and activation of calcium-regulated systems is a common event in several types of neuronal injury. This mechanism has been the focus of intense research, with the hope that a more complete understanding of how neuronal injury affects calcium-regulated systems will provide effective treatment options. This study examines one such calcium-stimulated enzyme, calcineurin, in the context of two common neurological pathologies, status epilepticus and traumatic brain injury.

Status epilepticus was induced by pilocarpine injection. NMDA-dependent increases in calcineurin activity were observed in cortical and hippocampal homogenates. Upon closer examination, the most profound increases in activity were found to be present in crude synaptoplasmic membrane fractions isolated

from cortex and hippocampus. A concurrent status epilepticus-induced increase in calcineurin concentration was observed in membrane fractions from cortex and hippocampus. Immunohistochemical analysis revealed an increase in calcineurin immunoreactivity in apical dendrites of hippocampal pyramidal neurons. We examined a cellular effect of increased dendritic calcineurin activity by characterizing a calcineurin-dependent loss of dendritic spines. Increased dendritic calcineurin led to increased dephosphorylation and activation of cofilin, an actin-depolymerizing factor. Calcineurin-activated cofilin induced an increase in actin depolymerization, a mechanism shown to cause spine loss in other models. Finally, via Golgi impregnation, we demonstrated that status epilepticus-induced spine loss is blocked by calcineurin inhibitors.

To demonstrate that the increase in dendritic calcineurin activity was not model-specific, we examined a moderate fluid-percussion model of brain injury. Calcineurin activity was significantly increased in hippocampal and cortical homogenates. This increased activity persisted for several weeks post-injury, and may be involved in injury-induced neuronal pathologies. Also similar to the SE model, calcineurin immunoreactivity was dramatically increased in synaptoplasmic membrane fractions from cortex and hippocampus, and immunohistochemistry revealed increased calcineurin content in dendrites of hippocampal CA1-3 pyramidal neurons. These changes in calcineurin distribution also persisted for several weeks post-injury.

These studies demonstrate a novel, cellular mechanism of calcium-mediated pathology in two models of neuronal injury. Elucidation of cellular events involved in the acute and chronic effects of brain trauma is essential for the development of more effective treatment options.

INTRODUCTION

Excitotoxic calcium influx and the subsequent activation of calcium-regulated systems is a common event in several types of neuronal injury [1]. This pathological mechanism has been the focus of intense research, with the hope that a more complete understanding of how neuronal injury affects calcium-regulated systems will eventually provide effective neuroprotective and therapeutic treatment options. The present study examines one such calcium-stimulated enzyme, calcineurin, in the context of two common neurological pathologies, status epilepticus and traumatic brain injury.

Calcineurin – Structure, Function, Regulation, and Neuronal Substrates:

Structure and Function:

Calcineurin (CaN) was first discovered as a calmodulin-dependent inhibitor of CaM Kinase II that was highly enriched in neuronal tissue [2]. CaN was subsequently identified as a calcium-calmodulin dependent serine-threonine phosphatase [3, 4]. As one of the few serine-threonine phosphatases directly regulated by a second messenger, CaN plays an important role in many cellular functions, including regulation of other phosphatases and kinases, regulation of apoptosis, modulation of neurotransmitter release and receptor function,

modulation of learning and memory [5], regulation of gene transcription, and activation of immune cells [6]. CaN's involvement in numerous essential cellular properties, coupled to its neuronal enrichment, have made the enzyme an intriguing subject of research into the mechanisms underlying neuronal injury and disease states.

CaN is composed of two subunits: the catalytic "A" subunit, and the regulatory "B" subunit. Each of these subunits is subject to a number of regulatory mechanisms. The 58-64 kDa catalytic A subunit consists of catalytic, calmodulin-binding, autoinhibitory, and calcineurin-B binding domains [7, 8]. In the presence of 20 micromolar calmodulin, calcineurin has a K_m of 0.6 μM for calcium. Calcium-calmodulin binding to CaN is highly cooperative, with a Hill coefficient of 2.5-3 [8, 9]. Binding of calcium/calmodulin to the calmodulin binding domain releases the catalytic domain from the influence of the autoinhibitory domain, permitting the enzyme's phosphatase activity [10, 11]. The existence of these functional domains is supported by proteolysis studies. Partial proteolytic cleavage of the A subunit by the calcium-stimulated protease calpain (as well as members of the caspase family) can result in the removal of both the autoinhibitory and calmodulin-binding domains, resulting in a constitutively active enzyme with greatly increased phosphatase activity [12-15].

The CaN A subunit exists in several isoforms, including Aα1, Aα2, Aβ1, and Aβ2 [8]. CaN A α and A β are both broadly expressed (including in most neurons and glia), although expression levels of the two isoforms vary between different cell types [16], and the α isoforms tend to be more strongly expressed in

neural tissue [16]. A testis-specific splice variant of CaN (CaN Aγ) exists in both rodents and humans [8], and may play a role in sperm maturation [17]. From a practical standpoint, no functional difference has been demonstrated between the various CaN A isoforms, and all are highly homologous [8].

CaN B, the 19 kDa regulatory subunit of the enzyme, is a member of the EF-hand superfamily of calcium-binding proteins [18]. CaN B is tightly bound to CaN A, even in very low (nanomolar) calcium concentrations [8]. CaN B can bind 4 calcium ions with high (K_d = 10^{-7}M) affinity, and several more with micromolar (K_d = 0.5 to 1 micromolar) affinity [18]. Binding of calcium to the high affinity sites appears to be structural, while binding of calcium to the low-affinity sites causes a small, calmodulin-independent activation of the enzyme. The presence of CaN B is also essential for the calcium/calmodulin-dependent activation of the enzyme; it has been suggested that binding of calcium to the low-affinity sites on CaN B induces a conformational change in the catalytic A subunit, facilitating calmodulin binding [19]. Mammalian CaN B exists in 2 isoforms, CaN B_1, found in all tissues, and CaN B_2, which is testis-specific. The structure of CaN B is highly conserved from yeast to man, and both isoforms are typically myristoylated on the N-terminal glycine, a post-translational modification that is not essential for function [20].

Regulation:

In addition to its regulation by calcium/calmodulin, CaN is also activated by other divalent cations, including nickel, magnesium and manganese [21], with

the most potent activation by Ni and the least by Mg. There is some debate about the physiological relevance of this activation, with some early studies suggesting that CaN requires one of these cations in addition to Ca for activity [22], while other researchers have not found any tightly associated Ni or Mn ions [23]. Calcineurin is sensitive to oxidation, and prolonged activation by calcium can result in inactivation of the enzyme through an oxidative mechanism [24]. Activity lost in this manner can be restored by ascorbate or another mild reducing agent in enzyme assays.

Various endogenous peptides have been identified that act as physiological inhibitors of CaN activity. One such peptide (calcineurin autoinhibitory peptide, referred to in the literature as CAIN or CAP) binds to the autoinhibitory domain of CaN [25]. This peptide has been shown to negatively modulate CaN-mediated endocytosis, demonstrating that it has some physiological function [26]. More research remains to be done on this topic. In addition to the autoinhibitory peptide, other endogenous CaN inhibitory proteins have been recently identified. These include the calcineurin B homologous protein (CHP) and calcipressin 1. CHP (and a highly similar protein, tescalcin, expressed during the development of mouse testes [27]) is highly homologous with both calcineurin B and calmodulin and is capable of calcium binding [28]. It has been shown to potently inhibit calcineurin when overexpressed in cultured cells or when added in purified form to calcineurin assays [28]. Calcipressin 1 is the peptide product of the DSCR1 gene, located in a region thought to be critical to the defects associated with Down's Syndrome [29, 30]. Calcipressin 1 is a

potent inhibitor of calcineurin [30, 31], through a mechanism that likely involves direct binding to the enzyme [30] and may involve competition with CaN substrates [32]. A final potential peptide regulator of CaN activity is the astrocyte calcium binding protein S100B, which seems to increase CaN activity [33], although this effect still requires further study.

Regulation of CaN by phosphorylation of the enzyme remains controversial. For example, CaN can be phosphorylated at the same site (Ser 411) by CaM kinase II and PKC [34-37]. While early research suggested that this phosphorylation modulated CaN activity [35], the effects were generally small and differed between activation and inhibition depending on the substrate and assay protocol used [38]. This site is rapidly autodephosphorylated by CaN itself [35]. CaN can also be phosphorylated at two sites by casein kinase I, no effect on CaN enzymatic activity has yet been attributed to this phosphorylation, and further research is required to determine its functional significance [39].

Finally, CaN is also regulated by its binding to the scaffolding protein AKAP79/150. In general, the AKAP family of proteins anchor protein kinase A near its substrates. Specifically, the AKAP79/150 molecule anchors PKA, CaN and PKC in the vicinity of AMPA receptors. Binding of CaN to the AKAP molecule results in an inhibition of CaN phosphatase activity [40].

Substrates and Potential Role in Disease States:

Calcineurin is highly enriched in neurons, and modulates a number of neuronal systems that are of interest in disease states. These systems include

management of neuronal calcium homeostasis, modulation of neurotransmitter function, and regulation of the neuronal cytoskeleton. An understanding of the role of CaN in these systems is essential to determining its role in clinical disease.

Maintenance of a low level of free intracellular calcium is essential to the proper function of neurons and allows calcium ions to work effectively as a second messenger in several key steps of neurotransmission. Due to its high affinity for calcium ions and relatively low dissociation constant for Ca^{2+} [2], CaN is one of the first post-synaptic enzymes activated after a calcium influx [41]. Thus CaN is ideally placed for the regulation of intracellular free calcium via negative feedback on several systems, including several types of voltage-gated ion channels, NMDA receptor-associated channels, and endoplasmic reticulum calcium stores.

Calcineurin has been shown to exhibit negative feedback on calcium entry through both L [42-44] and N [44, 45] type voltage-gated calcium channels (VGCC). In L-type channels, CaN overexpression reduced channel availability and increased the rate of channel inactivation in a cell line derived from rat neuroblastoma cells [42, 44]. These effects on L-type calcium currents were reversed by the inclusion of FK506 in the patch pipette, further implicating CaN in the effect [42]. A similar negative modulation of L-type channels has been seen in other, non-neuronal cell types, such as smooth muscle [46]. The precise mechanism for this effect has not yet been described, however the authors suggested that it was not G-protein mediated. This is in contrast to the regulation

of N-type calcium channels by CaN, which does appear to be G-protein mediated. In rat sympathetic neurons, CaN was shown to positively modulate the binding of an inhibitory G-protein to the N-type channel, enhancing channel inhibition. Addition of cyclosporin A in this study enhanced N-type calcium currents [45]. Some controversy exists over the CaN-dependent regulation of VGCC's. For example, one study has suggested that calcineurin *increases* L-type calcium channel activity in hippocampal neurons in culture [47]. The authors state that since VGCC regulation often varies greatly between cell types and even with the age of the neuron, it is possible for CaN to negatively modulate voltage sensitive calcium entry in some neurons while positively modulating it in others. If true, this hypothesis adds another layer of complexity to the role of CaN in regulating calcium entry.

In addition to its ability to retard calcium entry through some types of calcium channels, CaN also regulates intracellular calcium storage, particularly that of the endoplasmic reticulum. The ER is capable of sequestering calcium ions via a Mg/ATP-ase pump, then releasing this calcium in response to second messengers, including IP3 and calcium itself (through the ryanodine receptor). CaN has been shown to downregulate both the IP3 and ryanodine receptors through dephosphorylation of a PKC-dependent site [48, 49]. This dephosphorylation reduces the affinity of both receptors for their respective ligands, thus preventing excessive calcium discharge from the ER. CaN also regulates intracellular calcium dynamics on a transcriptional level. For example, CaN-mediated dephosphorylation of the transcription factor NF-ATc4 has been

shown to upregulate IP3 expression [50, 51]. CaN has also been shown (in some neuronal populations) to modulate expression of the plasma membrane calcium ATP-ase pump [52, 53] and the Na/Ca exchanger [54].

With the few exceptions noted above, the net effect of CaN is to provide negative feedback on calcium influx and ER calcium release, preventing excessive intracellular calcium levels in response to neuronal stimuli, and possibly downregulating downstream neurotransmission.

In excitatory neurons, CaN is highly enriched in the post-synaptic density. This places the enzyme in an ideal location for the regulation of neurotransmitter receptors. Indeed, several classes of receptors have been identified as either direct CaN substrates or indirectly regulated by CaN. These receptors include the NMDA-associated receptor, the AMPA/kainate glutamate receptor, and the $GABA_A$ receptor. In the PSD, CaN is highly bound to scaffolding proteins, including AKAP 79/150 [55, 56] and MAP-2. This interaction of CaN with these molecules serves several purposes. First, binding of CaN to specific molecular scaffolds aids in the compartmentalization of CaN substrates and downstream effectors, increasing the efficiency with which CaN regulates target mechanisms. For example, AKAP 79/150 holds CaN in a complex with PKA near AMPA receptors, facilitating the regulation of these receptors [55]. Additionally, binding of CaN to AKAP 79/150 directly regulates CaN activity. CaN activity has been shown to be decreased by approximately 25% when bound to the AKAP 79/150 molecule [40]. Finally, molecular scaffolds can recruit further neurotransmitter receptors and other PSD proteins in response to neuronal activity.

The anchoring of CaN near AMPA receptors by AKAP 79/150 suggests strongly that the enzyme may regulate these receptors. Recent research has demonstrated that this is, in fact, the case. CaN has been shown to negatively modulate these ligand-gated ion channels by several mechanisms. First, CaN appears to directly dephosphorylate the AMPA receptor GluR1 subunit at Ser 845 [57]. Phosphorylation at this serine site potentiates the response of AMPA receptors to glutamate [58], thus CaN-mediated dephosphorylation of this site depotentiates the receptor. Further evidence for CaN-mediated negative modulation of AMPA receptors is provided by a study where the calcineurin autoinhibitory peptide was diffused into neurons via patch pipette. Under the influence of the autoinhibitory peptide, the amplitude of glutamate-induced fast EPSC's increased [59]. Finally, some recent evidence suggests that CaN plays a role in NMDA receptor-triggered endocytosis of AMPA receptors, thus indirectly limiting AMPA receptor activity [60]. These mechanisms have all been proposed as a possible explanation of CaN's effects on LTP and LTD.

Calcineurin also appears to negatively modulate the other major class of glutamate-gated ion channels, NMDA receptors. Lieberman and Mody discovered that FK506 prolonged NMDA receptor channel open time in granule cells of the dentate gyrus [61], although they did not determine if this was due to a direct dephosphorylation of the receptor protein. A later study discovered that calcineurin was involved in glycine-insensitive desensitization of the NMDA receptor in outside-out patches from hippocampal neurons (a type of desensitization in which the NMDA receptor becomes desensitized to glutamate

due to extended binding of ligand to the receptor) [62]. Inhibition of CaN with an autoinhibitory peptide reduced desensitization of the receptor. It was subsequently discovered that this effect of CaN on NMDA receptor desensitization was due to a direct dephosphorylation of the receptor on the C-terminus of the NR2A subunit [63]. This densensitization of NMDA receptors was observed under more physiological conditions (and found again to be CaN-dependent) using synaptic NMDA receptors in hippocampal cell culture. Synaptic NMDA receptors were stimulated by causing glutamate release from presynaptic neurons. Desensitization was observed under these conditions, and desensitization was blocked through the use of CaN inhibitors [64].

$GABA_A$ receptors are the primary receptor responsible for the fast inhibitory response in neuronal tissue [65]. Several recent studies have demonstrated a down-regulation of $GABA_A$ receptor function by CaN [66-68]. This modulation of $GABA_A$ receptor function may occur through direct dephosphorylation of receptor subunits. For example, a recent study described a direct interaction of CaN with the gamma 2 subunit of GABA receptors. CaN-mediated dephosphorylation of this subunit was shown to produce long-term depression (LTD) of inhibitory synapses [69].

Finally, CaN also regulates a number of cytoskeletal elements. CaN has been shown to dephosphorylate several microtubule-associated proteins, including MAP2 and tau [70]. MAP2 is a protein that co-purifies with tubulin and is present in neuronal cell bodies, axons and dendrites, and is important for the crosslinking of microtubules to one another and to other cytoskeletal elements.

MAP2 is highly phosphorylated *in vivo*, and this phosphorylation seems to be involved in the crosslinking and assembly of microtubules. A number of studies have demonstrated a CaN-dependent dephosphorylation of MAP2. This dephosphorylation was induced by activation of the NMDA receptor in several studies, suggesting that CaN may regulate the microtubule structure in response to neuronal excitation. Like MAP2, tau has also been shown to crosslink microtubules to one another [71] and CaN has been shown to dephosphorylate tau [72]. In fact, exogenous CaN added to cultured neurons resulted in dephosphorylation of at least four tau phosphorylation sites [73], while reduction of CaN expression by antisense oligonucleotides resulted in hyperphosphorylation of tau at two sites [74]. Loss of CaN-mediated tau dephosphorylation has been a topic of intense interest in Alzheimer's disease, as hyperphosphorylated tau is a major component of the neurofibrillary tangles that are a hallmark of the disease [75]. In a more normal physiological role, CaN-mediated tau dephosphorylation has also been shown to be involved in the acquisition of polarity in cultured neurons [76]. Finally, in addition to its actions on microtubule-associated proteins, CaN is also capable of modulating actin stability. Calcineurin has been shown to be involved in extension of neuronal growth cones by encouraging actin depolymerization and turnover, likely by dephosphorylating a number of factors [77, 78]. CaN has also been observed to alter dendritic spine morphology, both in neuronal cultures and in a hippocampal slice model of LTD [79, 80]. Finally, CaN has been shown to regulate several actin-associated proteins, including cofilin and calponin [81]. Cofilin acts as an

actin-depolymerizing factor, and is stimulated by CaN-mediated dephosphorylation, while calponin is an actin binding protein that is associated with smooth muscle contraction. Both proteins have been identified in neurons and have been implicated in dendritic spine plasticity [82, 83].

Given its essential role in modulating neuronal excitability and its ability to regulate the architecture of the neuronal cytoskeleton, alterations in CaN expression or activity by disease states have a great deal of pathological potential. The present study investigates the role of CaN in two such conditions, traumatic brain injury and status epilepticus.

Traumatic Brain Injury:

Traumatic brain injury is a major cause of death and disability in the United States, particularly among young adults and the elderly [84], has been associated with a number of long-term neurological pathologies, including cognitive deficits and the development of post-traumatic epilepsy [85]. Limiting the mortality and long-term neurological pathology associated with these injuries has been a major focus of research for many years. A number of delayed processes are thought to contribute to the neuronal pathology associated with these injuries. The current hope is that a better understanding of these secondary processes will help provide neuroprotective clinical treatments for the brain-injured patient. Preventing this secondary damage of brain tissue may allow for better post-injury outcomes, especially in patients with mild to moderate

injuries, where the area of primary damage may be small. One pathological mechanism that has been of great interest is excitotoxic neuronal damage.

Following TBI, widespread neuronal depolarization leads to excessive release of glutamate [86]. The presence of such large amounts of excitatory neurotransmitter leads to toxic activation of post-synaptic receptors, influx of calcium ions, and pathological overactivation of calcium-stimulated systems. These calcium-stimulated enzymes and transcription factors are then thought to lead to a number of pathological changes in neurons, including axonal sprouting and synaptic reorganization, dendritic pull-back, neuronal hyperexcitability and cell death. This excessive glutamate release has been observed both in several animal models of injury and clinically (via the use of microdialysis probes) [87-89]. Interestingly, the rise in glutamate levels can be delayed anywhere from several hours to a day after the initial brain injury. Ideally, this presents a clinical window for the administration of neuroprotective agents. Unfortunately, efforts at pharmacological treatments that focus on this pathway, while promising in animal models, have been unsuccessful clinically [90]. A more complete understanding of the calcium-regulated mechanisms that are activated by this post-traumatic glutamate release may help with the development of more focused and effective treatment options.

A mounting body of evidence suggests that CaN may be one such TBI-modulated system. CaN activation has been observed *in vitro* in several studies of glutamate excitotoxicity [91, 92]. Additionally, both of the immunosuppressive CaN inhibitors, cyclosporin A and FK506 (tacrolimus), have been shown to be

neuroprotective in several animal models of TBI. Singleton and colleagues demonstrated protection by FK506 against diffuse axonal injury [93], this protection was shown to be a result of FK506 preventing TBI-induced impairment of axonal transport [93]. Some controversy exists over the mechanism of action of these inhibitors in TBI, as cyclosporin in particular has other actions in addition to inhibition of CaN, and may be providing neuroprotection through more than one pathway. Cyclosporin blocks the mitochondrial permeability transition pore, thought to be a key step in both the induction of apoptosis and axonal injury [94]. However, the efficacy of FK506 (which is more specific in its effects) in preventing a number of pathological processes tends to argue for a CaN-dependent mechanism. Further research is required to accurately determine the involvement of CaN in TBI-associated neuronal pathology.

Status Epilepticus:

Epilepsy and other seizure disorders are one of the most common neurological conditions in the United States today. These disorders can have a negative impact on quality of life for a number of reasons [95]. Depending on the patient's seizure frequency and severity, seizure disorders can limit cognitive development in children [96], prevent daily activities such as driving a car or working [97], and may require a lifetime of medication, often with unpleasant side effects [98, 99]. In spite of this, in most seizure disorders the seizures themselves are self-limiting – lasting a few minutes at most – and thus are not life threatening on their own. However, seizures that do not self-terminate after a few minutes

are life threatening and merit aggressive treatment. This condition of continuous seizure activity is known as status epilepticus (SE).

SE, affecting over 100,000 people annually [100], is defined as continuous seizure activity that exceeds thirty minutes in duration, or a number of individual seizures that total more than thirty minutes and between which the patient does not regain consciousness. SE can be subdivided into convulsive and non-convulsive SE (NCSE). Convulsive SE, which can be generalized (GCSE) or patrial manifests both behavioral and electrographic seizures, and is associated with a higher acute mortality. On the other hand, NCSE is characterized by electrographic seizures without convulsions and has several possible presentations, ranging from mild confusion to coma [101]. NCSE requires electroencephalography (EEG) for definitive diagnosis. Both subtypes of SE represent a severe neurological emergency associated with significant morbidity and mortality [102, 103]. SE is of particular concern in the elderly population, with a higher incidence among these patients. SE also has a markedly higher mortality rate among elderly patients, partly due to the greater incidence of other complicating conditions in this population [104].

Many of these cases of SE may be attributed to a causative event, such as an injury or illness. Underlying epilepsy is perhaps the most common cause of SE, especially in patients without adequate antiepileptic drug therapy [105]. Traumatic brain injury is also associated with the development of SE [106, 107]. The onset of continuous seizures often greatly complicates the treatment of traumatic brain injury and is associated with lower rates of recovery [108]. Other

causes of SE include brain neoplasms, drug overdose or withdrawal, infection, fever (especially in children) and stroke [105]. However, in many cases a causative event cannot be identified.

Regardless of the cause, SE requires urgent treatment to prevent long-term injury or mortality. Unfortunately, common anti-epileptics are not effective in some cases of SE, especially as the duration of the seizure activity increases [109]. As a result, SE often requires aggressive treatment with general anesthetics, placing the patient in a drug-induced coma to reduce or eliminate electrographic seizure activity. Additionally, patients require cardiovascular and respiratory support to help them survive the SE episode [110]. While termination of the seizure activity is essential for patient survival (particularly in GCSE), these treatments are not without risks and are not always optimally effective. Understanding why SE becomes refractory to first- and second-line treatments and devising new treatment options are currently major focuses of a number of research studies.

Even among patients that survive SE, long-term neurological complications are a common consequence of a prolonged seizure episode. Potential consequences of SE include cognitive deficits and the development of spontaneous recurrent seizures (i.e. epileptogenesis) [105, 111]. Developmental delay has been associated with SE in children, especially in non-febrile, non-idiopathic cases [96]. A more complete understanding of the cellular mechanisms underlying these pathologies may help limit the morbidity currently associated with continuous seizure activity.

As with TBI, glutamate-mediated excitotoxicity and calcium-mediated injury are thought to be a major cause of SE-mediated neuronal damage [1, 112]. Acutely, blockade of the NMDA receptor has been shown to preserve benzodiazepine efficacy well into SE, suggesting that calcium-regulated systems may be partially responsible for refractoriness to anti-epileptic drugs [113]. Additionally, blockade of glutamate receptors limits neuronal death in SE. Chronically, excitotoxic/calcium-mediated mechanisms are important in the development of several SE-associated pathologies. For example, in the pilocarpine model of SE, several studies have demonstrated that post-SE cognitive dysfunction and epileptogenesis were dependent on NMDA-receptor mediated calcium influx [114-116].

NMDA-mediated calcium influx leads to toxically high levels of calcium inside of neurons during the seizure event. However, this acute spike in free calcium is not the only source of excessive intracellular calcium implicated in the pathology of SE. It appears that calcium levels remain chronically high in neurons well after SE, due to a reset of the neuron's normal resting calcium levels [117, 118]. Additionally, after SE neurons respond more slowly to a calcium challenge, requiring more time to remove calcium once it has entered the neuron [119]. Since calcium is such a pervasive second messenger in cellular processes, this SE-induced increase in resting calcium concentrations can lead to chronic activation of calcium-stimulated enzymes and subsequent disregulation of synaptic function. Neuronal free calcium levels are normally maintained in at nanomolar concentrations through the actions of several calcium sinks, including

plasma membrane calcium pumps, calcium-binding proteins, and calcium sequestration by the mitochondria and smooth endoplasmic reticulum. Recent research has implicated at least one of these mechanisms in SE-induced altered calcium handling. Parsons et al [120] demonstrated that the ATP-dependent calcium pumps of the smooth ER are damaged by SE, resulting in an uncoupling of their ATP usage from their calcium pumping activity and a loss of efficiency in ER calcium sequestration. These calcium-related pathological mechanisms have made calcium-regulated systems an intriguing area of research in SE. One such calcium-regulated system that may play a role in the pathology of SE is CaN.

Some evidence points to a role for CaN in SE. As with TBI, CaN inhibitors have proven neuroptotective in some seizure models. Moriwaki et al demonstrated that CaN inhibitors prevented epileptogenesis and behavioral deficits after kainite-induced SE, although no effect was observed on the acute seizure activity of SE, suggesting that CaN may be important for the development of SE-associated chronic pathologies [121]. However, the mechanism underlying this neuroprotective effect has not been elucidated. Moia and colleagues observed a similar anti-epileptogenic effect in a kindling model, with administration of FK506 or cyclosporin A preventing electrical-stimulation kindling in rats [122]. In the same study, CaN was shown to translocate into post-synaptic membrane fractions as a result of kindling, possibly indicating that CaN modulates neuronal excitability post-synaptically during epileptogenesis. Sanchez et al. [123] suggested one potential seizure-induced post-synaptic effect of CaN in a model of hypoxic seizures in immature rats. In this study, CaN

activity was increased post-seizure, and this increase in CaN activity appeared to modulate the activity of the $GABA_A$ receptor. In spite of these intriguing results in other seizure models, no study has yet examined the effects of SE on CaN activity, or demonstrated the role of CaN in SE-associated pathology.

The present study characterizes the effects of two different models of neuronal injury on the activity and subcellular distribution of CaN. In chapter one, we examine basal and maximal CaN activity in forebrain homogenates after a one-hour SE event. In this chapter, we also describe SE-induced changes in CaN substrate kinetics. Finally, chapter one also examines the NMDA receptor-dependence of these changes in CaN activity, and determines whether the observed SE-induced changes in CaN activity are due to an overall increase in enzyme concentration. In chapter two, through the use of western and immunohistochemical analysis, we show an SE-dependent increase in the amount of CaN present in the post-synaptic region of hippocampal and cortical neurons. This SE-induced increase in synaptoplasmic CaN concentration is accompanied by a dramatic increase in CaN activity in this fraction. Chapter two also presents data on SE-induced changes in CaN enzyme activity in subcellular fractions taken from cortex and hippocampus. Taken together, the results presented in the first two chapters of this study describe a profound increase in post-synaptic CaN concentration and activity after one hour of SE, changes that could have major implications in the pathology of SE. In chapters three and four we present TBI-induced changes in CaN activity and post-synaptic concentration

in the moderate fluid percussion model of traumatic brain injury. These changes in CaN activity and subcellular distribution persist for several weeks post-injury, a time-course which corresponds to a number of TBI-associated pathologies. Finally, in chapter five, we discuss a major physiological consequence of SE-induced increases in post-synaptic CaN activity and concentration: loss of dendritic spines. CaN was shown to be part of a cellular mechanism of SE-induced dendritic spine loss, possibly implicating the enzyme in SE-induced chronic neurological pathology. Altogether, the results presented in this study provide compelling evidence that CaN is involved in neuronal damage in two disparate models of injury, and support the hypothesis that SE-induced increases in CaN activity lead to decreased dendritic spine density. Ideally, further research in this topic will provide a basis for future neuroprotective and therapeutic treatments.

CHAPTER I

A SIGNIFICANT INCREASE IN BOTH BASAL AND MAXIMAL CALCINEURIN ACTIVITY IN THE RAT PILOCARPINE MODEL OF STATUS EPILEPTICUS

INTRODUCTION

Status epilepticus (SE) is a severe medical condition, affecting 102,000 to 152,000 people per year in the United States [100, 103]. Defined as continuous seizure activity lasting thirty minutes or greater, SE is a life-threatening medical emergency, associated with significant mortality rates [103, 105, 124]. According to recent studies, status epilepticus results in between 22,000 and 42,000 fatalities every year in the U.S. [100, 103]. In addition, SE is also associated with physiological and neurochemical changes which take place during the seizure activity [105, 125, 126]. These cellular changes may later manifest themselves as spontaneous recurrent seizure activity (i.e. epilepsy), through a process known as epileptogenesis [105, 111]. Therefore, victims of status epilepticus incur both an immediate, serious risk of death, and another, long-term risk of developing recurrent seizure activity.

Modulation of intracellular calcium levels is important in a number of normal neuronal processes including regulation of gene expression, development of learning and memory, and neurotransmitter synthesis and release [127, 128]. However, alterations in calcium-regulated systems and loss of calcium homeostasis have also been implicated in many pathological conditions, such as ischemia [129-131], traumatic brain injury [132, 133], and SE [118, 120]. Specifically, influx of calcium through the NMDA subtype of glutamate receptor is suspected to be important for physiological changes occurring after SE [116, 118, 126]. NMDA-linked increases in intracellular calcium affect a number of calcium-controlled cellular mechanisms and enzymes including calcium/calmodulin-dependent kinase II (EC 2.7.1.123, CaM Kinase II) [127, 134], calpain I (EC 3.4.22.17) [135] and calcineurin (EC 3.1.3.16 CaN) [136].

Calcineurin is a calcium/calmodulin-stimulated phosphatase enriched in neural tissue [137]. CaN-mediated dephosphorylation is an important modulatory factor in many cellular processes, including development of learning and memory [138], regulation of LTP and LTD [139], and induction of apoptosis [140]. Additionally, CaN may depress the activity of the GABA receptor, an important inhibitory receptor in the brain [67]. These characteristics make CaN an intriguing enzyme for study in SE. In spite of this, no studies have yet focused on SE-dependent changes in CaN activity.

This study was undertaken to characterize changes in calcineurin activity in specific brain regions following status epilepticus. Basal and maximal CaN activities were investigated, with an NMDA-receptor activation-dependent

increase present in both. Since CaN regulates many important neuronal processes, an increase in the activity of this important enzyme may be involved in SE-induced alterations of neuronal function.

METHODS AND MATERIALS:

All materials were reagent grade and were purchased from Sigma Chemical Co. (St. Louis, MO) unless otherwise noted. Bio-Rad protein assay concentrate, sodium dodecyl sulfate (SDS), 2-mercaptoethanol, blotting grade dry milk, and Mini-Protean II SDS-PAGE apparatus and power supplies were purchased from Bio-Rad Laboratories (Richmond, CA). Okadaic Acid was purchased from BioMol (Plymouth Meeting, PA). ABC reagents were obtained from Vector Laboratories (Burlingame, CA). Absolute ethyl alcohol was purchased from AAPER Alcohol and Chemical Co. (Shelbyville, KY). Adult male Sprague-Dawley rats were obtained from Harlan Laboratories (Indianapolis, IN).

Pilocarpine model of status epilepticus:

All animal use procedures were in strict accordance with the Guide for the Care and Use of Laboratory Animals described by the National Institutes of Health and were approved by the Virginia Commonwealth University Animal Use Committee. SE was induced in adult male Sprague-Dawley rats by the method described in Mello et al [141]. Rats were handled regularly for approximately one week to acclimate them to handling prior to drug administration. Adult rats weighing 175-230g were injected intraperitoneally (i.p.) with 350mg/kg pilocarpine HCl, a potent muscarinic agonist. 30 minutes prior to the pilocarpine

injection, all rats were treated i.p. with 1mg/kg methylscopolamine. Methylscopolamine is a peripheral muscarinic antagonist; administering it prior to pilocarpine injection minimizes adverse peripheral effects. Control rats received all injections, except that pilocarpine was administered at 1/10th its seizure-inducing dose. Control animals did not exhibit any behavioral seizure activity. When appropriate, rats were injected with the non-competitive NMDA antagonist, MK-801 (4 mg/kg, i.p.), 20 minutes before pilocarpine injection. All drugs were dissolved in 0.9% saline.

Behavioral seizures typically began 20 minutes following pilocarpine injection. Seizures were rated according to the scale described by Racine [142]. Only animals reaching stage 5 seizures were included in this study. Stage 5 was classified as the most severe level of seizure activity, characterized by rearing and falling. Rats not responding to the initial pilocarpine injection received a second injection, often of a lower dose. Rats that still did not display stage 5 seizure activity following a second pilocarpine injection were excluded from the SE group [134].

Isolation and homogenization of brain regions:

Rats were rapidly decapitated after 1 hour of SE. Brains were dissected on a petri dish on ice to preserve post-mortem enzyme activity. Cortical, hippocampal, and cerebellar brain regions were quickly isolated and immediately homogenized with 10 strokes (up and down) at 12,000 rpm, using a motorized homogenizer (TRI-R Instruments, Inc. Rockville Center, NY). Brain regions were

homogenized into ice-cold homogenization buffer containing 5mM HEPES (pH 7.0), 7mM EGTA, 5mM EDTA, 1mM dithiothreitol (DTT), 0.3mM PMSF, and 300mM sucrose. Cortical regions were homogenized into 7ml of buffer, hippocampal regions into 3ml of buffer, and cerebellar regions into 5ml. All brain homogenates were normalized for protein, separated into aliquots and stored at –80°C until used.

pNPP assay of phosphatase activity:

Calcineurin activity was assayed using a modification of the procedure detailed by Pallen and Wang [143]. All reaction tubes were prepared on ice and contained the following: 25mM MOPS (pH 7.0), 1mM DTT, 2mM p-nitrophenol phosphate (pNPP). Some basal tubes also contained 2mM EGTA and 2mM EDTA. Maximal tubes contained the same reagents as basal reactions, with the addition of 2mM $MnCl_2$. Final reaction volumes were 1ml. Both Mn^{2+} and Ca^{2+}/calmodulin activate calcineurin in this assay; however, Mn^{2+} activates calcineurin more strongly than calcium [21]. Therefore, Mn^{2+} was used instead of calcium in maximal reactions to better visualize the cation-stimulated activity of the enzyme. When called for, 150nM okadaic acid, 50μM okadaic acid (sodium salt), or 100μM $NaVO_4$ was added to both basal and maximal tubes. Prior to use, the protein concentration of all homogenates was determined using the method of Bradford et al. [144]. Reactions were initiated by the addition of 200 mg/ml brain region homogenate. Unless otherwise specified, standard reactions were incubated at 37°C for 15 minutes in a shaking water bath. Tubes were then

removed from the water bath and placed in ice to stop the reaction. Absorbance of the reaction mixture was immediately measured at 405nm in a spectrophotometer (UV-2101, Shimadzu Scientific Instruments, Inc. Columbia, MD). Absorbance units were converted to nmol of pNP produced by comparison to a pNP concentration standard absorption curve.

pNPP substrate kinetics:

Basal reaction tubes were prepared containing 25mM MOPS, 1mM DTT, 2mM EGTA, 2mM EDTA, and 150nM okadaic acid to minimize the influence of other phosphatases on the results of the assay. Maximal reaction tubes contained 25mM MOPS, 1mM DTT, 2mM $MnCl_2$, and 150nM okadaic acid. All reaction tubes were prepared on ice. pNPP was added to the tubes for final concentrations of 0, 0.1, 0.2, 0.5, 1, 2, 4, 8, 16 and 24mM. CaN reactions were initiated by the addition of homogenate and assayed as described above. Values for K_m and V_{max} were obtained via a non-linear regression analysis of the substrate isotherm.

CaN protein level analysis:

Western analysis was performed essentially as described previously [145, 146]. Briefly, homogenates were resolved on SDS-PAGE and transferred to a nitrocellulose membrane using the Geni blot system (Idea Scientific, Minneapolis, MN). Nitrocellulose was then immersed for one hour in blocking solution containing phosphate buffered saline (PBS, pH 7.4), 0.05% (v/v) polyoxyethylene

sorbitan monolaurate (tween-20), 50 g/L Bio-Rad blotting grade dry milk, and horse serum (Vector Laboratories Inc., diluted 50 μl/10ml). The nitrocellulose membrane was then incubated with primary antibody in blocking solution for one hour. Anti-CaN A antibody (clone CN-A1, mouse monoclonal IgG, Sigma Chemical Co.) was diluted 1:10,000 for western analysis. Membranes were then washed three times in a wash solution containing PBS, tween-20, and dry milk. Nitrocellulose was then reacted with a secondary antibody in blocking solution for 45 minutes. The membrane was then washed three times and incubated with an avidin-biotinylated horseradish peroxidase complex for 30 minutes. Nitrocellulose was then washed three times in PBS for 10 minutes per wash. Blots were developed with a solution containing 10 ml PBS, 0.025% (v/v) H_2O_2, and 8 mg 4-chloro-1-napthol dissolved in 2ml of methanol. Specific immunoreactive bands were quantified by computer-assisted densitometry (Inquiry, Loats Associates, Westminster, MD).

Statistical analysis:

All statistical analysis of data was performed using GraphPad Prism 3.0 (GraphPad Software, San Diego, CA), or Sigma Stat 2.03 (SPSS Inc, Richmond, CA). Levels of phosphatase activity were compared to control using the Student's t-test (two-tailed distribution, unpaired or paired where appropriate) or one-way ANOVA with Tukey post analysis to control for type 1 errors in multiple comparisons. Values for V_{max} and K_m were determined by a non-linear regression curve for single-site substrate binding, included with the Prism software.

Computer assisted densitometric analysis was performed using Inquiry (Loats Associates Inc, Westminster, MD).

RESULTS:

Status epilepticus results in an increase in calcineurin activity in specific brain regions:

Calcineurin dephosphorylates the low molecular weight compound p-nitrophenolphosphate (pNPP) with high affinity, producing p-nitrophenol (pNP) [143]. It is possible to measure this dephosphorylation spectrophotmetricaly, providing a simple and accurate method for quantifying calcineurin activity. In the present study, CaN activity was measured via the pNPP assay in homogenates obtained from the cortex, hippocampus, and cerebellum of SE and control rats.

Both basal and maximal CaN activity were measured in SE and control animals (Figure 1). In every sample studied, SE caused an increase in phosphatase activity above control levels in both the cortex and hippocampus, but not the cerebellum. Average basal activity in control samples was 0.79 ± 0.10 μg pNP /min in cortical homogenates, and 0.86 ± 0.03 μg pNP/min in hippocampal homogenates. Following SE, basal CaN activity was elevated 48.6 ± 14.5% above control in the cortex (Figure 1A) (1.18 ± 0.04μg pNP/min, $p < 0.01$, n=6, two-tailed unpaired Student's t-test) and 20.8 ± 4.9% in the hippocampus (Figure 1B) (1.04±0.03μg pNP/min, $p < 0.001$, n=9). The elevated activity was biological, and could be eliminated by boiling the homogenate prior

to beginning the reaction. The increase was present in spite of the addition of ion chelators to the reaction mix (see methods).

Unlike homogenates from the cortex and hippocampus, basal activity in cerebellar homogenate was not significantly increased after SE. Basal activity in cerebellar homogenates isolated from control animals was 0.92 ± 0.08μg PNP/min. After SE, activity in the cerebellum was elevated to 1.00 ± 0.05μg PNP/min, an increase of 8.0 ± 10.1% (Figure 1C). This was not a significant increase ($p > 0.05$, n=7). The difference in the response of the cerebellum from that of the forebrain suggests that different mechanisms are involved in the expression of SE in the cerebellum from that of the forebrain.

Maximal activity, like basal activity, was increased after SE in both the cortex and hippocampus, but not the cerebellum. In cortical homogenates isolated from control animals, pNPP dephosphorylation was found to be 1.34 ± 0.18μg pNP/min. Following SE, maximal cortical dephosphorylation activity was elevated to 1.80 ± 0.05μg pNP/min, an increase of 34.2 ± 10.2% (Figure 1A, $p < 0.01$, n=6). An increase in maximal activity was also observed in hippocampal homogenates. Control maximal activity was 1.36 ± 0.05μg pNP/min. SE resulted in a 13.7 ± 5.1% increase in activity, to a post-SE value of 1.55 ± 0.02μg pNP/min. (Figure 1B, $p < 0.05$, n=9). No significant change in maximal activity was observed in the cerebellum. Control maximal activity was 1.54 ± 0.12μg pNP/min in cerebellar homogenates. After SE, maximal activity increased to 1.60 ± 0.08μg pNP/min. This was an increase of 4.0 ± 3.4% over control, which was not statistically significant (Figure 1C, $p > 0.05$, n=7).

The SE-dependent increase in CaN activity is due to an alteration in enzyme kinetics:

To further characterize the SE-dependent effect on calcineurin activity, several experiments were conducted in cortical homogenate to examine the effects of SE on CaN-mediated pNPP dephosphorylation kinetics. Figure 2 shows the linear regression analysis of the time course for pre-steady state pNPP dephosphorylation under basal and maximal CaN conditions. The slope of the linear regression for each condition was used to estimate the rate of pNPP dephosphorylation. The rate of CaN-dependent dephosphorylation of pNPP in cortical homogenates from control animals was estimated to be 0.26 μg/min under basal conditions. SE resulted in a 36.7 ± 7.6% increase in the rate of pNPP dephosphorylation, to 0.36 μg/min (Figure 2A, $p < 0.001$, n=3, unpaired student's t-test). The increase in pNPP dephosphorylation rate was also observed in maximal CaN reactions (Figure 2B). The rate of control pNPP dephosphorylation was 0.68 μg/min under maximal conditions. SE resulted in a significant increase in pNPP dephosphorylation, to a value of 0.80 μg/min (17.6 ± 4.7%, $p < 0.05$, n=3, unpaired student's t-test). The data demonstrate a significant increase in both basal and maximal pNPP dephosphorylation rates in cortical homogenate

To determine the effect of SE on CaN affinity for pNPP, cortical homogenates from SE and control animals were tested in the presence of specific pNPP concentrations. (Figure 3). Through non-linear regression analysis of the data, maximal pNPP dephosphorylation (V_{max}) and substrate affinity (K_m)

for the dephosphorylation of pNPP were calculated. The control value for V_{max} was 1.21 ± 0.06μg pNP/min under basal reaction conditions. Following SE, V_{max} increased to 1.46 ± 0.03μg pNP/min, an increase of 20.5 ± 5.3% above the control value ($p < 0.05$, n=3, two-tailed unpaired Student's t-test). Substrate affinity was also increased under basal conditions. In homogenates isolated from control animals, K_m was found to have a value of 1.25 ± 0.22mM. Post-SE, K_m decreased to 0.54 ± 0.06mM. This decrease in K_m corresponded to a 56.8 ± 14.5% increase in substrate affinity in SE homogenates when compared to control ($p < 0.05$, n=3). Under maximal conditions, V_{max} was also increased after SE. In control homogenates, V_{max} was determined to be 1.73 ± 0.05μg pNP/min. Following SE, V_{max} was elevated to 1.93 ± 0.04μg pNP/min, an increase of 12.8 ± 3.5% over control ($p < 0.05$, n=3). Substrate affinity appeared to increase in SE homogenates under maximum conditions; however, this difference was not statistically significant ($p > 0.05$, n=3).

The increase in both basal and maximal pNPP dephosphorylation is due to CaN:

The enzyme activity observed in the various brain regions is consistent with CaN activity: calcineurin dephosphorylates pNPP readily, is stimulated by Mn^{2+}, and is most active at pH 6.8 - 7.0 [21, 143]. However, pNPP is a versatile substrate, and is also dephosphorylated by some tyrosine and alkaline phosphatases [147]. All experiments were conducted at a neutral, rather than alkaline, pH (see methods). Therefore, it would be expected that alkaline

phosphatases have only a minimal contribution to the observed dephosphorylation of pNPP. To rule out tyrosine phosphatases and other serine/threonine phosphatases, the phosphatase inhibitors sodium orthovanadate and okadaic acid were tested.

Sodium orthovanadate ($NaVO_4$) is a potent inhibitor of tyrosine phosphatases (IC50 = 10μM) [148]. Additionally, orthovanadate is a strong inhibitor of the Mn^{2+}-stimulated activity of calcineurin (IC_{50} = 1μM) [149]. It does not, however, inhibit any non-Mn^{2+} stimulated calcineurin activity [149]. Dephosphorylation reactions were carried out in cortical homogenates in the presence of 100μM $NaVO_4$ under both basal and maximal (Mn^{2+}-stimulated) conditions (Figure 4). The addition of orthovanadate did not cause any significant change in basal pNPP dephosphorylation in either control or SE homogenates ($p > 0.05$, n=4, one-way ANOVA). Therefore, even in the presence of $NaVO_4$, basal pNPP dephosphorylation in homogenates isolated from SE animals was still significantly greater when compared to control homogenates ($p < 0.001$, n=4, unpaired student's t-test). Thus, SE induced a $NaVO_4$-resistant increase in pNPP dephosphorylation. The data support the hypothesis that the SE induced dephosphorylation was not due to tyrosine phosphatases.

As expected, the inclusion of orthovanadate did have a significant effect on maximal pNPP dephosphorylation. Orthovanadate reduced maximal enzyme activity to basal levels in both SE and control homogenates. The addition of $NaVO_4$ reduced control maximal activity from 1.19μg pNP/min to 0.62μg pNP/min, a decrease of 48.1 ± 4.6% ($p < 0.001$, n=4, two-tailed paired student's

t-test). In SE homogenates, maximal activity was reduced by 40.7 ± 8.9%, from 1.67μg pNP/min to 0.99μg pNP/min ($p < 0.001$, n=4). The $NaVO_4$-inhibited maximal activity was significantly greater in SE homogenates when compared to control homogenates ($p < 0.001$, n=4, two-tailed unpaired student's t-test). Since orthovanadate specifically inhibits only Mn^{2+}-stimulated CaN activity, the observed inhibition of maximal activity, but not basal activity, is consistent with CaN-dependent dephosphorylation.

To further characterize the CaN-dependent dephosphorylation of pNPP, okadaic acid was utilized. Okadaic acid (OA) is a potent inhibitor of serine/threonine phosphatases 1 and 2A [150], with an IC_{50} of 10-15 nM for PP1, and an IC_{50} of 100 pM for PP2A. Okadaic acid is also an inhibitor of calcineurin, although with a much lower affinity (IC_{50} =5mM) [150]. This difference in sensitivity makes OA a valuable tool in differentiating between the activities of these three phosphatases. CaN activity was first assayed in the presence of 150nM OA, a concentration sufficient to inhibit both PP1 and 2A, but not high enough to significantly affect CaN activity. The inclusion of 150nM OA did not significantly affect pNPP dephosphorylation in cortical homogenates (Fig. 5A). The lack of OA-dependent inhibition was observed under both basal and maximal conditions for CaN activation. SE basal activity in the presence of 150nM OA was 1.03μg pNP/min, only 1.7% lower than the 1.05μg pNP/min that was measured in the absence of inhibitor. This difference was not significant ($p > 0.05$, n=4, two-tailed paired student's t-test). SE maximal activity was 2.14μg pNP/min in the absence of inhibitor, and 2.00μg pNP/min in the presence of

150nM OA, a decrease of 8.3% that was not statistically significant ($p > 0.05$, n=4). Similarly, control basal activity was not significantly modified by low concentrations of OA ($p > 0.05$, n=4). Control basal activity in the absence of OA was 0.62μg pNP/min, and in the presence of OA activity was 0.69μg pNP/min. Control maximal activity was 1.61μg pNP/min without OA and 1.68μg pNP/min with OA, a difference of 4.7% ($p > 0.05$, n=4). These results indicated that PP1 and 2A are not responsible for the SE-dependent increase in phosphatase activity observed under either basal or maximal conditions.

Dephosphorylation of pNPP was also carried out at a higher concentration (50μM) of OA. This concentration of OA was high enough to block the activity of CaN, and was found to significantly decrease pNPP dephosphorylation in both control and SE cortical homogenates (Fig. 5B). Maximal activity in control homogenates was reduced from 1.29μg pNP/min to 1.20μg pNP/min by the addition of inhibitor (a decrease of 8.8 ± 2.8%, $p < 0.01$, n=6). Similarly, maximal activity was reduced in SE homogenates by 10.7 ± 4.2%, from a value of 1.57μg pNP/min without inhibitor to a value of 1.40μg pNP/min in the presence of OA ($p < 0.01$, n=6, two-tailed paired student's t-test). However, basal activity was not inhibited by 50μM OA in control homogenates ($p>0.05$, n=6). Under basal reaction conditions, most of the required ions for CaN activation are either not present or bound to chelators, and CaN activity in control basal reactions is probably very limited. Therefore, it is not surprising that 50μM OA does not inhibit the control basal pNPP dephosphorylation. However, it is interesting to note that the SE basal activity, unlike the control basal activity, was inhibited by high-

concentration OA. Basal activity in the SE homogenate was reduced from 1.06μg pNP/min to 0.94 μg pNP/min by the addition of 50μM OA, a decrease of 11.2 ± 4.4% ($p < 0.01$, n=6). The data suggest that SE results in the production of a Ca^{2+}-independent form of CaN that is sensitive to inhibition by high concentrations of OA. However, the activity in SE homogenates was not entirely reduced to control levels by the addition of 50μM OA. This may be due to the solubility or efficacy limits of OA as a CaN inhibitor under these conditions, or it may suggest that another, OA-insensitive phosphatase is also contributing to the observed SE-dependent increase in phosphatase activity.

The lack of response to low concentrations of OA, the significant inhibition by high concentration OA, and the distinctive reaction of the homogenate to orthovanadate, all strongly suggest that CaN is responsible for the observed increase in activity. In addition, the response of the SE homogenate to high concentration OA under basal conditions suggests that the observed increase in basal activity is due to the presence of a calcium independent form of CaN.

The increase in enzyme activity is not due to an increase in protein:

A potential explanation for the observed SE-dependent changes in CaN activity and kinetics is an increase in the amount of enzyme present in the cell. To investigate this possibility, western blot analysis was performed on homogenate isolated from the cortex and hippocampus (Figure 6). Cerebellar homogenate was not tested since there was no SE-dependent change in CaN activity in the cerebellum. Immunoreactivity of the catalytic A subunit was

determined using a monoclonal antibody to CaN A (CN-1, Sigma, St. Louis, MO). In both the cortex (Figure 6A) and hippocampus (Figure 6B), a single band with molecular weight of 61kDa was resolved. This size corresponds with the size of the CaN A subunit [8]. Computer assisted densitometric analysis was performed on SE and control fractions (see methods and materials). Optical density of the immunoreactive band in SE homogenate was found to be 93.62 ± 3.01% of control in the cortex and 104.17 ± 14.57% of control in the hippocampus. No significant difference in the density of the 61kDa band was found in either brain region, indicating equal total amounts of the enzyme in both SE and control animals in both regions ($p>0.05$, $n=4$, two-tailed unpaired student's t-test). The data suggest that the increase in enzyme activity was not due to increased protein synthesis, but due to another mechanism, such as post-translational modification of the enzyme, or increased Ca/CaM binding to the enzyme following SE.

The increase in calcineurin activity occurs through an NMDA-dependent mechanism:

Calcium influx through the NMDA subtype of glutamate receptor is essential for the development of a number of SE-dependent alterations in neurochemical and physiological processes [115, 120, 127, 134]. To investigate the involvement of NMDA-regulated calcium influx on the SE-dependent increase in calcineurin activity, MK-801 was used to block the NMDA receptor-associated calcium channel during seizure activity. Pre-injection of MK-801 has been shown

to prevent many of the NMDA-receptor dependent consequences of SE, but does not prevent or inhibit the pilocarpine-induced seizures in this model [115].

Cortical (Figure 7A) and hippocampal (Figure 7B) homogenates from MK-801 treated SE animals were assayed for phosphatase activity via the pNPP assay as described. Injection of MK-801 alone (no SE) did not induce a significant change in calcineurin activity. However, MK-801 injection did block the SE-induced increase in calcineurin activity. In the cortex, basal calcineurin activity in MK-801 animals was 0.88μg pNP/min, only slightly higher than the control activity of 0.82μg pNP/min. The observed increase was not statistically significant (7.2 ± 16.8% increase over control, $p > 0.05$, n=4, one-way ANOVA with Tukey post-hoc analysis). Maximal activity of MK-801 and control animals was also not significantly different: 1.38μg pNP/min for control homogenates and 1.48μg pNP/min for MK-801 homogenates (an increase of 7.1 ± 11.4%, $p > 0.05$, n=4). Cortical calcineurin activity was significantly higher in pilo-SE animals than in either control or MK-801 treated animals. SE basal CaN activity was 1.21μg pNP/min, an increase of 37.8 ± 11.0% over the MK-801 group ($p < 0.05$, n=4). Maximal activity was 1.86μg pNP/min, 26.0 ± 6.8% higher than that of the MK-801 homogenates ($p < 0.05$, n=4). This data suggests that NMDA-dependent calcium influx during SE is essential for the observed increase in calcineurin activity in the cortex.

Hippocampal homogenates from MK-801 treated animals had significantly lower basal and maximal CaN activity than hippocampal SE homogenates ($p < 0.05$, n=4, one-way ANOVA with Tukey post-hoc analysis). However, unlike the

cortex, CaN activity was not entirely reduced to control levels by MK-801 pre-injection. A significant increase in CaN activity was still found in MK-801 homogenates (Figure 7B). The MK-801 basal value of 1.23μg pNP/min was elevated 19.1% above the control value of 1.03μg pNP/min, but still significantly lower than the activity in SE homogenates, which was 1.35μg pNP/min, or a 31.1% increase over control ($p < 0.05$, n=4). Likewise, maximal activity was elevated above control in the MK-801 group, with a value of 1.67μg pNP/min, a 24.6% increase over the control value of 1.34μg pNP/min. However, this increase was not as large as the increase in activity found in SE homogenates. SE maximal activity was 31.3% above control, with a value of 1.76μg pNP/min. This suggests that either the MK-801 did not entirely block the NMDA receptor in hippocampal neurons, or that the SE-dependent increase in calcineurin activity is controlled by additional mechanisms in the hippocampus. Overall, NMDA receptor activation was found to play a significant role in the SE-induced increase in CaN activity in both brain regions.

DISCUSSION:

Understanding the cellular and molecular changes that take place during SE is essential to understanding the physiological mechanisms that cause this severe seizure activity. This study characterizes the changes in both basal and Mn^{2+}-stimulated CaN activity in specific brain regions following SE. The data demonstrate a significant increase in CaN activity in cortical and hippocampal homogenates. The increase in phosphatase activity in cortical homogenates was

found to be OA-sensitive. SE did not significantly affect CaN activity in homogenates isolated from the cerebellum. In addition, the SE-induced increase in CaN activity was NMDA-receptor activation-dependent. The present study is the first definitive investigation of SE-dependent modulation of calcineurin activity. The data supports the hypothesis that SE results in an NMDA-dependent increase in both basal and maximal calcineurin activity in the rat forebrain, but not in the cerebellum.

There are several possible mechanisms that could account for the increase in CaN-mediated dephosphorylation. Calcineurin is a calcium/calmodulin-stimulated enzyme [8] and would be stimulated by increased intracellular calcium concentrations. SE induces a loss of function of the endoplasmic reticulum Mg^{2+}/Ca^{2+} ATPase [120]. This enzyme sequesters calcium ions into the microsomes of the smooth ER, providing a high-affinity mechanism for regulating intracellular calcium concentration [151, 152]. After SE, ATPase-mediated uptake of calcium into the microsomes is less efficient [120], which could potentially result in higher than normal resting calcium concentrations inside the cell. In fact, an increase in intracellular free calcium has been found during and after SE [118]. The increased intracellular calcium associated with SE could be responsible for activating CaN above its normal physiological level. However, it is unlikely that increased calcium observed *in vivo* is directly responsible for the increase in CaN activity following SE observed in this study. Increasing chelator concentrations did not effect the SE-induced increase in CaN dephosphorylation (Data not shown). Additionally, no difference

in free calcium between SE and control homogenates was present, as determined by calcium-specific electrode measurements as described by Parsons et al [130] (93-20 calcium electrode, Orion, Boston, MA). Thus, the effects of any alterations in intracellular free calcium would be minimal under the conditions used in the present study.

Another possible explanation for the observed increase in CaN activity is an increase in the amount of enzyme present in the cell. This is unlikely, since it would require translation of a significant amount of enzyme in a relatively short amount of time (animals actively seized for slightly less than 1 hr). Western analysis of SE and control homogenates further eliminated this possibility, as no significant increase in total enzyme level was observed in any brain region studied.

Another possible mechanism is post-translational modification of CaN, producing a more active form of the enzyme. One such modification could be limited proteolysis by the calcium-stimulated neutral protease, calpain I. Calpain may be activated by the increased intracellular calcium concentrations present during and after SE. Supporting this hypothesis, calpain is activated in other neurotraumatic events that involve glutamate excitotoxicity, such as ischemia [153] and traumatic brain injury [154]. Calpain proteolysis could account for the increased V_{max}, decreased K_m, and increased enzyme activity observed post-SE in this study. Calpain cleaves the catalytic CaN A subunit, removing the calmodulin binding domain and creating a highly active, 43 kDa, calcium-independent form of the enzyme [12, 14]. Some researchers also surmise that

calpain-mediated proteolysis removes the autoinhibitory domain present in the A subunit [14], although other studies suggest that this may not be the case [155].

Significant proteolysis of CaN was not responsible for the observed alteration in enzyme function, since no decrease in total enzyme was observed in western analysis of the SE homogenate. Additionally, no degradation products reacted with the anti-CaN A antibody. However, it is possible that the total amount of enzyme broken down by calpain was too small to detect in the western analysis that was used. Calpain-degraded CaN is reported to be 1100% more active than normal enzyme, while SE produced only a 20-50% increase in activity. The magnitude of this difference suggests that, if the calcium-independent 43 kDa fragment is present, it constitutes only a small amount (3-5%) of total enzyme. A difference in protein levels of this magnitude would be difficult to detect through western blot analysis. It is also possible that the epitope recognized by the antibody was no longer present following proteolysis, explaining why no small fragments appeared on the western blot.

Finally, post-translational modification other than calpain proteolysis may be taking place, activating CaN through another, unidentified mechanism. For example, calcineurin is phosphorylated at the same location by both protein kinase C and CaM kinase II, inhibiting the enzyme through a decrease in substrate affinity [35, 37]. Calcineurin and CaM kinase II share a similar distribution in the brain [156], and regulation of CaN by CaM kinase II is not unlikely. However, long-lasting inhibition of CaM kinase II has been observed following SE in multiple models [134, 157, 158]. It is possible that a decrease in

the CaM kinase II-mediated phosphorylation of CaN produces a net increase in the amount of active calcineurin. While this mechanism would account for the observed increase in maximal calcineurin activity, it does not explain the SE-dependent development of calcium-independent CaN activity.

Calcium influx through the NMDA receptor has been implicated in many of the physiological changes that take place following SE [115, 134]. For this reason, it was of interest to determine if the observed SE-dependent increase in CaN activity was also NMDA-dependent. Blocking the NMDA receptor-associated Ca^{2+} channel with MK-801 completely prevented the SE-dependent increase in CaN activity in the cortex, and significantly reduced the magnitude of the increase in the hippocampus. This data suggests that calcium influx through the NMDA-receptor associated channel is involved in the SE-induced increase in calcineurin activity.

The increase in CaN activity described in this study was not observed in the cerebellum. Although pilocarpine-induced seizure activity generalizes into the cerebellum, many SE-induced physiological changes do not develop in this region. For example, CaM kinase II activity is altered in the cortex and hippocampus following SE, but not in the cerebellum [134]. Similarly, the spontaneous recurrent seizures that develop following pilocarpine treatment do not generalize into the cerebellum [141]. Considering this, it is not surprising that SE-induced increase in calcineurin activity was not noted in the cerebellum. It is possible that SE activates different mechanisms in the cerebellum than in the forebrain, or that an enzyme or receptor necessary for the SE-dependent

activation of CaN is not present in the cerebellum.

The observed SE-dependent increase in CaN activity has broad physiological implications. Neuronal mechanisms which are regulated by CaN dephosphorylation under normal conditions could be highly altered as a result of elevated enzyme activity. One important CaN-mediated mechanism is modulation of the $GABA_A$ receptor. GABA receptors are the primary receptor responsible for the fast inhibitory response in neuronal tissue [65], and play a major role in preventing the neuronal hyperexcitability associated with epilepsy and SE [124]. Several recent studies have demonstrated an inhibitory modulation of $GABA_A$ receptor function by CaN [66-68, 159, 160]. A post-SE elevation in CaN activity may result in increased dephosphorylation of $GABA_A$ receptors, producing a net disinhibition of cellular excitability. This hypothesis is strengthened by the fact that recent studies have described a post-SE decrease in $GABA_A$ activity [161]. Chronic increases in CaN-mediated dephosphorylation, could lead to a long-term loss of GABA receptor function, which may play a role in epileptogenesis. The results of one kindling study already suggest that calcineurin may have an epileptogenic role [122], and disinhibitory mechanisms have been found to be epileptogenic in several studies.

This study is the first to detail an SE-dependent effect on calcineurin activity. The results presented above describe an SE- induced increase in CaN activity which has far-reaching implications, from possible avenues for SE treatment to a potential role in development of epilepsy following SE. While this study focused on the total enzyme pool contained in the homogenate, future

studies will investigate the effect of SE on CaN activity in specific cellular fractions, as well as on purified enzyme. A great deal of further research on this topic is possible, offering exciting insight into the mechanisms underlying status epilepticus.

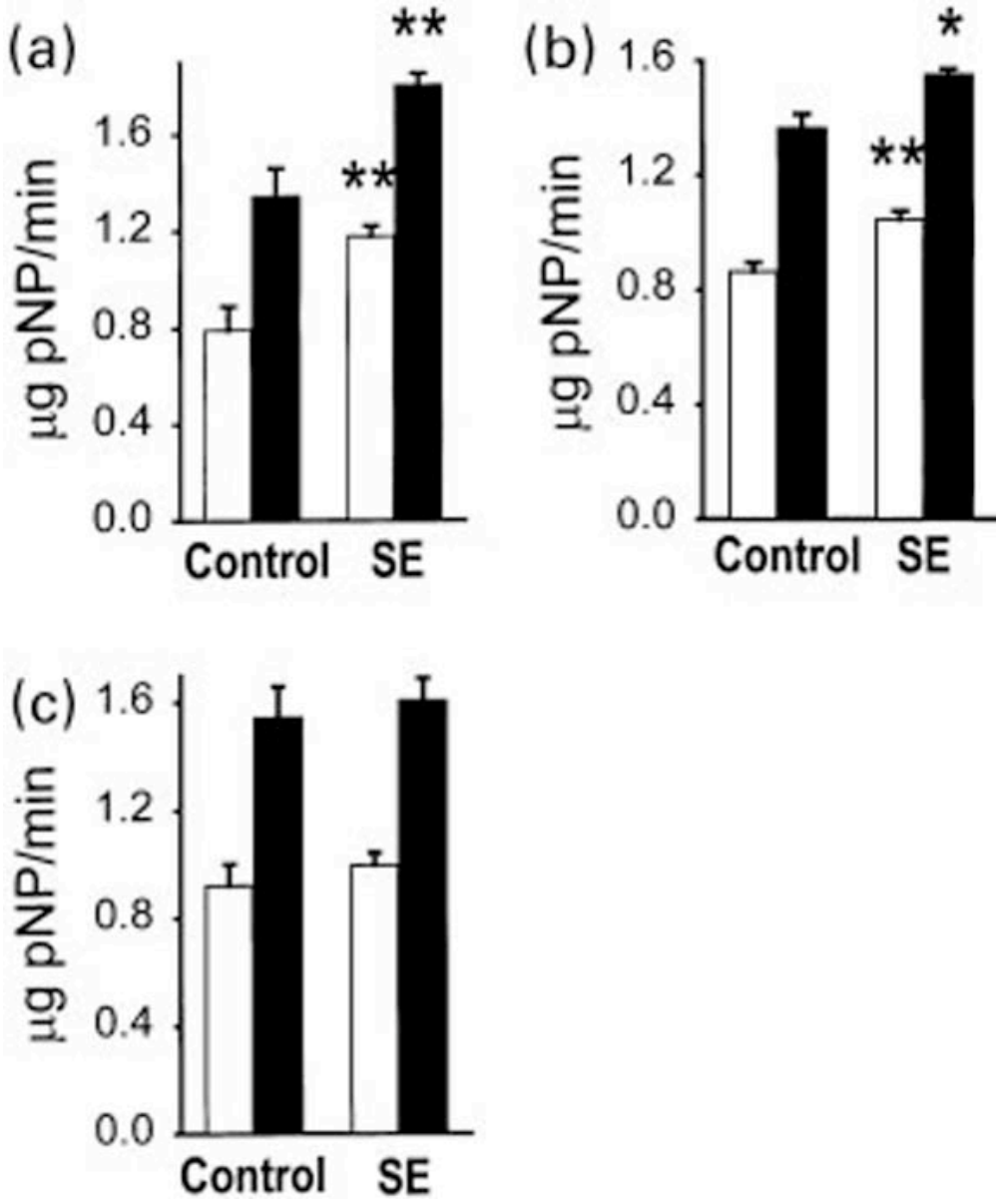

Figure 1. SE resulted in a significant increase in basal and maximal CaN activity. Basal (white) and maximal (black) calcineurin activity was assayed in cortical, hippocampal, and cerebellar homogenates isolated immediately after 1 hour of SE. A) Cortical homogenates isolated from SE animals displayed a significant increase in both basal and maximal CaN activity. (** $p < 0.01$, n=6, two-tailed unpaired Student's t-test). B) Basal and maximal CaN activity was also elevated in the hippocampal homogenates isolated from SE animals when compared to control animals (* $p < 0.05$, n=9; ** $p < 0.01$, n=9, two-tailed unpaired Student's t-test). C) No significant differences were observed in either basal or maximal calcineurin activity in cerebellar homogenates.($p>0.1$, n=7).

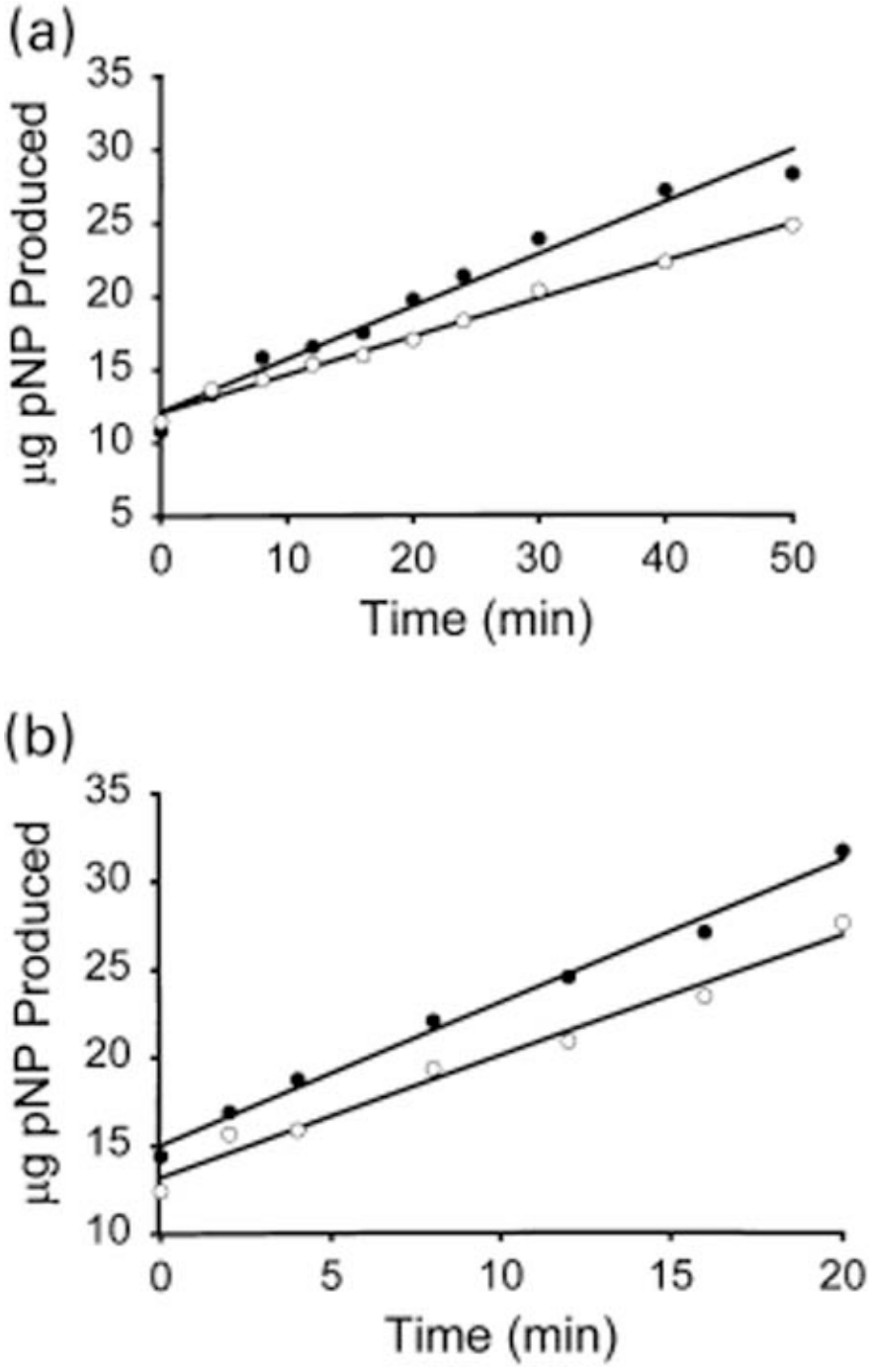

Figure 2. SE modulates the rate of CaN-mediated dephosphorylation in rat cortical homogenates.

CaN dephosphorylation reactions were performed in cortical homogenates isolated from control (white circles) and SE (black circles) animals. Basal (A) and maximal (B) CaN reactions were allowed to continue for specific time intervals, and the corresponding activities plotted to determine reaction rate. The portion of the reaction shown is during the linear (pre-steady state) portion of the reaction A) Under basal conditions, the reaction rate (as indicated by linear regression analysis of the data with time as the independent variable and μg pNP produced as the dependent variable. r^2 = 0.992) was 0.257μg/min in control homogenates (white circles). CaN-mediated dephosphorylation in SE cortical homogenates (black circles) occurred at a rate of 0.355μg/min. This represents an increase of 36.72 ± 7.6% when compared to the control rate. B) Maximal dephosphorylation occurred at a rate of 0.684μg/min in control homogenates, as indicated by linear regression analysis (r^2 = 0.991). The maximal reaction rate in SE homogenates was 0.804μg/min, an increase of 17.55 ± 4.74% over the control rate. Data represents an average of three experiments.

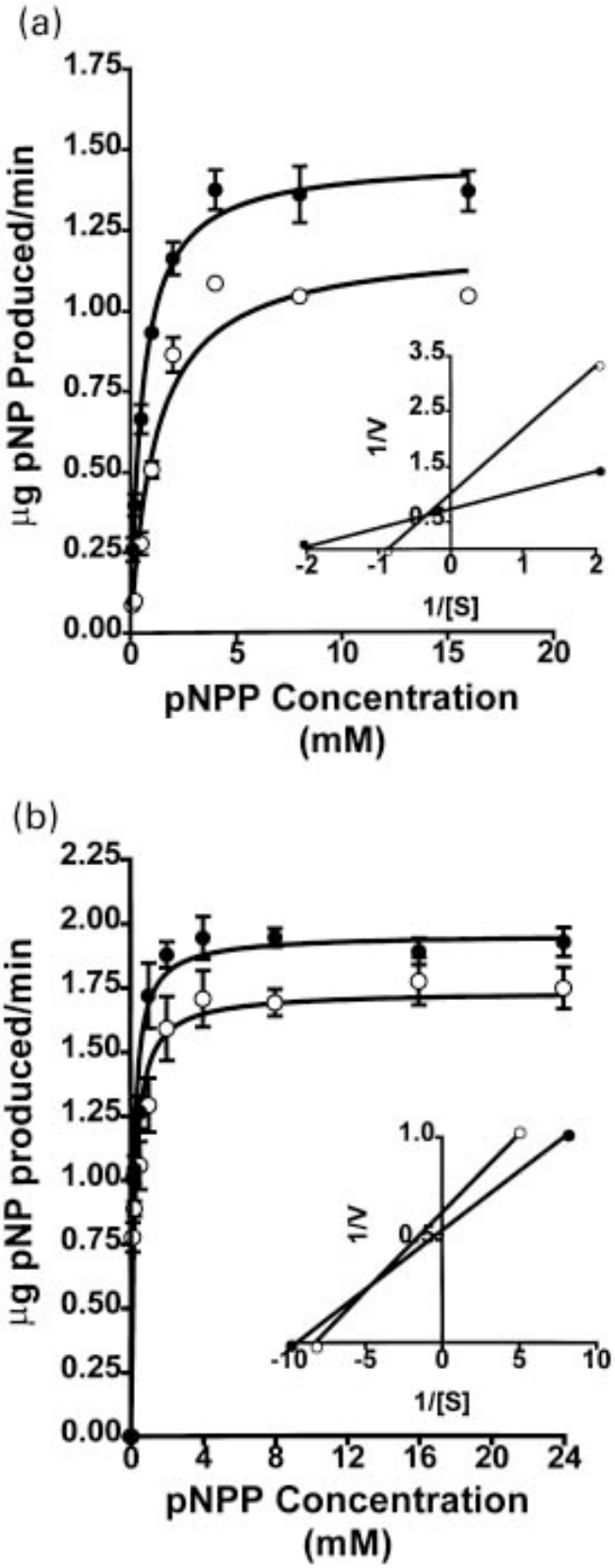

Figure 3. SE alters CaN substrate affinity in rat cortical homogenates.

Substrate affinity (K_m) and maximal pNPP dephosphorylation (V_{max}) for CaN were determined under basal and maximal conditions for SE and control cortical homogenates. A) SE increased both K_m and V_{max} for pNPP dephosphorylation by CaN under basal conditions. A substrate concentration isotherm was generated under basal dephosphorylation conditions in cortical homogenates isolated from control animals (white circles) and SE animals (black circles). Both V_{max} and substrate affinity were increased in SE homogenates when compared to control. Inset: Linweaver-Burk plots of data from control and SE homogenates. SE resulted in an increase in maximal dephosphorylation (V_{max}) under basal conditions. V_{max} for SE homogenates (black circles) was higher than that of control homogenates (white circles) ($p < 0.05$, n=3, student's t-test). K_m was increased after SE. ($p < 0.05$, n=3). B) SE increased V_{max} for pNPP dephosphorylation under conditions for maximal CaN activity. Substrate concentration isotherms under maximal dephosphorylation conditions were generated in cortical homogenates isolated from control (white circles) and SE (black circles) animals. Maximal dephosphorylation was increased in SE homogenates when compared to control. However, substrate affinity in SE and control homogenates was not significantly different under maximal conditions. Inset: Linweaver-Burk plot of substrate isotherms from control and SE homogenates. V_{max} was increased in SE homogenates ($p < 0.05$, n=3). Substrate affinity appeared to increase, however the change was small and not statistically significant ($p > 0.05$, n=3).

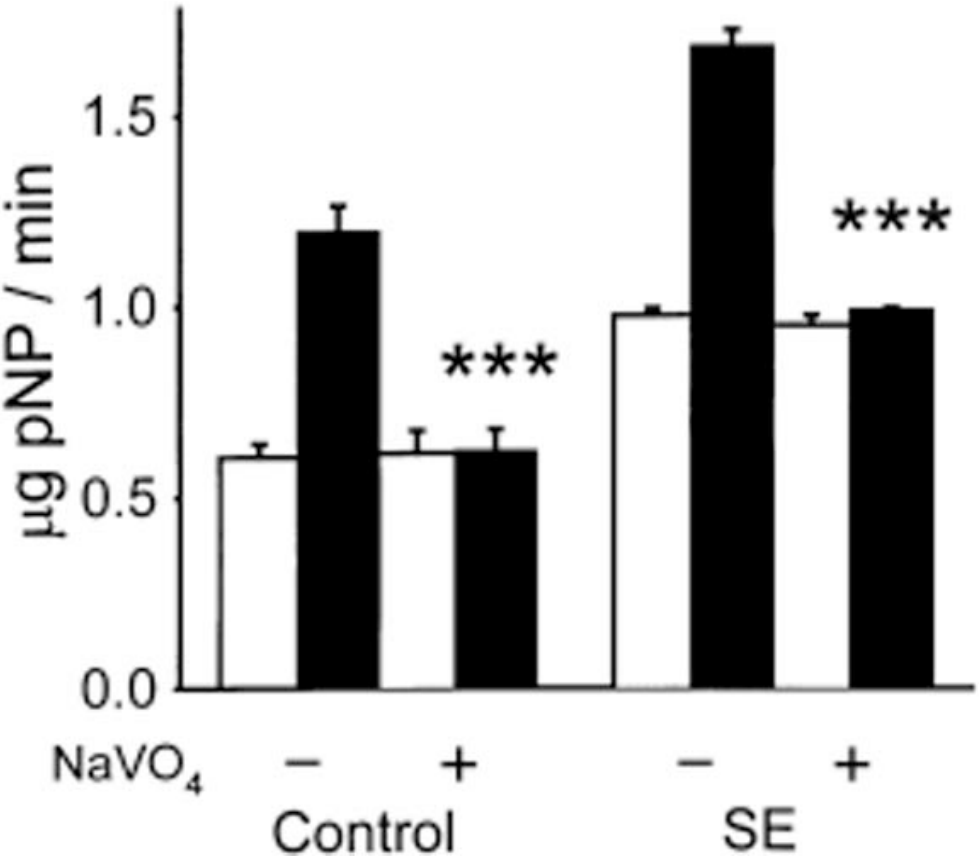

Figure 4. The SE-induced increase in pNPP dephosphorylation was not due to tyrosine phosphatase activity.

Cortical homogenates were isolated from control and SE rats and subjected to basal (white bars) and maximal (black bars) reaction conditions. The reactions were performed in the absence (-) or presence (+) or 100μM $NaVO_4$. This level of $NaVO_4$ is sufficient to inhibit tyrosine phosphatases and Mn^{2+}-stimulated CaN activity. The inclusion of $NaVO_4$ did not significantly affect basal pNPP dephosphorylation, but resulted in complete inhibition of Mn^{2+}-stimulated pNPP dephosphorylation (*** $p < 0.001$, n=4, Student's t-test)

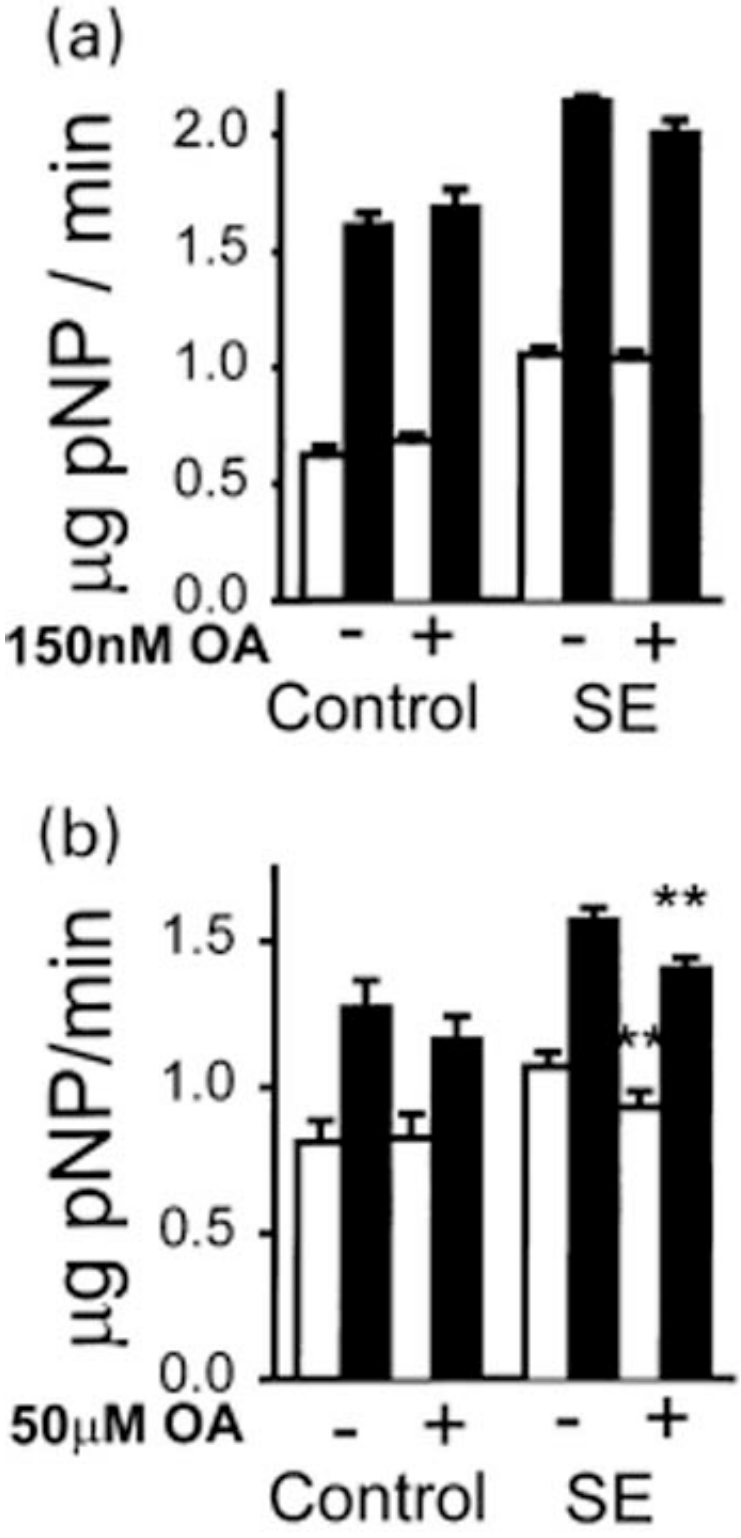

Figure 5. The SE-induced increase CaN activity was inhibited by okadaic acid in a concentration-dependent manner.

A) Low concentration OA has no significant effect on pNPP dephosphorylation in cortical homogenate. The addition of 150nM okadaic acid did not affect pNPP dephosphorylation under either basal or maximal activity in homogenates isolated from either SE or control animals ($p > 0.05$, n=4). This suggests that neither PP1 (IC_{50} for OA: 10-15nM) nor PP2A (IC_{50}: 100pM) is responsible for the measured activity. B) High concentration of OA results in significant inhibition of pNPP dephosphorylation. 50μM okadaic acid inhibited maximal activity in both control and SE cortical homogenates (** $p<0.01$, n=6, two-tailed paired student's t-test). Maximal activity was inhibited by 10.65% in SE homogenates, and by 6.61% in homogenate isolated from control animals. High concentration OA also inhibited basal activity by 11.17% in SE homogenates (** $p<0.01$, n=6, two-tailed paired student's t-test), but did not inhibit pNPP dephosphorylation in control homogenates ($p>0.05$, n=6, two-tailed paired student's t-test). The data suggests that SE results in an OA-sensitive increase in pNPP dephosphorylation, measured under both basal and maximal conditions for CaN activity.

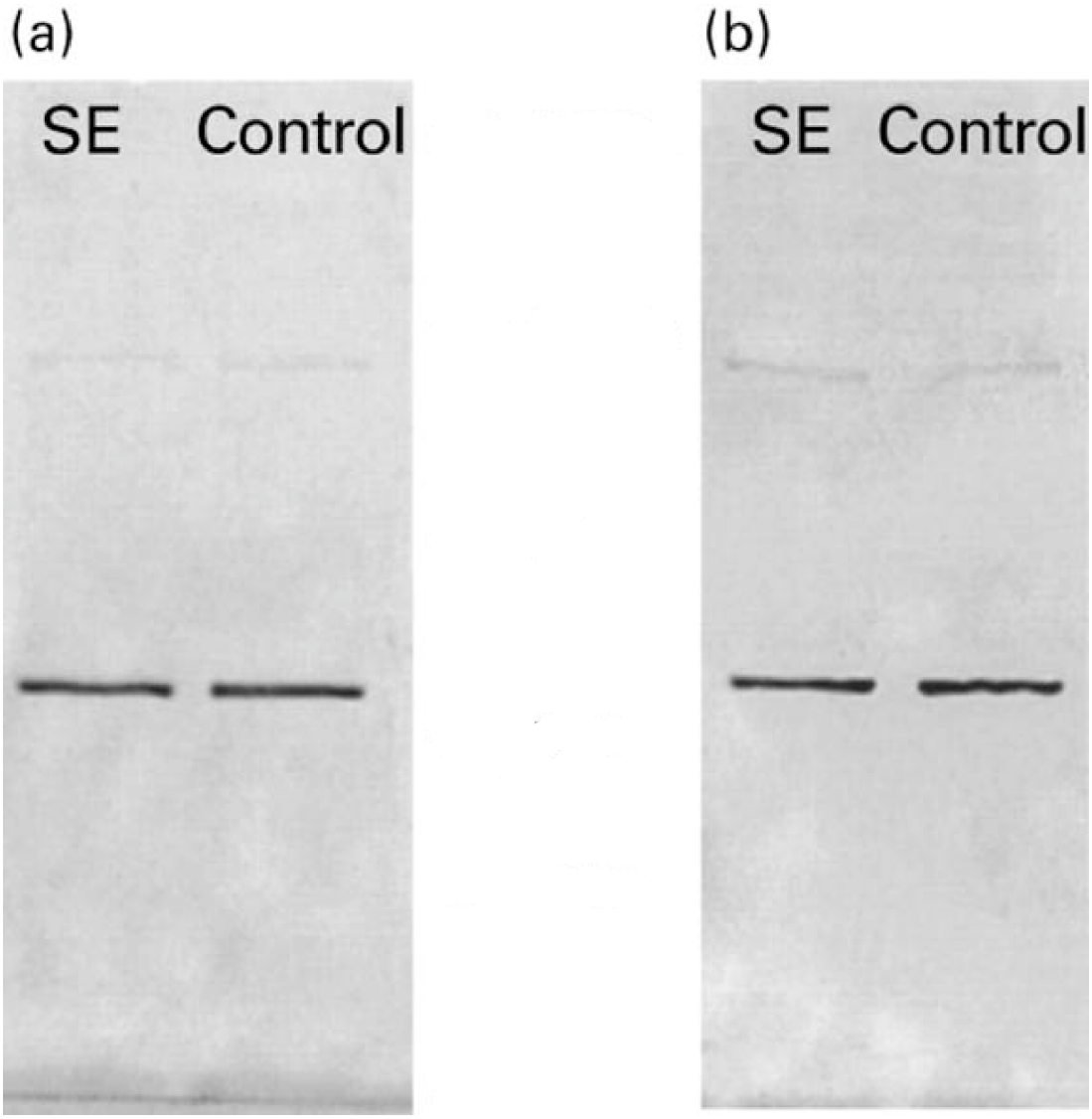

Figure 6. The post-SE increase in CaN activity was not due to a SE-induced increase in CaN protein expression.

To determine if SE results in increased CaN enzyme levels, homogenates from control and SE rats were subjected to western analysis. Cortical (A) and hippocampal (B) homogenates were resolved on SDS-PAGE and blotted to nitrocellulose (see methods). The resulting blots were reacted a monoclonal antibody against the A subunit of CaN. SE did not result in a significant alteration of CaN immunoreactivity in any brain region studied. A) Immunoreactivity was 93.62 ± 3.01% of control enzyme levels in cortical homogenates isolated from SE animals. B) CaN immunoreactivity in hippocampal homogenates isolated from SE animals was 104.17 ± 14.57% of the control enzyme level.

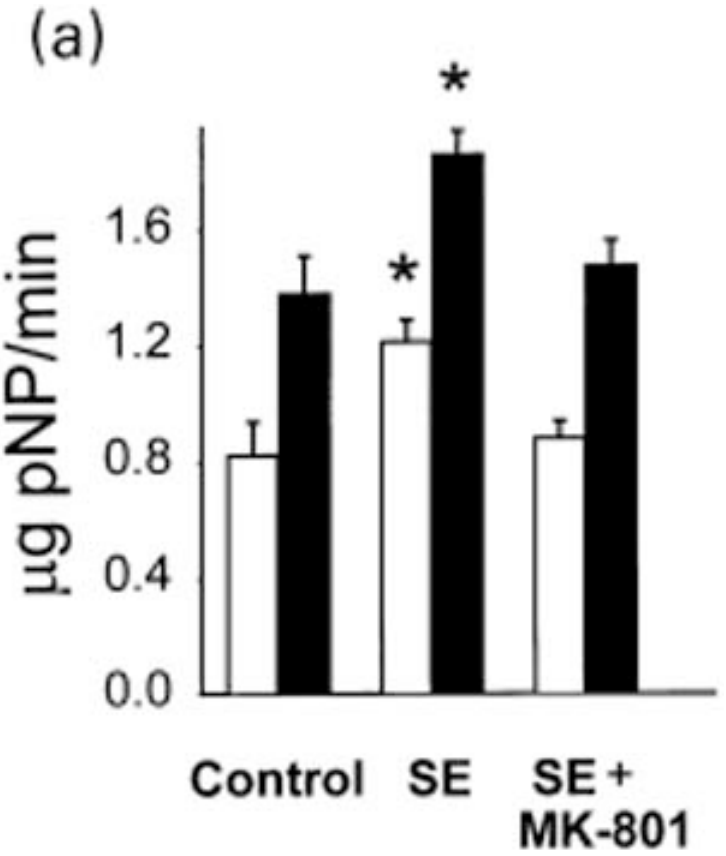

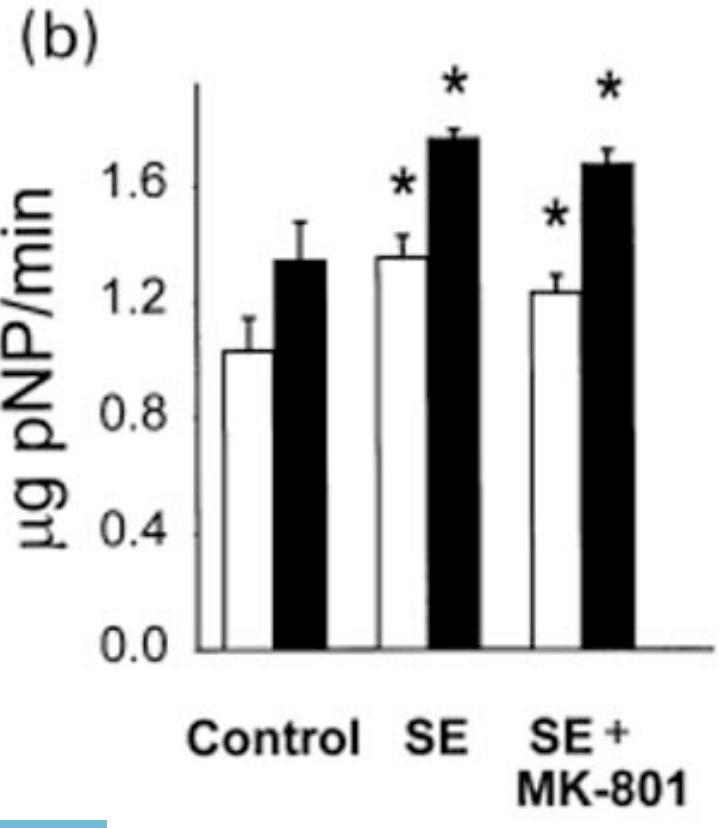

Figure 7. MK-801 pretreatment prevented the SE-dependent increase in CaN activity in cortical homogenates. A) Preinjection of animals with MK-801 (a non-competitive NMDA antagonist) completely prevented the SE-dependent increase in CaN activity in cortical homogenates. CaN activity in MK-801 cortical homogenates was not significantly different from that of control homogenates for both basal (white) and maximal (black) activities ($p > 0.05$, n=4, one-way ANOVA with Tukey post-hoc analysis). SE homogenates had significantly higher activity than both MK-801 and control homogenates under both basal and maximal conditions (*$p < 0.05$, n=4). B) MK-801 pre-treatment reduced, but did not completely prevent, the SE-dependent increase in CaN activity in hippocampal homogenates. MK-801 treated animals had significantly lower CaN activity than SE animals under both basal (white) and maximal (black) conditions ($p < 0.05$, n=4). However, both basal and maximal hippocampal CaN activity in MK-801 animals was significantly higher than that of control animals ($p < 0.05$).

CHAPTER II

STATUS EPILEPTICUS-INDUCED CHANGES IN THE SUBCELLULAR DISTRIBUTION AND ACTIVITY OF CALCINEURIN IN RAT FOREBRAIN

INTRODUCTION:

Status epilepticus (SE) is a severe medical emergency affecting more than 100,000 people per year in the United States [100, 103]. Victims of SE are at risk for both immediate mortality and long-term neurological pathologies associated with the disorder [105, 111, 124]. Previous research has shown many of these pathological consequences to be associated with calcium and calcium-regulated systems [115, 126]. Calcium's central role in the pathology of SE has made characterization of calcium-regulated systems an important area for further study in SE.

One calcium-regulated enzyme of particular interest is the calcium-stimulated phosphatase, calcineurin (CaN). CaN's enrichment in forebrain neurons and its key role in the modulation of many neuronal processes make it an intriguing enzyme for study. For example, CaN regulates gene transcription through the NFAT family of molecules [6, 162], modulates the function of both the GABA and NMDA receptors [63, 67, 68, 163, 164], affects cytoskeletal

architecture through dephosphorylation of microtubules and associated proteins [70-72], regulates neurotransmitter release [165], and may be involved in the initiation of apoptosis [91, 166]. All of these processes may play a role in the pathology of SE, warranting a closer look into any association between CaN and SE.

Several recent studies have, in fact, suggested an association between CaN and seizure activity. For instance, Kurz et al. [167] described an SE-dependent increase in CaN activity in the forebrain, while Moia et al. [122] suggested that CaN activity may be essential for the development of seizures in a kindling model. While these findings suggest the involvement of CaN in the development of seizure activity, more research is needed to elucidate the physiological role of this enzyme in SE. For example, the ability to localize SE-induced changes in enzyme activity and concentration to specific subcellular compartments would provide valuable clues to the role of CaN in the pathology of SE.

The present study examined the effects of SE on enzyme activity and the sub-cellular distribution of CaN in the cortex and hippocampus. CaN activity was assayed in sub-cellular fractions isolated from both of these regions, and CaN concentration in each fraction was determined by western analysis. Additionally, immunohistochemical studies were conducted on hippocampal tissue from SE and control animals. A significant SE-dependent increase in CaN activity was observed in synaptosomal and crude nuclear fractions. This increase was accompanied by a significant increase in CaN concentration in these fractions as

demonstrated by western analysis. In addition, immunohistochemical studies revealed an apparent increase in CaN levels in the apical dendrites of CA1 neurons in the hippocampus following SE.

METHODS AND MATERIALS:

Materials:

All materials were reagent grade and were purchased from Sigma Chemical Co. (St. Louis, MO) unless otherwise noted. Bio-Rad protein assay concentrate, sodium dodecyl sulfate (SDS), 2-mercaptoethanol, blotting grade dry milk, and Mini-Protean II SDS-PAGE apparatus and power supplies were purchased from Bio-Rad Laboratories (Richmond, CA). ABC reagents were obtained from Vector Laboratories (Burlingame, CA). Absolute ethyl alcohol was purchased from AAPER Alcohol and Chemical Co. (Shelbyville, KY). Adult male Sprague-Dawley rats were obtained from Harlan Laboratories (Indianapolis, IN).

Pilocarpine model of status epilepticus:

All animal use procedures were in strict accordance with the Guide for the Care and Use of Laboratory Animals described by the National Institutes of Health and were approved by the Virginia Commonwealth University Animal Use Committee. SE was induced in adult male Sprague-Dawley rats by the method described in Mello et al [141]. Rats were handled regularly for approximately one week to acclimate them to handling prior to drug administration. Adult rats

weighing 175-230g were injected intraperitoneally (i.p.) with 350mg/kg pilocarpine HCl, a potent muscarinic agonist. 30 minutes prior to the pilocarpine injection, all rats were treated i.p. with 1mg/kg methylscopolamine. Methylscopolamine is a peripheral muscarinic antagonist; administering it prior to pilocarpine injection minimizes adverse peripheral effects. Control rats received all injections, except that pilocarpine was administered at $1/10^{th}$ its seizure-inducing dose. Control animals did not exhibit any behavioral seizure activity. All drugs were dissolved in 0.9% saline.

Behavioral seizures typically began 20 minutes following pilocarpine injection. Seizures were rated according to the scale described by Racine [142]. Only animals reaching stage 5 seizures were included in this study. Stage 5 was classified as the most severe level of seizure activity, characterized by rearing and falling. Rats not responding to the initial pilocarpine injection received a second injection at on half of the initial dose (175 mg/kg). Rats that still did not display stage 5 seizure activity following a second pilocarpine injection were excluded from the SE group.

Isolation and homogenization of brain regions:

Rats were rapidly decapitated after 1 hour of SE. Brains were dissected on a petri dish on ice to preserve post-mortem enzyme activity. Cortical, hippocampal, and cerebellar brain regions were quickly isolated and immediately homogenized with 10 strokes (up and down) at 12,000 rpm, using a motorized homogenizer (TRI-R Instruments, Inc. Rockville Center, NY). Brain regions were

homogenized into ice-cold homogenization buffer containing 5mM HEPES (pH 7.0), 7mM EGTA, 5mM EDTA, 1mM dithiothreitol (DTT), 0.3mM PMSF, and 300mM sucrose. Cortical regions were homogenized into 7ml of buffer, hippocampal regions into 3ml of buffer, and cerebellar regions into 5ml. All brain homogenates were either separated into aliquots and stored for later use, or subjected to the differential centrifugation procedure described below.

Isolation of sub-cellular fractions:

Sub-cellular fractions were isolated by a differential centrifugation procedure as modified from Edelman et al [168]. Brain region homogenate was first centrifuged at 5000g for 10 minutes, to produce a crude nuclear pellet (P1) and a supernatant (S1). The P1 pellet was resuspended in homogenization buffer, separated into aliquots, and stored at -80°C until used. The S1 was centrifuged for 30 minutes at 18,000g to produce the crude synaptoplasmic membrane/mitochondiral pellet (P2) and a supernatant (S2). The P2 pellet was resuspended in ½ the original volume of the homogenate (3.5mL for cortex, 2.5mL for cerebellum, 1.5mL for hippocampus), then separated into aliquots and stored at -80°C until used. The S2 was subjected to another centrifugation, at 100,000g for 60 minutes. The resulting supernatant (S3) was separated into aliquots and stored for later use. The P3 pellet was resuspended in homogenization buffer (700μL for cortex, 500μL for cerebellum, 300μL for hippocampus), and likewise separated into aliquots and stored at -80°C for later use.

pNPP assay of phosphatase activity:

Calcineurin activity was assayed using the procedure detailed by Pallen and Wang [143] as modified by Kurz et al. [167]. All reaction tubes were prepared on ice and contained the following: 25mM MOPS (pH 7.0), 1mM DTT, 2mM p-nitrophenol phosphate (pNPP). Some basal tubes also contained 2mM EGTA and 2mM EDTA. Maximal tubes contained the same reagents as basal reactions, with the addition of 2mM $MnCl_2$. Where appropriate, 120μM gossypol, 50μM okadaic acid (sodium salt), or 100μM sodium orthovanadate was added to the reaction mixture. Final reaction volumes were 1ml. Both Mn^{2+} and Ca^{2+}/calmodulin activate calcineurin in this assay; however, Mn^{2+} activates calcineurin more strongly than calcium [21]. Therefore, Mn^{2+} was used instead of calcium in maximal reactions to better visualize the cation-stimulated activity of the enzyme. Prior to use, the protein concentration of all homogenates was determined using the method of Bradford et al. [144]. Reactions were initiated by the addition of 200 μg/ml of homogenate or the appropriate subcellular fraction. Reactions were incubated at 37°C for 15 minutes in a shaking water bath. Tubes were then removed from the water bath and placed in ice to stop the reaction. Absorbance of the reaction mixture was immediately measured at 405nm in a spectrophotometer (UV-2101, Shimadzu Scientific Instruments, Inc. Columbia, MD). Absorbance units were converted to nmol of pNP produced by comparison to a pNP concentration standard absorption curve.

CaN immunoblotting procedure:

Western analysis was performed essentially as described previously [145]. Briefly, homogenates were resolved on SDS-PAGE and transferred to a nitrocellulose membrane using the Geni blot system (Idea Scientific, Minneapolis, MN). Nitrocellulose was then immersed for one hour in blocking solution containing phosphate buffered saline (PBS, pH 7.4), 0.05% (v/v) polyoxyethylene sorbitan monolaurate (tween-20), 50 g/L Bio-Rad blotting grade dry milk, and horse serum (Vector Laboratories Inc., diluted 50 μl/10ml). The nitrocellulose membrane was then incubated with primary antibody in blocking solution for one hour. Anti-CaN A antibody (clone CN-A1, mouse monoclonal IgG, Sigma Chemical Co.) was diluted 1:10,000 for western analysis. Membranes were then washed three times in a wash solution containing PBS, tween-20, and dry milk. Nitrocellulose was then reacted with a secondary antibody in blocking solution for 45 minutes. The membrane was then washed three times and incubated with an avidin-biotinylated horseradish peroxidase complex for 30 minutes. Nitrocellulose was then washed three times in PBS for 10 minutes per wash. Blots were developed with a solution containing 10 ml PBS, 0.025% (v/v) H_2O_2, and 8 mg 4-chloro-1-napthol dissolved in 2ml of methanol. Specific immunoreactive bands were quantified by computer-assisted densitometry (Inquiry, Loats Associates, Westminster, MD).

Immunohistochemical analysis:

SE was induced in male Sprague-Dawley rats as described above. After one hour of SE, rats were anesthetized with halothane and transcardially perfused with a solution containing 4% paraformaldehyde and 0.1% glutaraldehyde. Brains were then removed and allowed to post-fix in the perfusion fixative for 24hr. Brains were then blocked to allow sectioning of the dorsal hippocampus, embedded in agar and coronally sectioned into serial 40 μm sections on a Leica VT1000S vibratome (Leica Microsystems, Bannockburn, IL). Sections were stored in 12 well culture plates until used.

For immunohistochemical staining, sections were incubated for 30 minutes in normal serum at 37°C. Sections were then incubated overnight with a polyclonal anti-CaN A antibody at a dilution of 1:50,000. Following incubation with the primary antibody, sections were then washed 4X with phosphate-buffered saline (PBS, pH 7.4) for 15 minutes per wash. The tissue was then incubated in secondary antibody for 1 hour at 37°C. Sections were washed 3X in PBS, then placed in Vectastain ABC reagent for 2 hours. The first hour of incubation in ABC was performed at 37°C, the second hour at room temperature. Sections were then washed 2X in PBS for 10 minutes per wash, and 1X in Tris-Base (pH 7.6) It was essential to wash in Tris-Base at this step because the staining procedure requires most of the phosphate to be washed out of the tissue to work properly. The tissue was then stained with a glucose oxidase-DAB-nickel preparation.

Statistical analysis:

All statistical analysis of data was performed using GraphPad Prism 3.0 (GraphPad Software, San Diego, CA). Levels of phosphatase activity or concentration were compared to control using the Student's t-test (two-tailed distribution, unpaired or paired where appropriate), or using one-way ANOVA with Tukey post-test to control for type one errors in multiple comparisons. Computer assisted densitometric analysis was performed using Inquiry (Loats Associates Inc, Westminster, MD).

RESULTS:

CaN-mediated dephosphorylation of pNPP:

Fractions were isolated from the cortex and hippocampus of control and SE animals. In both the hippocampal and cortical homogenates, overall post-SE CaN activity was significantly increased. In hippocampal homogenates, SE resulted in a 21.2 ± 4.7% increase in basal CaN activity, and a 20.8 ± 5.0% increase in maximal activity when compared to control animals. Similarly, in cortical homogenates isolated from SE animals, basal CaN activity was 49.3 ± 13.6% of control, and maximal activity was elevated 34.3 ± 13.9% above control values. This overall increase in CaN activity in the homogenate is consistent with the findings of previous studies [167] and establishes a baseline to which the activities of individual fractions may be compared.

The effects of several inhibitors were tested to confirm that the observed increase in pNPP dephosphorylation was due to an increase in CaN activity and not due to contamination from other phosphatases (Figure 8). The results obtained are consistent with a previous characterization of the pNPP assay [167]. The addition of okadaic acid (a potent inhibitor of PP1 and PP2A) did not effect either basal or maximal pNPP dephosphorylation, suggesting PP1 and PP2A are not responsible for the observed increase in activity. The effects of sodium orthovanadate (NaVO4) on pNPP dephosphorylation were also tested. NaVO4 is a potent inhibitor of tyrosine phosphatases; however, it also inhibits the Mn^{2+} stimulated activity of CaN. In this study, sodium orthovanadate did not affect the SE-induced increase in basal activity; however, under maximal reaction conditions, NaVO4 blocked pNPP dephosphorylation down to basal levels in homogenates isolated from both control and SE animals. These results are consistent with CaN activity, and suggest that tyrosine phosphatases are not involved in the SE-dependent increase in enzyme activity. Finally, gossypol (120 μM), a specific CaN inhibitor [169], was tested. Co-incubation with gossypol blocked the SE-induced increase in both basal and maximal CaN activity ($p<0.05$, $n=3$), suggesting CaN is responsible for the increase. The data demonstrate that the SE-induced increase in pNPP dephosphorylation is due to CaN and not due to another phosphatase.

Selective modulation of CaN by SE in specific subcellular fractions:

An SE-dependent increase in CaN activity was observed in the P1 pellet from both cortical and hippocampal tissue. The P1, or crude nuclear pellet, contains nuclei and other large molecular weight fractions. In hippocampal P1 isolated from control animals, basal CaN activity was 3.8 ± 0.01 μg pNP/min/mg. Following SE, this value increased by 13.1 ± 4.7%, to 4.3 ± 0.2 μg pNP/min/mg ($p < 0.05$, n=3). Under maximal conditions, CaN activity in control hippocampal P1 was 6.1 ± 0.1 μg pNP/min/mg. SE induced a 10.6 ± 2.9% increase in the maximal CaN activity, to a value of 6.8 ± 0.2 μg pNP/min/mg ($p < 0.05$, n=3).

SE also induced a significant increase in basal and maximal enzyme activity in cortical P1 fractions (Figure 9). Under basal reaction conditions, CaN activity in control P1 was 3.1 ± 0.9 μg pNP/min/mg. Following SE, basal activity increased 29.4 ± 11.9 % to 4.1 ± 0.6 μg pNP/min/mg ($p < 0.05$, n = 9). Maximal activity in cortical P1 isolated from control animals was 6.2 ± 0.1 μg pNP/min/mg. Following SE, maximal CaN activity increased by 14.88 ± 3.3 % to a value of 7.1 ± 0.2 μg pNP/min/mg ($p < 0.001$, n = 9). The increase in activity in both the hippocampus and cortical P1 was similar to that observed in homogenate.

In crude synaptoplasmic membrane (P2) fractions isolated from forebrain homogenates, SE resulted in a significant increase in both basal and maximal CaN activity (Figure 9). Average basal CaN activity measured in control hippocampal P2 was 2.7 ± 0.7 μg pNP/min/mg. Following SE, this value was elevated to 4.8 ± 0.3 μg pNP/min/mg, an increase of 77.8 ± 25.9% ($p < 0.05$, n=3, Student's t-test). Control maximal activity in hippocampal P2 was 7.0 ± 0.8 μg

pNP/min/mg. After SE, activity increased 56.4 ± 16.3% over control, to a value of 10.9 ± 0.8 μg pNP/min/mg ($p < 0.05$, n=3). This increase is more than double the overall increase observed in hippocampal homogenate.

In cortical P2, a large, SE-dependent increase in CaN activity was observed under both basal and maximal reaction conditions (Figure 9). Average basal CaN activity in control samples was 2.7 ± 0.4 μg pNP produced/ min/ mg of protein. Following SE, this value increased to 5.6 ± 0.7 μg pNP/min/mg, an increase of 107.4 ± 29.6% ($p < 0.01$, n=6). Maximal activity in cortical P2 isolated from control animals was 7.4 ± 0.6 μg pNP/min/mg. In SE animals, this value was increased by 54.0 ± 10.7%, to a value of 11.4 ± 0.6 μg pNP/min/mg ($p < 0.01$, n=6). This increase was also more than twice the overall increase observed in cortical homogenates in this study.

Unlike the other membrane-rich fractions, cortical P3 did not display any significant, SE-dependent change in CaN activity (Figure 9). In cortical P3 isolated from control animals, basal activity was 1.8 ± 0.2 μg PNP/min/mg. After SE, activity in the P3 decreased to 1.7 ± 0.1 μg PNP/min/mg, an increase of 5.5 ± 4.1% which was not statistically significant ($p > 0.05$, n=3). Maximal activity in control cortical P3 was 3.4 ± 0.1 μg PNP/min/mg, while in SE P3 this value was 3.1 ± 0.1 μg PNP/min/mg. This difference was also not statistically significant ($p > 0.05$, n=3). It was not possible to test hippocampal P3 due to the extremely low protein yield present in this fraction. The lack of an SE-dependent increase in activity in this fraction indicated that the post-SE increase in activity observed in

the P1 and P2 fractions was not due to a nonselective precipitation of CaN during SE.

No significant SE-induced change in CaN activity was observed in the cytosolic (S3) fraction isolated from either hippocampus or cortex. However, it is interesting to note that under both basal and maximal conditions, CaN activity appeared to decrease slightly (Figure 9). This is particularly interesting considering that overall CaN activity increased by 35-50% in the cortical homogenate. In S3 isolated from control hippocampi, basal CaN activity was 1.3 ± 0.1 μg PNP/min/mg. Following SE, this value decreased by 10.8 ± 18.5% to 1.1 ± 0.2 μg PNP/min/mg ($p > 0.05$, n=4). Under maximal reaction conditions, CaN activity in S3 isolated from control animals was 4.4 ± 0.4 μg PNP/min/mg. In S3 from SE animals, CaN activity was 3.8 ± 0.1 μg PNP/min/mg, a decrease of 13.6 ± 13.4% from control ($p > 0.05$, n=4). Similarly, in cortical S3, control CaN activity was 2.3 ± 0.2 μg PNP/min/mg under basal conditions. Following SE, this value decreased by 8.6 ± 8.8% to a value of 2.1 ± 0.1 μg PNP/min/mg ($p > 0.05$, n=8). Under maximal conditions, control CaN activity was 9.1 ± 0.3 μg PNP/min/mg in the cytosol. In cytosolic fractions isolated from SE animals, this value decreased 14.4 ± 9.8% to 7.8 ± 0.9 μg PNP/min/mg ($p > 0.05$, n=8).

SE resulted in increased synaptoplasmic CaN in both the hippocampus and cortex.

The increase in activity observed in the P2 fraction in both the hippocampus and cortex was far larger than that observed in any other fraction

or the homogenate. This increase in activity could be accounted for by an increase in the amount of enzyme present in this fraction, either through new synthesis of CaN or by translocation from other areas of the cell. To examine this hypothesis, western analysis of homogenate from all fractions and brain regions was performed, using an antibody directed against the catalytic A-subunit of the enzyme (CN-1, Sigma, St. Louis, MO). In all fractions, a band with molecular weight of approximately 61kDa was resolved. This corresponds with the size of the CaN A subunit [8]. In P2 isolated from cortical homogenates, two other bands were sometimes observed. Both of these bands were determined to be due to non-specific binding of the secondary antibody (anti-mouse IgG), as they were also observed when the primary antibody was omitted from the reactions.

In the P2 fraction, a large increase in CaN A immunoreactivity was observed in both the hippocampus and cortex (Figure 10). Optical density of the 61kDa band in fractions from SE animals was 194.9 ± 31.04% of control in the hippocampus ($p < 0.05$, n=5), and 207.2 ± 22.3% of control in the cortex ($p < 0.001$, n=6). No significant difference in immunoreactivity was detected in any other sub-cellular fraction.

SE results in increased CaN A immunoreactivity in apical dendrites of hippocampal CA1 neurons.

To further characterize the SE-dependent increase in CaN activity and concentration observed in the P2 fraction, immunohistochemical studies were performed on paraformaldehyde-fixed coronal sections from SE and control

animals. Hippocampal sections from control animals demonstrated diffuse staining throughout the pyramidal cell layer, with the exception of the pyramidal cell nuclei (Fig. 11A, C). Faint CaN immunoreactivity was observed in the surrounding cortex (data not shown). This diffuse staining remained unchanged following SE. Therefore, the intensity of cortical staining was used as a background value to compare control and SE images. When viewed under 400X magnification, individual pyramidal neurons could be visualized (Fig. 11E). The cytoplasm of these cells demonstrated very diffuse CaN-reactive staining. The darkest staining was seen around the plasma membrane of these neurons. Occasional dendritic processes demonstrated CaN immunoreactivity; however, many apical dendrites could not be individually visualized in control sections. These histological findings were in agreement with previous studies demonstrating the presence of CaN in the hippocampal formation, particularly in the plasma membrane and in neurites [170, 171].

Hippocampal sections from SE animals demonstrated several qualitative changes when compared to control sections (Fig. 11B). Similar to the control sections, diffuse CaN-reactive staining was present throughout CA1-3. However, this staining was noticeably more intense in the SE sections. Staining was still relatively poor in the surrounding cortex in the SE sections. In addition to the increased level of staining in the pyramidal neurons, an intensely stained band could be seen near the pyramidal cell layer of the hippocampus in SE sections. At 400X magnification this intense staining was found to be present around the plasma membranes and throughout the apical dendrites of pyramidal neurons

(Fig. 11F). Unlike the control sections, CaN immunoreactivity was absent from the nuclei of pyramidal neurons from SE animals as well as those from control animals. It was not possible to visualize any axonal processes leading from the pyramidal cells, nor were any darkly stained processes observed in axonal layers of the hippocampus, suggesting that the increased CaN immunoreactivity was post- rather than presynaptic. Finally, no interneurons were detected in control or SE sections, suggesting an absence of CaN in these neurons which is in agreement with previous research [172].

DISCUSSION:

Recent research suggests a physiological role for CaN in the pathology of seizure disorders [122, 167]. However, much remains to be discovered about the effects of SE on CaN and the physiological ramifications of these effects. Since CaN regulates many neuronal processes [67, 70, 164-166], understanding how SE effects the activity of specific subcellular pools of CaN is warranted. The present study demonstrated a significant, SE-dependent increase in CaN activity in the synaptosomal (P2) and nuclear (P1) fractions isolated from rat cortex and hippocampus. Additionally, a significant, SE-dependent increase in CaN concentration was observed in P2 fractions isolated from hippocampal and cortical tissue. No significant increase in CaN activity or concentration was observed in the cortical P3 fraction, confirming that the observed increase was not due to nonspecific precipitation of CaN protein during SE. Can activity in the hippocampal P3 was not assessed due to low protein yield in this fraction.

Immunohistochemical staining of hippocampal tissue revealed increased CaN staining in apical dendrites of the CA1 region. These data suggest that SE induces a translocation of CaN into specific subcellular compartments, where it may play an important role in the pathophysiology of SE.

A significant increase in CaN activity was observed in the nuclear (P1) pellet fraction. While this is a relatively crude fraction, the observed increase in activity may represent translocation of enzyme into the nucleus or cell membrane. There are precedents for nuclear translocation of calcineurin. For example, CaN is capable of dephosphorylating the NFAT family of molecules. Although originally described in the immune system [6], several members of the NFAT family have been identified in neuronal tissue [173, 174]. Following dephosphorylation by CaN, both the enzyme and NFAT move to the nucleus of the cell, where the NFAT molecule regulates gene transcription. Previous studies have shown alteration of gene transcription to be an important pathological mechanism in SE and epileptogenesis [175-177]. CaN-regulated mechanisms, similar to the NFAT mechanism described above, may play an important role in this modulation of gene expression.

A large, significant increase in both CaN activity and enzyme concentration was observed in the P2 fraction. The P2 fraction is highly enriched in both crude synaptoplasmic membrane and mitochondria [168]. Previous studies have not detected significant amounts of CaN in purified mitochondrial preparations [171]; however, it is possible that SE induces a translocation of enzyme to these organelles. CaN plays an essential role in several apoptotic

pathways [91, 166]. Movement of the enzyme to the mitochondria would likely facilitate these apoptotic mechanisms, resulting in increased cell death.

An alternative hypothesis on the apparent increase in enzyme concentration observed in both western and immunohistochemical studies is that prolonged SE modulates the immunoreactivity of CaN. Pathological changes in protein immunoreactivity have been observed before [146]. The changes in enzyme immunoreactivity would have to be a primary structural change, since it is observed in both western and immunohistochemical analyses. The altered immunoreactivity would also explain why a significant increase in CaN concentration is observed in the P1 and P2 fractions without a significant loss of enzyme in the other subcellular fractions studied.

On the other hand, the increase in CaN concentration in the P2 fraction may represent a true increase of enzyme at the synaptoplasmic membrane. Immunohistochemical data demonstrated a significant increase in CaN staining in the pyramidal cell layers, particularly the CA1 region, of hippocampus isolated from SE animals. The observation that the increased staining is confined to hippocampal pyramidal neurons suggests that SE may induce a unique mechanism in these cells that is not present in other hippocampal neurons. The histochemical data also suggest that the increase in CaN concentration is occurring primarily post-synaptically, in the dendrites of affected cells. This increase in enzyme concentration places approximately double the control amount of enzyme in the post-synaptic region of neurons, where it may modulate neurotransmitter receptors.

The $GABA_A$ receptor is a particularly important CaN-regulated system in the study of SE. GABA receptors are the primary receptor responsible for the fast inhibitory response in neuronal tissue [65], and play a major role in preventing the neuronal hyperexcitability associated with epilepsy and SE [124]. Several recent studies have demonstrated an inhibitory modulation of $GABA_A$ receptor function by CaN [66-68, 159, 160]. This modulation of $GABA_A$ receptor function may occur through direct dephosphorylation of receptor subunits. $GABA_A$ receptors have a critical phosphorylation level required for optimal function. A post-SE elevation in CaN concentration in the dendrites could result in highly increased dephosphorylation of $GABA_A$ receptors, producing a net disinhibition of cellular excitability. An increase in CaN activity during and immediately after SE, such as the one described in this study, could lead to short-term loss of $GABA_A$ receptor function. This acute loss of inhibitory tone could lead to increased seizure propagation, failure of seizure termination, or resistance to antiepileptic drug treatment.

Additionally, high levels of CaN in the synaptic region of neurons may have several other pathological effects. CaN indirectly modulates the activities of the serine/ threonine phosphatases PP1 and PP2A through dephosphorylation of their respective inhibitors [178-180]. Thus, an increase in CaN activity could result in an accompanying increase in the activity of PP1 and 2A in neurons, with numerous downstream effects. CaN also is capable of dephosphorylating microtubules [70, 181], altering dendritic stability [79] and affecting the outgrowth of developing neurites [78].

The observed SE-dependent change in CaN concentration and activity could result from either increased synthesis of CaN or translocation of the enzyme from other cellular compartments. Several previous studies have observed that there is no significant, post-SE increase in the concentration of CaN in whole cell homogenate [167, 182], nor has any post-seizure increase in CaN mRNA been detected [182]. The lack of a SE-dependent net increase in CaN protein concentration or mRNA expression strongly suggests that SE does not induce synthesis of the enzyme. Indeed, it seems unlikely that animals undergoing the high physiological stress of SE, and studied at an acute post-SE time point, would have the necessary time and capacity to synthesize the amount of CaN represented by the increase.

Translocation of the enzyme may account for the increased levels of CaN detected in the P2 fraction. Movement of CaN to the synaptosomal fraction from other cellular compartments would suggest that a concurrent decrease in CaN concentration should be detected in other sub-cellular fractions. However, no significant decrease in CaN concentration was detected in any of the fractions isolated in this study, although the slight decrease in CaN activity observed in the cortical cytosol may suggest some loss of enzyme. This discrepancy may be due to the relatively small volume of the P2 fraction when compared to the cytosol; the effect of the translocation to the synaptosomes may simply be diluted by the large volume of the cytosolic compartment.

This study is the first to demonstrate a post-SE increase in CaN concentration and activity in specific subcellular compartments. The increase in

CaN activity in the nuclear-enriched P1 fraction suggests that CaN may alter gene expression. Alterations in gene expression may be responsible for many of the long-term effects of SE, such as the post-SE development of spontaneous seizure activity (epileptogenesis). On the other hand, the large increase in CaN activity and concentration in the synaptosomal P2 fraction suggests a CaN-modulated alteration in neurotransmitter receptor function. This mechanism could be responsible for many of the acute effects of SE, as well as playing a role in the resistance to anti-epileptic drugs seen in some instances of SE. Further research into these topics may help to clarify the pathological mechanisms of SE, and may help to develop more effective anti-epileptic drugs, ultimately leading to more effective treatment of this life-threatening and debilitating condition.

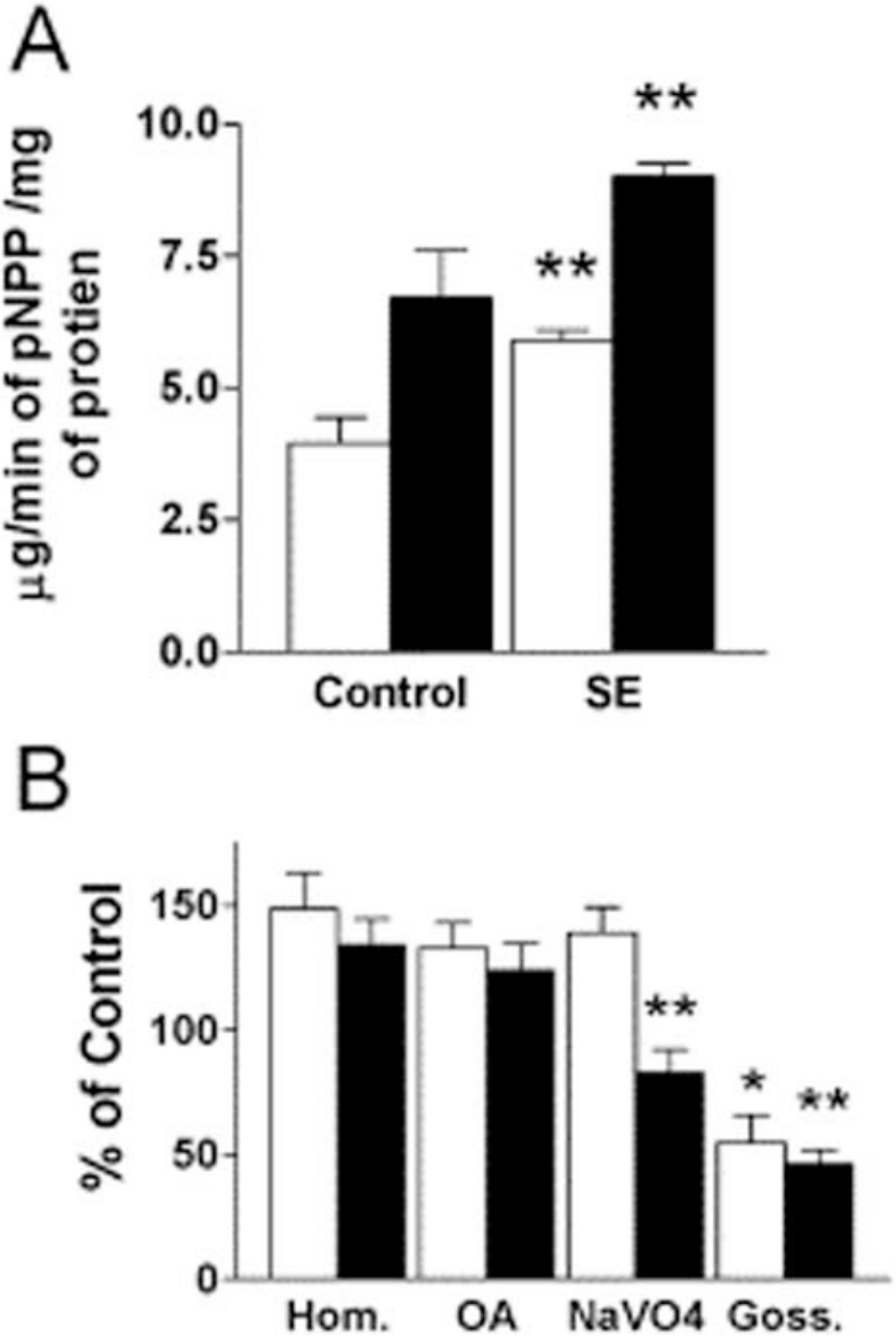

Figure 8. Prolonged SE resulted in increased CaN activity in cortical homogenates.

SE induced a significant increase in both basal and maximal pNPP dephosphorylation. (A) Basal (white) and maximal (black) CaN activity was determined in cortical homogenates isolated from both control and SE animals. SE resulted in an approximately 50% increase in basal activity and a 34% increase in maximal pNPP deposphorylation when compared to homogenate protein isolated from control animals. (B) The prolonged SE-induced increase in pNPP dephosphorylation was due to CaN activity. Basal (white) and maximal CaN reactions were performed in the presence of okadaic acid (OA; 50 μM), sodium orthovanadate (NaVO4; 100 μM) and the CaN-selective inhibitor, gossypol (Goss.; 120 μM). OA did not affect either basal or maximal pNPP dephosphorylation, suggesting that PP1 and PP2A did not significantly contribute to the observed dephosphorylation of pNPP. As expected, the tyrosine and activated CaN inhibitor NaVO4 blocked maximal pNPP dephosphorylation. However, NaVO4 did not affect the SE-induced increase in basal dephosphorylation of pNPP. In addition, the CaN-selective inhibitor, gossypol, blocked both basal and maximal increased pNPP dephosphorylation. $^{*}P < 0.05$ different from no drug homogenate; $^{**}P < 0.01$ different from no drug homogenate; $^{***}P < 0.001$, paired Student's *t* test, $n = 3$ each group.

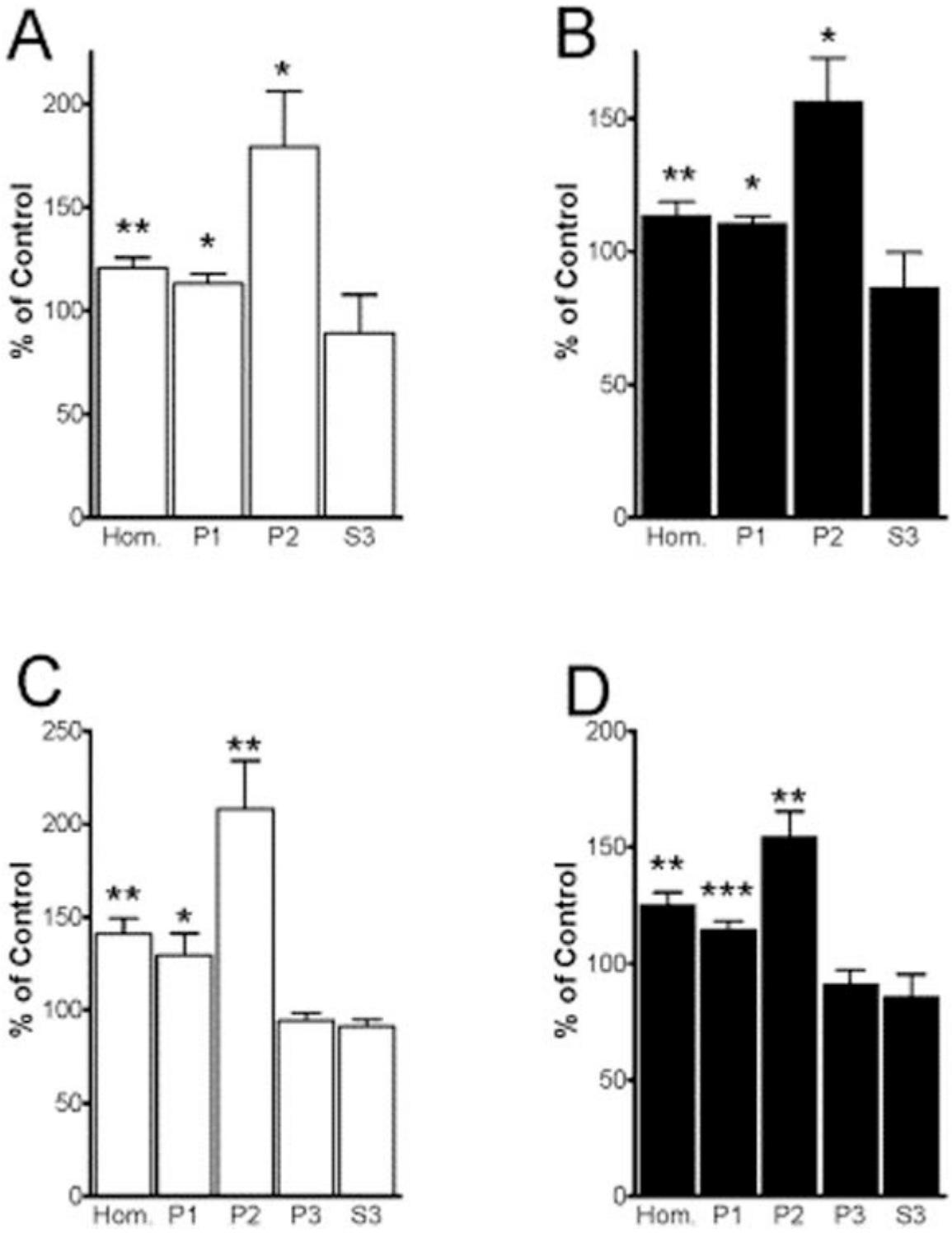

Figure 9. The SE-induced increase in CaN activity was observed in specific subcellular fractions.

SE-induced a significant increase in hippocampal CaN activity. Basal (A) and maximal (B) CaN activity was determined in specific subcellular fractions isolated from hippocampal homogenates. Significant increases in CaN activity were observed in the nuclear-enriched P1 fraction, as well as the mitochondrial and SPM-enriched P2 fractions. No significant change in CaN activity was observed in the cytosolic fraction (S3). Additionally, no change was observed in the endoplasmic reticulum-enriched P3 fraction isolated from cortical tissue. The lack of increase in the P3 fraction suggests that the increased CaN activity in the nuclear and SPM fractions was not due to nonspecific precipitation of the enzyme subunits. CaN activity was not assessed in hippocampal P3 due to low protein yield in this fraction. SE also resulted in increased CaN activity in specific subcellular fractions isolated from cortical homogenates. Basal (C) and maximal (D) CaN activity was determined in specific subcellular fractions isolated from cortical homogenate. SE resulted in a significant increase in nuclear and synaptoplasmic membrane fractions but not in endoplasmic reticulum or cytosolic fractions when compared to control fractions. No changes were observed in any fraction isolated from the cerebellum (data not shown). *$P < 0.05$ different from control, Student's *t* t test. **$P < 0.01$ different from control, Student's *t* test. See text for specific *n* values.

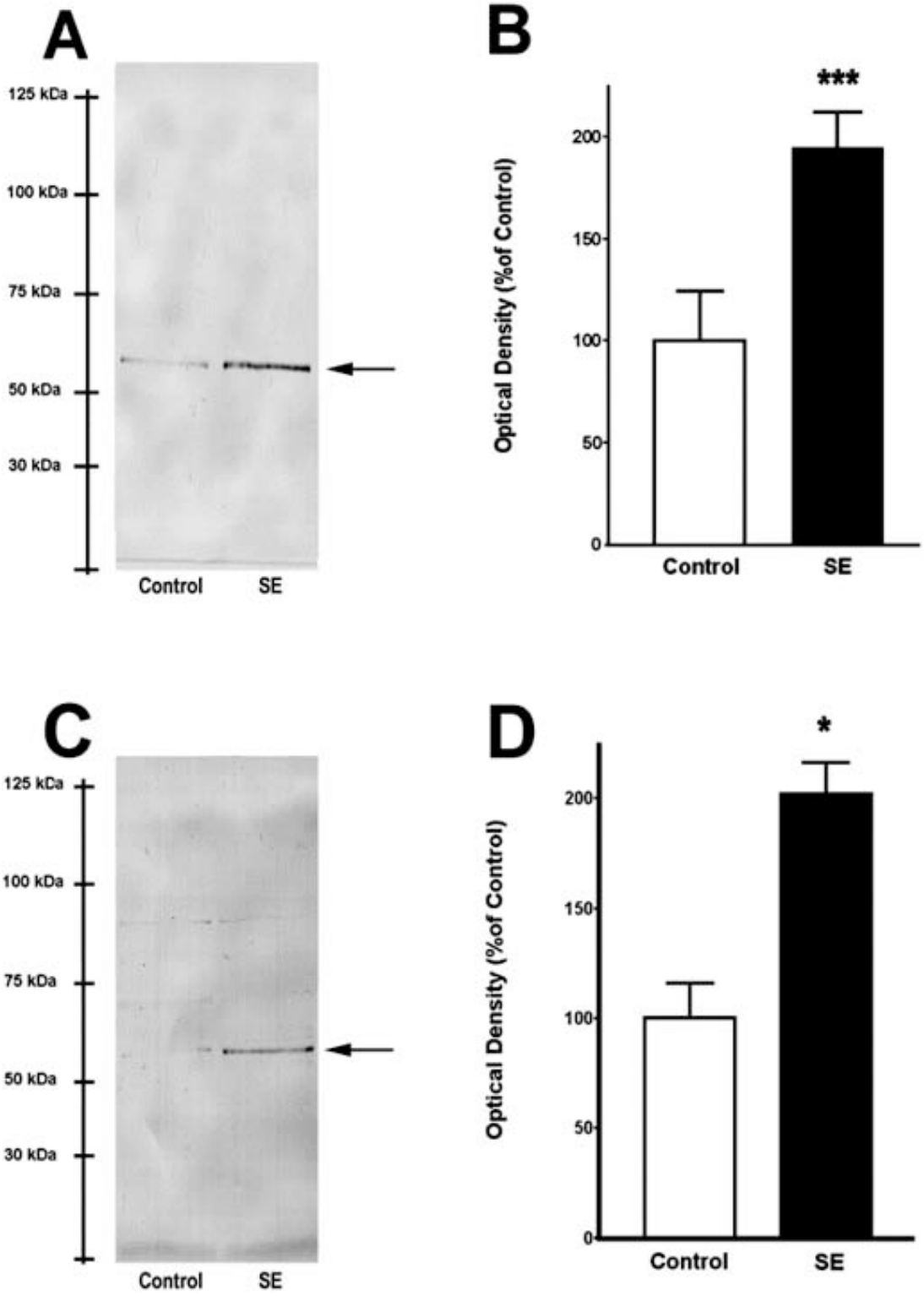

Figure 10. SE resulted in a significant increase in CaN protein levels in the SPM-enriched P2 fraction. (A) SPM-enriched hippocampal protein isolated from control (C) and SE (SE) rats was subjected to Western analysis and tested with a specific antibody directed against the A subunit of CaN. There was a selective increase in immunoreactivity toward CaN observed in the SPM-enriched fraction. (B) SE resulted in an almost 2-fold increase in CaN immunoreactivity in the SPM-enriched P2 subfraction. Immunoreactivity was quantified by computer-assisted densitometry (see Materials and methods). SE resulted in a significant, 95% increase in CaN immunoreactivity. *$P < 0.05$, $n = 5$, Student's t test. (C) SPM-enriched cortical protein isolated from control (C) and SE (SE) rats was subjected to Western analysis and tested with a specific antibody directed against the A subunit of CaN. There was a selective increase in immunoreactivity toward CaN observed in the SPM-enriched fraction. (D) SE resulted in a significant, 107% increase in CaN immunoreactivity ($n = 6$) in the SPM-enriched P2 subfraction. *$P < 0.05$, Student's t test. ***$P < 0.001$, Student's t test.

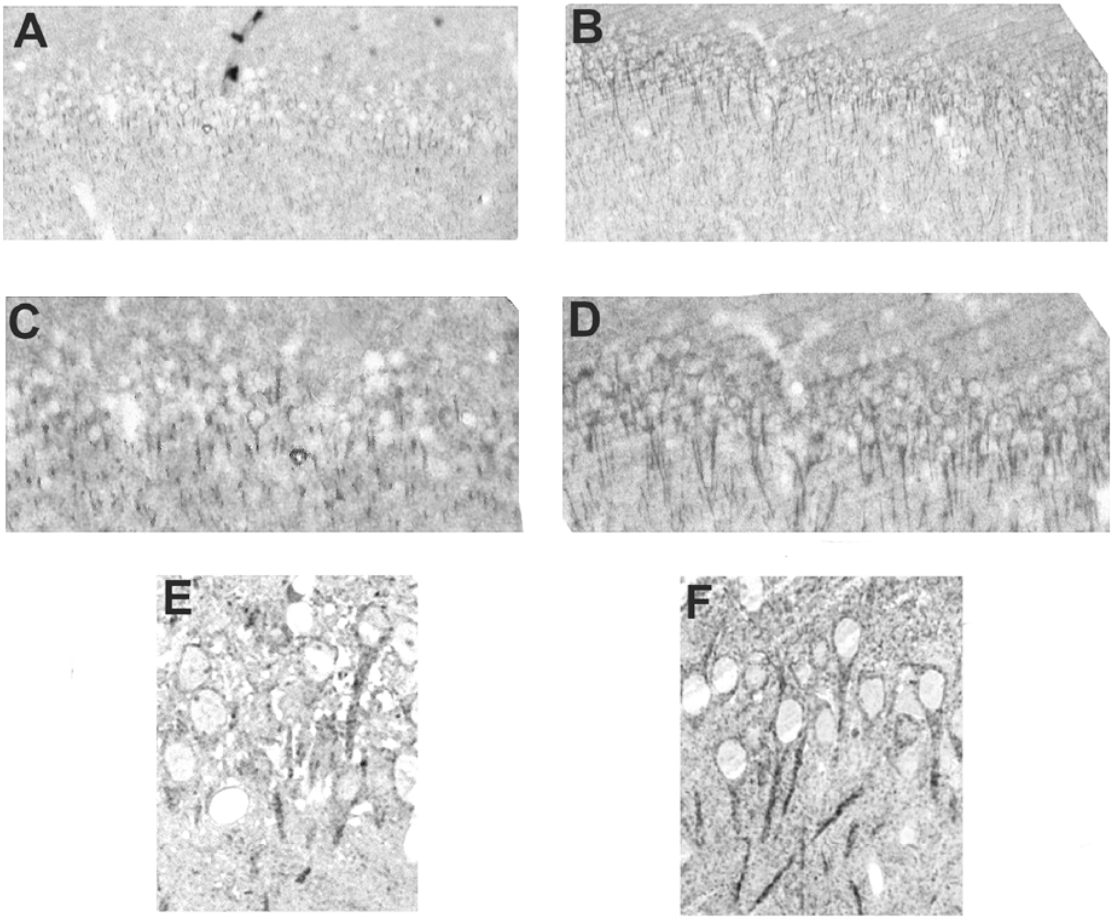

Figure 11. SE resulted in increased immunoreactivity of CaN in the dendritic processes of hippocampal CA1 neurons. Animals were subjected to prolonged SE or sham protocols, perfused, and studied for CaN immunoreactivity (see Materials and methods). (A) low magnification (40× original magnification) of dorsal hippocampus from control animal. Hippocampi from control animals displayed a nondescript, evenly distributed CaN immunoreactivity. (B) Low magnification of dorsal hippocampi isolated from an animal subjected to prolonged SE. Overall, an increase in immunoreactivity is observed in the hippocampal pyramidal region (both A and B are balanced for CaN immunoreactivity observed in nearby entorhinal cortex). (C) 100x original magnifaction and (E) 400x magnification, of CA1 pyramidal neurons in A. The CaN immunoreactivity appeared evenly distributed with the only substantial staining being cytosolic. (D) and (F) Higher magnification of CA1 pyramidal neurons isolated from animals subjected to prolonged SE displayed increased immunoreactivity, especially in the apical dendritic areas. Together with the data in Fig 2.3 the data suggest that SE induced a translocation of CaN into postsynaptic processes in CA1 pyramidal neurons.

CHAPTER III

A SIGNIFICANT INCREASE IN BOTH BASAL AND MAXIMAL CALCINEURIN ACTIVITY FOLLOWING FLUID PERCUSSION INJURY IN THE RAT

INTRODUCTION:

Traumatic brain injury is one of the major causes of death and disability in the United States today [183]. The initial traumatic insult to neuronal tissue can lead to significant pathology; however, much of the pathology associated with TBI also involves secondary damage to the tissue surrounding the primary injury site [183, 184]. Multiple cellular signals and mechanisms trigger significant physiological changes in neuronal tissue in the hours and days after TBI. These events occur in tissue not directly damaged by the primary insult, and result in such diverse effects as the formation of reactive astrocytes, alterations in neuronal excitability and receptor function, and induction of apoptosis [184]. It is this secondary phase of TBI that offers the most promise for treatment in the clinical setting; presumably a window exists following the initial injury during which much of this secondary damage could be prevented by pharmacological agents. Prevention of this later and more widespread stage of injury would drastically reduce the long-term consequences of severe TBI. Unfortunately,

clinical and laboratory testing of many neuroprotective agents up to this point has proven disappointing [90]. Clearly, more research into the cellular mechanisms occurring following TBI is needed to further our understanding of secondary neuronal damage and death.

Calcium and calcium-regulated systems play a central role in the spread of neuronal damage after TBI [132]. Therefore, calcium-modulated systems are an intriguing area for study when attempting to understand the cellular changes taking place after brain injury. One calcium-modulated enzyme that may prove important in studies of neuronal injury is the neuronally-enriched phosphatase, calcineurin.

Calcineurin is a calcium/calmodulin-stimulated serine/ threonine phosphatase that is highly enriched in neuronal tissue [137]. As the only identified calcium-regulated phosphatase, calcineurin has an important physiological role. CaN regulates neuronal excitability through modulation of both the GABA and NMDA receptors [64, 67, 68], plays a key role in the development of learning and memory [138], and is an important modulator of neuronal apoptosis [140, 185]. CaN also regulates the synthesis of nitric oxide, a free radical potentially important in TBI [186], and an isoform of CaN may modulate the formation of reactive astrocytes [187, 188]. In spite of the relevance of CaN to many of the pathological consequences of TBI, little research has been done detailing the effects of brain injury on calcineurin activity.

The present study investigates the effect of moderate central fluid percussion injury on CaN activity in rat brain homogenate from the cortex,

hippocampus and cerebellum. Both basal and maximal (cation-stimulated) CaN activity were assayed in all three brain regions. A TBI-dependent increase in CaN activity was observed in both the cortex and hippocampus, and this increase in CaN activity was found to persist two to three weeks post-injury.

MATERIALS:

All materials were reagent grade and were purchased from Sigma Chemical Co. (St. Louis, MO) unless otherwise noted. Bio-Rad protein assay concentrate, sodium dodecyl sulfate (SDS), 2-mercaptoethanol, blotting grade dry milk, and Mini-Protean II SDS-PAGE apparatus and power supplies were purchased from Bio-Rad Laboratories (Richmond, CA). ABC reagents were obtained from Vector Laboratories (Burlingame, CA). Adult male Sprague-Dawley rats were obtained from Harlan Laboratories (Indianapolis, IN).

METHODS:

Surgical preparation and fluid percussion injury:

All animal use procedures were in strict accordance with the Guide for the Care and Use of Laboratory Animals described by the National Institutes of Health and were approved by the Virginia Commonwealth University Animal Use Committee. Adult male Sprague-Dawley rats weighing between 300 and 350g were surgically prepared under sodium pentobarbital anesthesia (54 mg/kg intraperitoneally). Animals were placed in a stereotactic frame and the scalp

sagitally incised. A 4.8 mm hole was then trephined into the skull over the sagittal suture midway between bregma and lambda. A nickel-plated screw was placed 1mm rostral to bregma, and a second screw was inserted 1mm caudal to lambda. A modified female Luer-Loc syringe hub (2.6 mm inside diameter) was placed over the exposed dura and bonded in place with a cyanoacrylate adhesive. Dental acrylic was then poured around the syringe hub and screws. The scalp was then sutured, bacitracin was applied to the wound, and the animal was returned to its home cage.

Twenty-four hours following the surgical procedure, the rats were again anesthetized (4% isoflurane in a carrier gas mixture of 70% N_2O and 30% O_2). Rats in the sham-injury (control) group were anesthetized and connected to the injury device, but the pendulum was not released. Rats in the injured group were anesthetized and subjected to a moderate (2.1 ± 0.1 atm) level of fluid percussion injury. The Luer-Loc fitting, screws, and dental cement were then removed from the skull. Following recovery, rats were returned to their home cages and allowed to survive for 24 hours, one week, two weeks, three weeks or four weeks prior to being sacrificed.

Fluid percussion injury device:

The fluid percussion injury device used in these experiments is identical to that described by Dixon et al. [189]. Briefly, the device consisted of a Plexiglas cylinder reservoir 60cm long and 4.5cm in diameter. At one end of the cylinder was a rubber-covered Plexiglas piston mounted on O-rings. The opposite end of

the cylinder had a metal housing 2cm long, containing a transducer. A 5mm tube with a 2mm inner diameter was fitted at the end of the metal housing. The tube terminated with a male Luer-Loc fitting. This fitting was connected to a female Luer-Loc fitting that had been chronically implanted over the exposed dura of the rat. The entire system was filled with isotonic saline. The injury was produced by a metal pendulum that struck the piston of the injury device. The injury device injected a small volume of saline into the closed cranial cavity and produced brief displacement of brain tissue. The magnitude of injury was controlled by varying the height from which the pendulum was released. The resulting pressure pulse was measured externally by a pressure transducer (model EPN-0300A*-100A, Entran Devices, Fairfield, NJ) and recorded on a storage oscilloscope (model 5111, Tektronix, Beaverton, OR).

Isolation and homogenization of brain regions:

Rats were anesthetized and decapitated 24 hours, one week, two weeks, three weeks, and four weeks after injury. Brains were dissected on a petri dish on ice to reduce post-mortem alteration of enzyme activity. Cortical, hippocampal, and cerebellar brain regions were quickly isolated and immediately homogenized with 10 strokes (up and down) at 12,000 rpm, using a motorized homogenizer (TRI-R Instruments, Inc. Rockville Center, NY). Brain regions were homogenized into ice-cold homogenization buffer containing 5mM HEPES (pH 7.0), 7mM EGTA, 5mM EDTA, 1mM dithiothreitol (DTT), 0.3mM PMSF, and 300mM sucrose. Cortical regions were homogenized into 7ml of buffer, hippocampal

regions into 3ml of buffer, and cerebellar regions into 5ml. All brain homogenates were normalized for protein, separated into aliquots and stored at -80°C until used.

PNPP assay of calcineurin activity:

CaN activity was quantified using the procedure described in detail by Kurz et al. [167]. Briefly, the reactions were performed as follows. All reaction tubes were prepared on ice and contained the following: 25mM MOPS (pH 7.0), 1mM DTT, 2mM p-nitrophenol phosphate (pNPP). Maximal tubes contained the same reagents as basal reactions, with the addition of 2mM $MnCl_2$. Final reaction volumes were 1ml. Prior to use, the protein concentration of all homogenates was determined using the method of Bradford [144]. Reactions were initiated by the addition of 200 μg/ml brain region homogenate. Reactions were incubated at 37°C for 15 minutes in a shaking water bath. Tubes were then removed from the water bath and placed in ice to stop the reaction. Absorbance of the reaction mixture was immediately measured at 405nm in a spectrophotometer. Absorbance units were converted to nmol of pNP produced by comparison to a pNP concentration standard absorption curve.

RII phosphopeptide assay:

Each fraction was subjected to 1% triton X-100 for 1h at 4° C. Samples were then spun at 100,000 g in a tabletop centrifuge. The resulting supernatant will be passed through a centrifugal filter device with a 10,000 MW cutoff

(MicroCon filters, Amicon). These steps are necessary to remove endogenous phosphate from the assay, otherwise background phosphate would overwhelm the detection protocol. The final, phosphate-free solution was then balanced for protein as above. Reaction tubes contained the following: 50 mM Tris-HCl, 6 mM $MgCl_2$, 0.5 mM $CaCl_2$, 15 μM RII phosphopeptide and 5 μg of protein. Reaction tubes were incubated for 15 min at 37°C in a shaking water bath. Reactions were terminated by the addition of 2X the reaction volume of a malachite green-based agent (Calbiochem). Reactions were read at 620 nm in a UV-Vis spectrophotometer (Cary 50). Increased absorbance in this system indicates increased phosphate release from the CaN substrate. Absorbances were compared to a phosphate standard curve.

pNPP substrate kinetics:

Basal reaction tubes were prepared containing 25mM MOPS, 1mM DTT, 2mM EGTA, 2mM EDTA, and 150nM okadaic acid to minimize the influence of other phosphatases on the results of the assay [167]. Maximal reaction tubes contained 25mM MOPS, 1mM DTT, 2mM MnCl2, and 150nM okadaic acid. All reaction tubes were prepared on ice. pNPP was added to the tubes for final concentrations of 0, 0.1, 0.2, 0.5, 1, 2, 4, 8, 16 and 24mM. CaN reactions were initiated by the addition of homogenate and assayed as described above. Values for K_m and V_{max} were obtained via a non-linear regression analysis of the substrate isotherm.

Western blot analysis:

Western analysis was performed essentially as described previously [167]. Briefly, homogenates were resolved on SDS-PAGE and transferred to a nitrocellulose membrane using the Geni blot system (Idea Scientific, Minneapolis, MN). Nitrocellulose was then immersed for one hour in blocking solution containing phosphate buffered saline (PBS, pH 7.4), 0.05% (v/v) polyoxyethylene sorbitan monolaurate (tween-20), 50 g/L Bio-Rad blotting grade dry milk, and the appropriate normal serum (Vector Laboratories Inc., diluted 50 μl/10ml). The nitrocellulose membrane was then incubated with primary antibody in blocking solution for one hour. Anti-CaN A antibody (clone CN-A1, mouse monoclonal IgG, Sigma Chemical Co.) was diluted 1:10,000 for western analysis, and anti β-tubulin antibody was diluted 1:1,000. Membranes were then washed three times in a wash solution containing PBS, tween-20, and dry milk. Nitrocellulose was then reacted with a secondary antibody in blocking solution for 45 minutes. The membrane was then washed three times and incubated with an avidin-biotin horseradish peroxidase complex for 30 minutes. Nitrocellulose was then washed three times in PBS for 10 minutes per wash. Blots were developed with a solution containing 10 ml PBS, 0.025% (v/v) H_2O_2, and 8 mg 4-chloro-1-napthol dissolved in 2ml of methanol. Specific immunoreactive bands were quantified by computer-assisted densitometry (Inquiry, Loats Associates, Westminster, MD).

Statistical analysis:

All statistical analysis of data was performed using GraphPad Prism 3.0 (GraphPad Software, San Diego, CA), or Sigma Stat 2.03 (SPSS Inc, Richmond, CA). Levels of phosphatase activity were compared to control using the Student's t-test (two-tailed distribution, unpaired) or one-way ANOVA with Tukey post analysis to control for type 1 errors in multiple comparisons. Values for Vmax and Km were determined by a non-linear regression curve for single-site substrate binding, included with the Prism software. Computer assisted densitometric analysis was performed using Inquiry (Loats Associates Inc, Westminster, MD).

RESULTS:

Central fluid percussion injury results in an increase in calcineurin activity in specific brain regions:

CaN activity was quantified in homogenates from the cortex, hippocampus and cerebellum under both basal and maximal reaction conditions. In both the cortex and hippocampus CaN activity was significantly elevated after TBI. In hippocampal homogenates, TBI induced a significant increase in phosphatase activity above control levels under both basal and maximal conditions (Figure 12A). Average basal CaN activity measured in sham hippocampal homogenates was 3.63 μg pNP produced/min/mg of protein. Following TBI, this value was elevated to 5.01 μg pNP/min/mg, an increase of 38.2% ($p < 0.001$, n=10, Student's t-test). Control maximal activity in hippocampal homogenates was 7.36

μg pNP/min/mg. After injury, activity increased 28.6% over control, to a value of 9.47 μg pNP/min/mg ($p < 0.05$, n=10).

TBI induced a significant increase in both basal and maximal CaN activity in cortical homogenates. However, the increase in CaN activity was substantially smaller than that observed in hippocampal homogentates (Figure 12B). Average basal CaN activity in control samples was 3.49 μg pNP/min/mg. Following TBI, this value increased to 4.11 μg pNP/min/mg, and increase of 17.8% ($p<0.05$, n=6). Maximal activity in cortical homogenates isolated from sham animals was 6.99 μg pNP/min/mg. In injured animals, this value was increased by 14.6%, to a value of 8.01 μg pNP/min/mg ($p < 0.05$, n=6). The increase in both the cortical and hippocampal homogenates was present despite the addition of ion chelators to the reaction mix (see methods).

Changes in pNPP dephosphorylation were caused by CaN:

Previous studies [167] have demonstrated a high degree of CaN-specificity in the pNPP assay. For the present study, these results were futher confirmed by the use of gossypol, a specific CaN inhibitor (Figure 13). Under basal reaction conditions, the addition of gossypol decreased pNPP dephosphorylation in cortical homogenates isolated from control animals from 3.49 μg pNP produced/min/mg of protein to 1.38 μg pNP produced/min/mg, a decrease of 60.4%. Likewise, in cortical homogenates isolated from injured animals, pNPP dephosphorylation was reduced by 65.9% in the presence of gossypol, from 4.11 μg pNP produced/min/mg to 1.40 μg pNP produced/min/mg.

Under maximal reaction conditions, the addition of gossypol resulted in a 74.2% decrease in pNPP dephosphorylation in control homogenates, from 7.36 μg pNP produced/min/mg to 1.89 μg pNP produced/min/mg. pNPP dephosporylation was similarly decreased in cortical homogenates isolated from injured animals, from 9.47 μg pNP produced/min/mg to 1.94 μg pNP produced/min/mg in the presence of gossypol, a decrease of 79.5%. In the presence of gossypol, there was no significant difference between control and injured values for pNPP dephosporylation ($p < 0.01$, $n = 10$) suggesting that any TBI-dependent alterations in pNPP dephosphorylation were due to CaN.

The TBI-dependent increase in CaN activity persists several weeks post-injury:

CaN activity was assayed in both the cortex and hippocampus to determine the duration of the TBI-dependent increase in enzyme activity. In addition to the acute time-point discussed above, both basal and maximal CaN activity were measured at one week, two weeks, three weeks, and four weeks post-injury. The post-injury increase in CaN activity persisted two to three weeks after the TBI event; however, the magnitude of the increase in activity decreased with time in both hippocampal and cortical homogenates.

In cortical homogenates isolated from injured animals, basal CaN activity was 124% of control activity at the one week time point ($p < 0.01$, $n=3$). Two weeks post-injury, basal CaN activity was 121% of control basal activity ($p <$

0.01, n=6), and three weeks post-injury, basal CaN activity was 108.6% of control values ($p < 0.05$, n=3). At the four week post-TBI time point, basal CaN activity in homogenates isolated from TBI animals was 97.6% of control basal activity, a difference that was not significant (Figure 14A).

Similarly, at the one week time point, maximal CaN activity in cortical homogenates from injured animals was increased to 120.4% of control activity ($p < 0.01$, n=3). Two weeks post-injury, CaN activity was increased to 115.6% of control in cortical homogenates isolated from injured animals ($p < 0.05$, n=6). No significant increase in maximal CaN activity was observed at either the three or four week time point (Figure 14B).

The time-course of increased CaN activity in hippocampal homogenates demonstrated a pattern similar to that of cortical homogenates. Basal activity in homogenates isolated from injured animals was 132.3% of control one week post-injury ($p < 0.01$, n=3). At two weeks post-injury, basal CaN activity was 128.4% of control activity ($p < 0.01$, n= 6), and at three weeks post-injury, basal CaN activity was 114.4% of control activity in hippocampal homogenates ($p < 0.05$, n=3). At four weeks post-injury, there was no longer a statistically significant TBI-dependent increase in basal CaN activity (Figure 14C).

Maximal CaN activity remained elevated for two weeks post-injury in hippocampal homogenates. One week post-injury, maximal CaN activity was 126.2% of control activity in hippocampal homogenates isolated from injured animals ($p < 0.01$, $n = 3$). Two weeks post-injury, maximal CaN activity was 124.1% of control activity ($p < 0.01$, n=6). By three weeks post-injury, maximal

CaN activity had receeded to 104% of control activity, a difference which was not statistically significant ($p > 0.05$, n=3). At four weeks post injury, maximal CaN activity in hippocampal homogenates isolated from injured animals was indistinguishable from that of control animals (Figure 14D).

TBI induces an alteration in CaN enzyme kinetics in both the cortex and hippocampus:

Other models of cerebral trauma have been shown to alter apparent substrate affinity of CaN [167]. Therefore, to further characterize the effect of TBI on CaN activity, substrate affinity (K_m) and maximal dephosphorylation rate (V_{max}) were examined (see Materials and Methods). Substrate concentration isotherms of the pNPP dephosphorylation reaction were examined in both cortical and hippocampal homogenates, and under both basal and maximal reaction conditions. In hippocampal homogenates, the maximal rate of pNPP dephosphorylation was increased approximately 22% under basal reaction conditions (Figure 15A). In homogenates from control animals, V_{max} was 4.17 μg pNP/min/mg. In TBI homogenates, this value was elevated to 5.09 μg pNP/min/mg ($p < 0.001$, n=3). The apparent K_m was not significantly affected by TBI under basal conditions in the hippocampus. In control homogenates, the apparent K_m was 0.94 mM. Following TBI, the substrate affinity increased (decreased K_m) by 5.3% to 0.89 mM. However, the TBI-induced increase in substrate affinity was not statistically significant ($p>0.05$, n=3).

Under maximal CaN reaction conditions in hippocampal homogenates, the apparent V_{max} was significantly increased, while substrate affinity was not significantly altered by TBI (Figure 15B). In hippocampal homogenates isolated from control animals, V_{max} was 8.64 μg pNP/min/mg. Following TBI, this value increased by 14.4% to 9.88 μg pNP/min/mg ($p<0.001$, n=3). Substrate affinity was not altered under maximal dephosphorylation conditions in the hippocampus. In homogenates from both control and injured animals, the apparent K_m was approximately 0.20 mM ($p>0.05$, n=3).

Under both basal and maximal conditions in the cortex, V_{max}, but not K_m, was significantly increased following brain injury (Figure 16A). Under basal conditions, the apparent V_{max} in homogenates isolated from control animals was 6.88 μg pNP/min/mg. In animals subjected to TBI, this value increased 11.5% to 7.67 μg pNP/min/mg ($p<0.01$, n=3). In control homogenates, the K_m for basal reaction conditions was 0.95 mM pNPP. Following TBI, this value decreased slightly to 0.90 mM pNPP, a decrease of 5.3% that was not statistically significant. ($p>0.05$, n=3). Under maximal conditions in the cortex (Figure 16B), the apparent V_{max} was 10.82 μg pNP/min/mg. After injury, this value was significantly increased by 9.8% to 11.88 μg pNP/min/mg ($p<0.01$, n=3). K_m was not significantly altered under maximal reaction conditions in cortical homogenates. The control value for K_m was 0.68 mM, following TBI, this value decreased by 7.3% to 0.63 mM. This difference was not statistically significant ($p>0.05$, n=3).

TBI did not affect CaN activity in the cerebellum:

While significant increases in CaN activity were found in both the cortex and hippocampus following TBI, no increase was found in cerebellar homogenates. In fact, values for CaN activity appeared to decrease slightly (Figure 17). Under basal reaction conditions, the average control CaN activity in cerebellar homogenates was 3.84 μg pNP/min/mg. Following TBI, basal activity was 3.51 μg pNP/min/mg, a decrease of 8.6% that was not statistically significant ($p>0.05$, $n=6$). Maximal activity in sham cerebellar homogenates was 9.15 μg pNP/min/mg. Following TBI, this value decreased by 4.1%, to 8.78 μg pNP/min/mg ($p>0.05$, $n=6$). Although the decrease in neither basal nor maximal activity was statistically significant, the response of the cerebellum was remarkable due to the obvious difference from the significant increases in activity found in the other brain regions. To determine if significant post-TBI neuronal cell loss in the cerebellum contributed to the lack of increase and lower activities observed in this study, homogenates were assayed for the presence of a neuron-specific marker. Western analysis of cerebellar homogenates from control and TBI animals was performed using an antibody directed against β-tubulin (Clone TUJ1, Covance, Richmond, CA). This method has been shown to be an accurate assay for neuronal concentration [190, 191]. No significant difference in β-tubulin immunoreactivity was found between cerebellar homogenates from sham injured animals (Figure 18). This suggests that a roughly similar amount of neuronal tissue remained in the cerebellar homogenate 24 hours post-TBI, and that

neuronal cell loss was likely not responsible for the lower CaN activities observed in the cerebellum.

The observed increase in CaN activity was not due to an increase in the amount of CaN present:

A possible explanation for the increase in CaN activity observed in the hippocampus and cortex is the increased synthesis of enzyme following TBI. To examine this hypothesis, western analyses of homogenate from all brain regions were performed, using an antibody directed against the catalytic A-subunit of the enzyme (CN-1, Sigma, St. Louis, MO). In all three brain regions, a single band with molecular weight of approximately 61 kDa was resolved. This corresponds with the size of the CaN A subunit [8]. Computer-assisted densitometric analysis was performed on TBI and control fractions (see Materials and Methods). Optical density of the immunoreactive band in cortical TBI homogenate was found to be 94.8% of control density (Figure 19A). In the hippocampus, CaN immunoreactivity in TBI homogenate was 103.4% of control (Figure 19B) and in the cerebellum, immunoreactivity was 107.1% of control (Figure 19C). The density of the immunoreactive bands was not significantly different in any region tested ($p>0.05$, $n=3$ for all regions). The data suggest that an increase in CaN synthesis was not responsible for the increase observed in the cortex and hippocampus, nor was a decrease in the amount of CaN present responsible for the slight decrease in CaN activity in the cerebellum.

DISCUSSION:

The present study is the first to demonstrate a significant increase in CaN activity following fluid percussion brain injury. TBI induced a significant increase in both basal and maximal CaN activity in both the hippocampus and cortex, which persisted two to three weeks after injury. No increase in CaN activity was observed in the cerebellum. TBI-dependent increases in both substrate affinity and maximal reaction rate were demonstrated in the hippocampus and cortex. The significant increase in CaN activity was not due to an increase in the amount of CaN present in the homogenate. An increase in the activity of this important neuronal phosphatase has broad physiological implications, and may be an important step in the development of the pathological consequences of TBI.

Several possible mechanisms exist to explain the TBI-induced elevation in CaN activity. Significant increases in intracellular calcium concentrations have been demonstrated following TBI in several model systems, including the fluid percussion model used in this study [192, 193] and in hippocampal neurons in culture [194, 195]. Calcineurin is a calcium/calmodulin-stimulated enzyme, and would be highly sensitive to an increase in intracellular free calcium concentrations. Therefore, it is reasonable to suspect altered intracellular calcium levels were responsible for increased CaN activation following TBI. There is precedent to assume that increased intracellular calcium could account for altered enzyme activity lasting well after the event, as was the case in this study. The study of intracellular calcium described by Fineman et al. [193] detected increased intracellular calcium up to 4 days post TBI (the longest time-point

used), while studies in culture have detected persistent alterations in calcium entry and homeostatic mechanisms [194, 195]. However, under the reaction conditions employed in the present study, any increased Ca^{2+} should have been adequately buffered. In addition, increasing ion-chelator concentrations in the reaction mix did not significantly effect calcineurin activity in this assay (Data not shown). Therefore, increased intracellular Ca^{2+} alone cannot account for the observed increase in CaN activity.

It is possible that TBI alters the expression of CaN, resulting in a greater amount of the enzyme being present in neuronal cells after injury. An increase in the amount of CaN would explain both the increase in the apparent pNPP dephosphorylation rate without the alteration in substrate affinity following TBI. However, western analyses of cortical and hippocampal homogenates did not detect a significant change in the amount of CaN present in the tissue. This suggests that increased synthesis of CaN is not responsible for the results demonstrated in this study.

CaN activity may be increased after TBI due to post-translational modification of the enzyme. There are several intriguing possible modifications of the enzyme that could result in alterations in CaN activity similar to those observed in this study. For example, limited proteolysis of the CaN A subunit by the calcium-stimulated protease calpain I produces a highly active, calcium-independent form of CaN [12, 14]. Interestingly, several studies have demonstrated a TBI-dependent increase in calpain I activity, possibly due to increased intracellular calcium levels [154, 196]. Increased calpain activity could

result in higher levels of the partially digested, highly active form of CaN. However, the 43 kDa activated CaN fragment was not detected by the western analysis performed in this study, nor was a significant reduction in CaN A immunoreactivity detected, indicating that a large amount of the enzyme was not broken down by calpain. This does not completely discount proteolysis as a possible mechanism for the TBI-induced increase in CaN activity. Partially digested CaN is reported to have a basal activity 1100% higher than that of the holoenzyme [14]. An increase of this magnitude suggests that, if the activated 43 kDa fragment is present after TBI, it constitutes only a small amount (less than 5%) of total enzyme. A difference in protein levels of this magnitude would be difficult to detect through western blot analysis. It is also possible that the epitope recognized by the antibody was no longer present following proteolysis, explaining why no small fragments appeared on the western blot.

Other post-translational regulatory mechanisms also affect CaN activity. Phosphorylation of CaN by both PKC and CaM Kinase II has been shown to inactivate the enzyme [197]. Additionally, the membrane-associated protein AKAP79 binds CaN, also inactivating the enzyme [56]. A TBI-induced alteration in any of these mechanisms could result in the observed increase in CaN activity.

The TBI-dependent increase in CaN activity described in this study was not observed in the cerebellum. In fact, a small decrease in CaN activity was observed in all samples. Although, this decrease was not significant, it is interesting when considered in context of the significant increases observed in the other tow brain regions. Central fluid percussion injury produces a large

amount of strain on the brainstem and nearby structures, with death often resulting from brainstem injury in severe FPI [198, 199]. Therefore, it was possible that physical damage and death of neurons in this region may have contributed to the lower CaN activity. Western analysis for β-tubulin, a neuron-specific marker, did not detect a significant difference between TBI and sham homogenates. Additionally, western analysis of CaN did not detect a significant difference in CaN A immunoreactivity. Therefore, loss of CaN protein was not a contributing factor confounding a potential TBI-induced increase in enzyme activity. The data suggest that TBI modulated different mechanisms in the cortex and hippocampus than in the cerebellum.

The moderate fluid percussion injury used in this study results in numerous cognitive deficits, including memory dysfunction [200], loss of spatial navigation skills [201], and sensorimotor deficits [202]. These deficits are often worst in the days and weeks immediately following TBI. Increased CaN activity may play a role in this cognitive dysfunction. CaN plays a modulatory role in both LTP and LTD of neurons. CaN also modulates major inhibitory receptors, such as the GABAA receptor, and major excitatory receptors, such as the NDMA receptor. Additionally, recent research suggests a major role for CaN in the process of learning and memory. An increase in CaN activity could disrupt any of these processes, playing a role in the cognitive deficits that follow TBI. Interestingly, recent studies have shown cyclosporin A (CsA), a potent CaN inhibitor, to be beneficial in preserving cognitive and motor function following TBI [203, 204]. CsA has other functions as well, most notably blocking the formation

of the mitochondrial transition pore [205], and thus it is impossible to clearly attribute its neuroprotective function to the inhibition of CaN. However, these results, in combination with those of the present study, clearly identify CaN as an important area for further TBI-related research.

Among the physiological roles of CaN, modulation of the $GABA_A$ receptor is of particular interest. The $GABA_A$ receptor is the primary inhibitory receptor in the brain, and is essential for the control of neuronal excitability [65]. Several recent studies have demonstrated a down modulation of $GABA_A$ receptor function by CaN [66-68, 159]. A post-TBI elevation in CaN activity may result in increased dephosphorylation of $GABA_A$ receptors, resulting in a net disinhibition of cellular excitability. A loss of GABA function could produce cognitive and motor deficits, as well as possibly being epileptogenic. It is interesting to note that a recent study found antagonism of the $GABA_A$ receptor to be detrimental to recovery of cognitive function after TBI [206].

Another major cellular mechanism modulated by calcineurin is apoptosis. Several studies have shown CaN to be an essential link in apoptotic pathways [140, 185]. Additionally, artificially high levels of CaN activity predisposes neuronal cells to apoptosis [207]. When a truncated, highly active form of the enzyme was overexpressed in neuronal cells, even normally sub-lethal stimuli were capable of inducing apoptotic cell death. The increased CaN activity demonstrated in the present study, particularly the larger increases in the hippocampus, may make neurons in these regions more likely to undergo apoptosis. Recent literature suggests that apoptotic cell death may play an

important role in the pathology of TBI, making this mechanism an intriguing area for further study [208-210].

The results presented in this study describe a TBI-induced increase in CaN activity that persists up to three weeks post-injury. The relatively persistent nature of this increase suggests a major role for CaN in TBI-related pathologies, with the enzyme playing a role in both immediate neuronal dysfunction and possibly inducing chronic neurological changes. Further research into the role of CaN in TBI may provide a new avenue for clinical treatment of brain injury. For example, the calcineurin inhibitors cyclosporin A and FK506 have both shown promise as neuroprotective agents in several models of TBI, although debate exists about their mechanism of action [93, 94, 211]. Future research is needed to detail the physiological role of calcineurin in TBI and the mechanism responsible for the observed increase in CaN activity. This research will offer useful insight into the biochemical mechanisms occurring during traumatic brain injury.

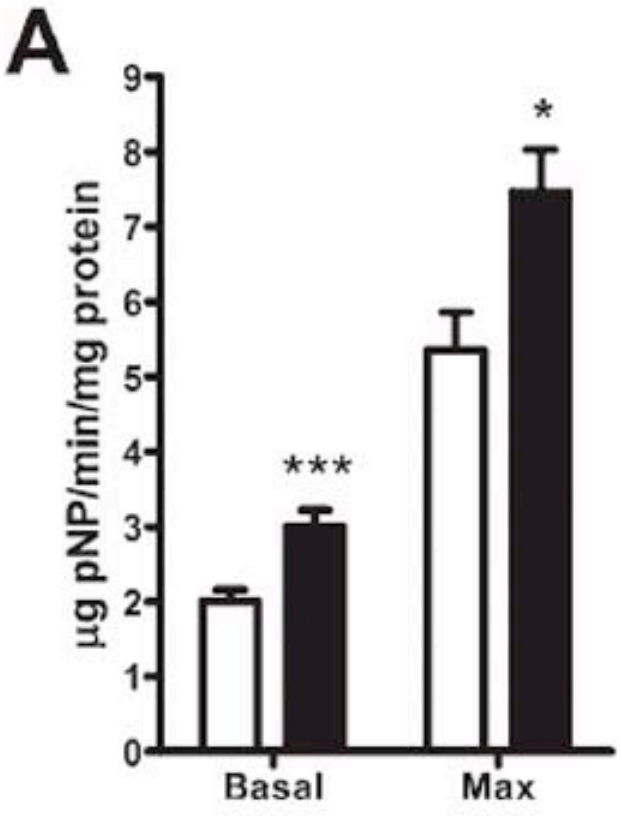

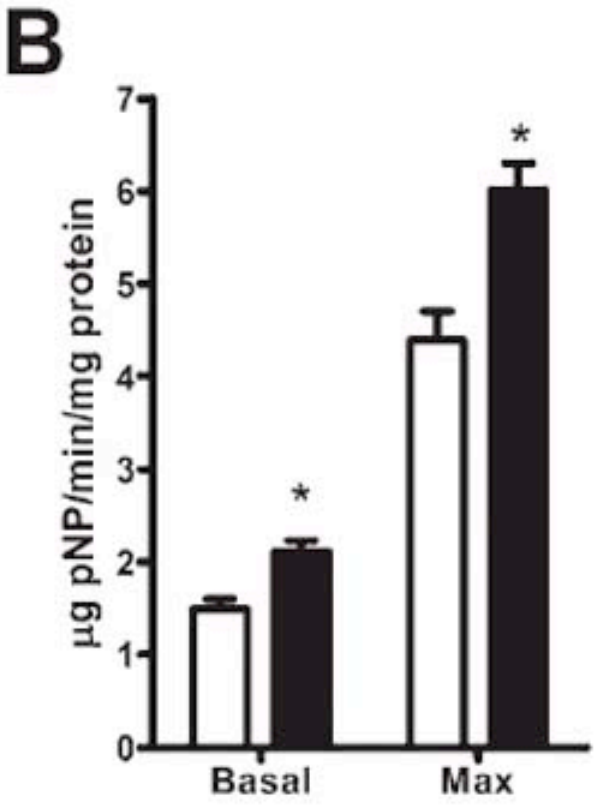

Figure 12. TBI resulted in a significant increase in basal and maximal CaN activity. Basal (white) and maximal (black) calcineurin activity were assayed in hippocampal and cortical homogenates isolated 24 h after moderate fluid-percussion injury. (A) Hippocampal homogenates isolated from injured animals displayed a significant increase in both basal (52.2%) and maximal (34.3%) CaN activity. (B) A TBI-dependent increase in CaN activity was also observed in cortical homogenates, although this increase was smaller than that observed in the hippocampus. Basal CaN activity was elevated by 44.9% and maximal CaN activity was increased by 39.1% when compared to control homogenates (***$p < 0.001$, *$p < 0.05$, $n = 10$, Student's t-test).

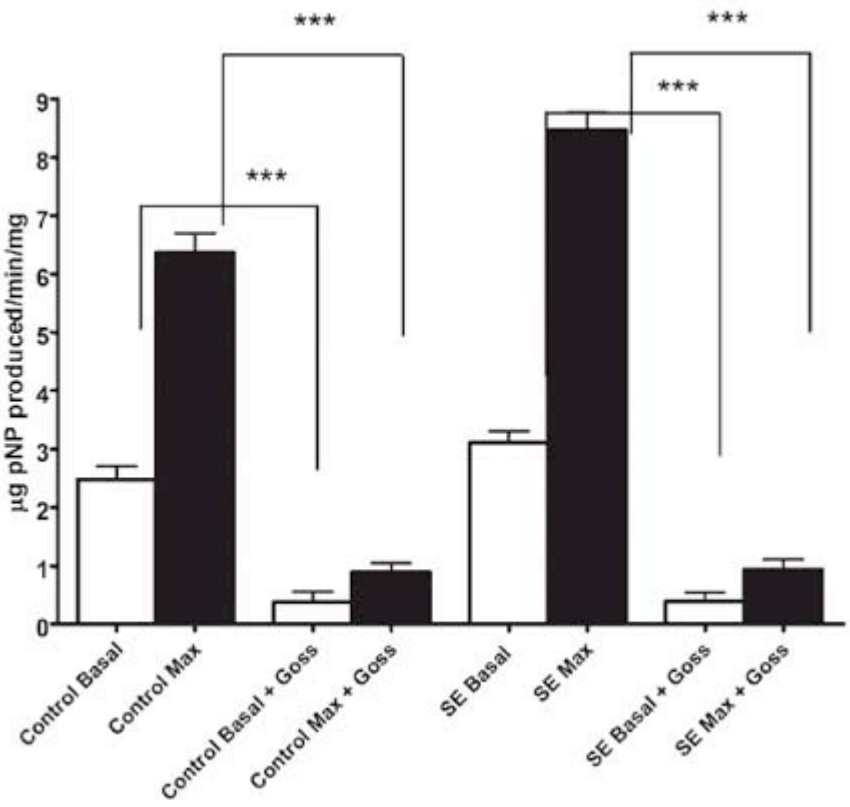

Figure 13. The observed increase in pNPP dephosphorylation is CaN-specific. Cortical homogenates from injured and control animals 24 h post-injury were subjected to basal (white bars) and maximal (black bars) reaction conditions in the presence and absence of gossypol, a CaN-specific inhibitor. In the presence of gossypol, both basal and maximal pNPP dephosphorylation were significantly reduced in control and injured homogenates (***$p < 0.001$, $n = 10$, Student's *t*-test). When gossypol was added to the reaction, basal pNPP dephosphorylation was not significantly different from maximal pNPP dephosphorylation in either control or TBI homogenates ($p > 0.05$, $n = 10$). Finally, control and TBI pNPP dephosphorylation were not significantly different in the presence of gossypol ($p > 0.05$, $n = 10$), indicating that the observed injury-dependent increase in pNPP dephosphorylation was due to CaN activity.

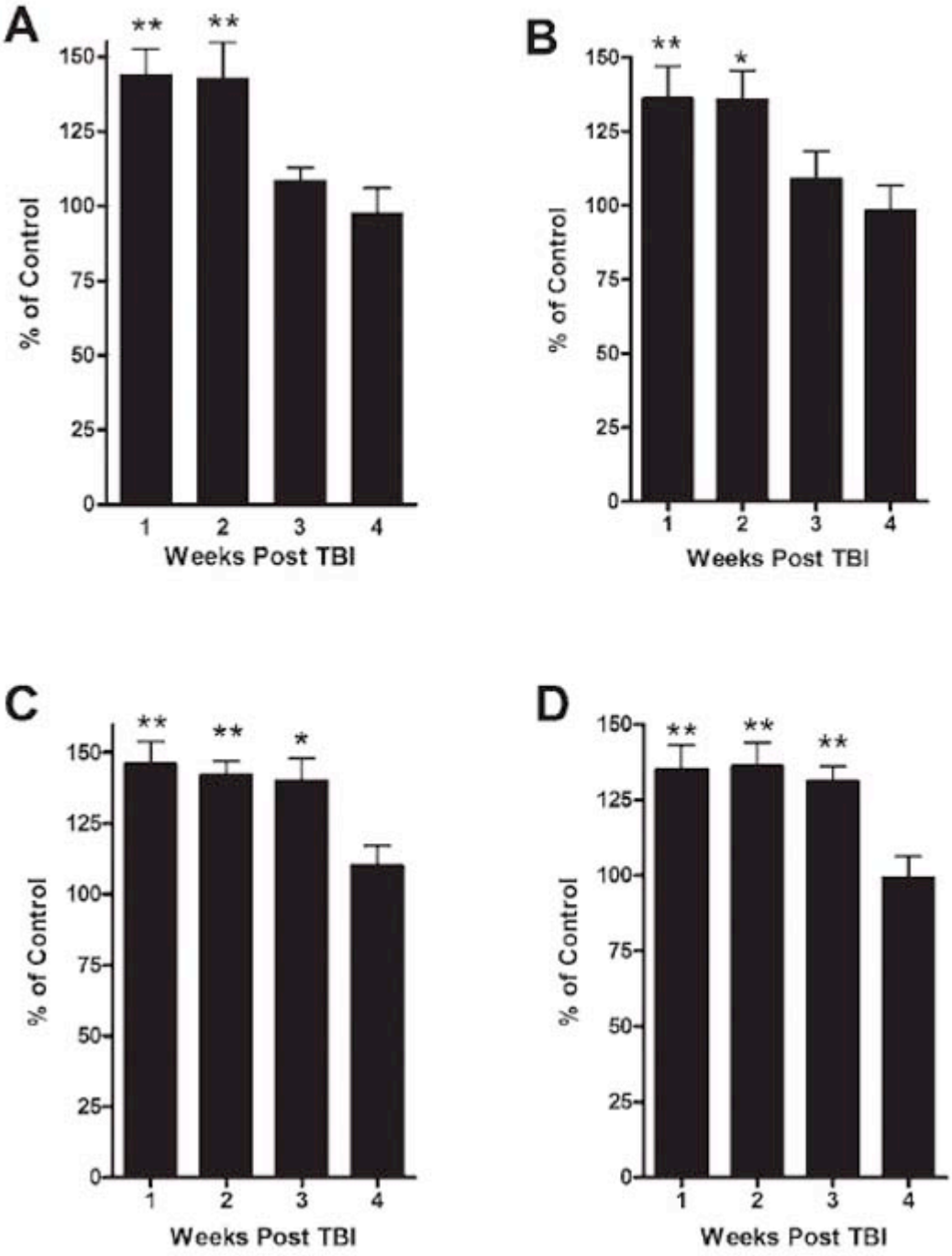

Figure 14. The TBI-induced increase in CaN activity lasts several weeks post-injury. Cortical and hippocampal homogenates from injured and control animals were isolated at 1, 2, 3, and 4 weeks post-injury. Under basal reaction conditions, CaN activity remained significantly elevated in cortical homogenates (**A**) at 1 and 2 weeks post-injury. At 3 and 4 weeks post-injury, basal CaN activity was not significantly different from control values. Under maximal conditions, CaN activity in cortical homogenates (**B**) was significantly elevated at 1 and 2 weeks post-injury. At 3 and 4 weeks post-injury, maximal CaN activity was not significantly different from control. In hippocampal homogenates, CaN activity was significantly elevated under basal conditions (**C**) post-injury at 1, 2, and 3 weeks post-injury. At 4 weeks post-injury, basal CaN activity was not significantly different from control. Under maximal reaction conditions, CaN activity was elevated in hippocampal homogenates (**D**) at 1, 2, and 3 weeks postinjury. At 4 weeks post-injury, maximal CaN activity was not significantly different from control (**$p < 0.01$, *$p < 0.05$, $n = 8$ for all groups, one-way ANOVA with Tukey post-hoc analysis).

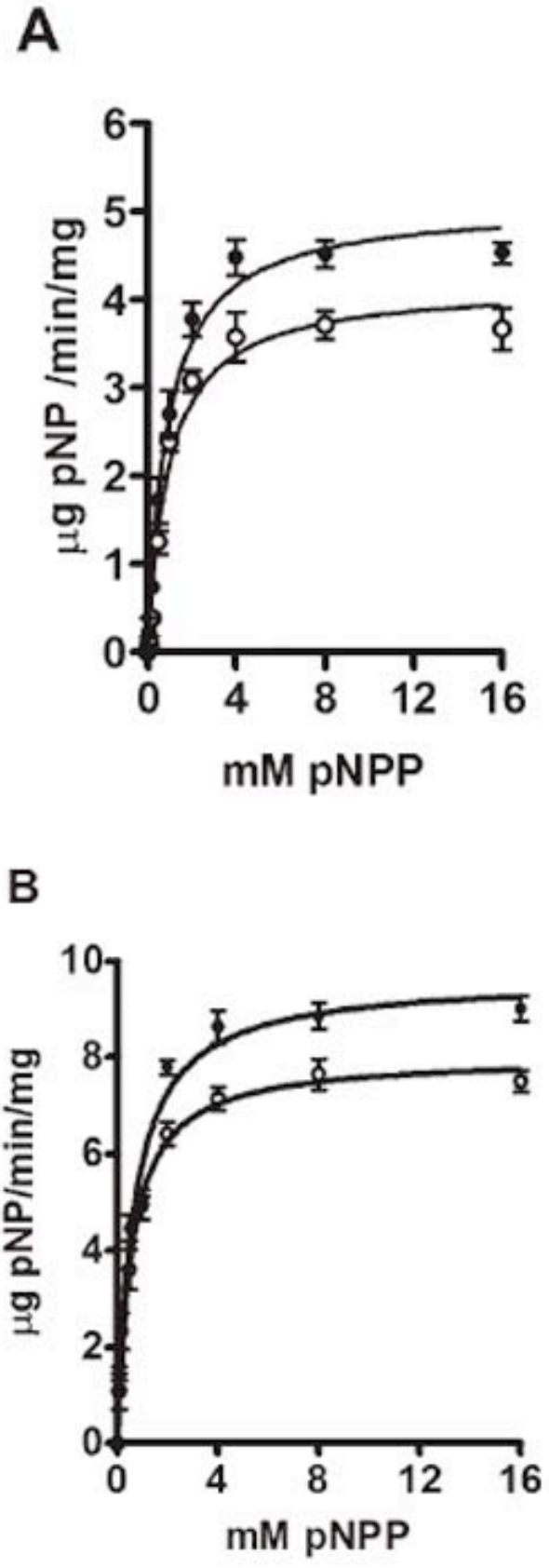

Figure 15. TBI modulated CaN enzyme kinetics in hippocampal homogenates. Substrate concentration isotherms were constructed in hippocampal homogenates isolated from control and TBI animals. (**A**) Basal CaN reactions were performed in control (open circles) and TBI (closed circles) homogenates. TBI resulted in a 27.4% increase in apparent Vmax ($p < 0.001$, $n = 3$). However, substrate affinity was not significantly affected (5.0% decrease in Km, $p > 0.05$, $n = 3$). (**B**) Maximal CaN reactions were performed in homogenates isolated from control (open circles) and TBI (closed circles) animals. Like basal CaN reactions, TBI resulted in a significant (20.2%, $p < 0.001$, $n = 3$) increase in apparent Vmax, without a significant increase in substrate affinity (Km not changed).

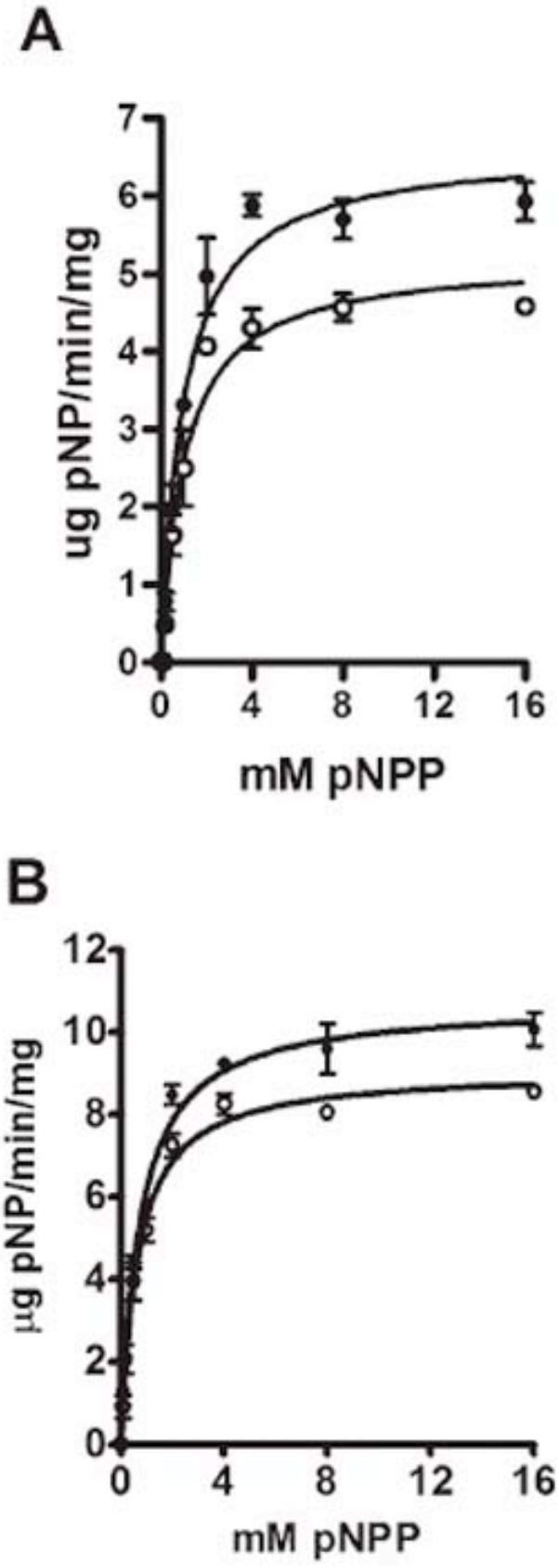

Figure 16. TBI modulated CaN enzyme kinetics in cortical homogenates.

Substrate concentration isotherms were constructed in cortical homogenates isolated from control and TBI animals. Cortical homogenates displayed a significant increase in CaN activity. (**A**) Basal CaN reactions were performed in control (closed circles) and TBI (open circles) homogenates. TBI resulted in a 22.3% increase in apparent Vmax ($p < 0.01$, $n = 3$). However, substrate affinity was not significantly affected (5.3% difference in Km, $p > 0.05$, $n = 3$). (**B**) Maximal CaN reactions were performed in homogenates isolated from control (open circles) and TBI (closed circles) animals. Like basal CaN reactions, TBI resulted in a significant (15.2%, $p < 0.01$, $n = 3$) increase in apparent Vmax, without a significant increase in substrate affinity (6.7%, $p > 0.05$, $n = 3$).

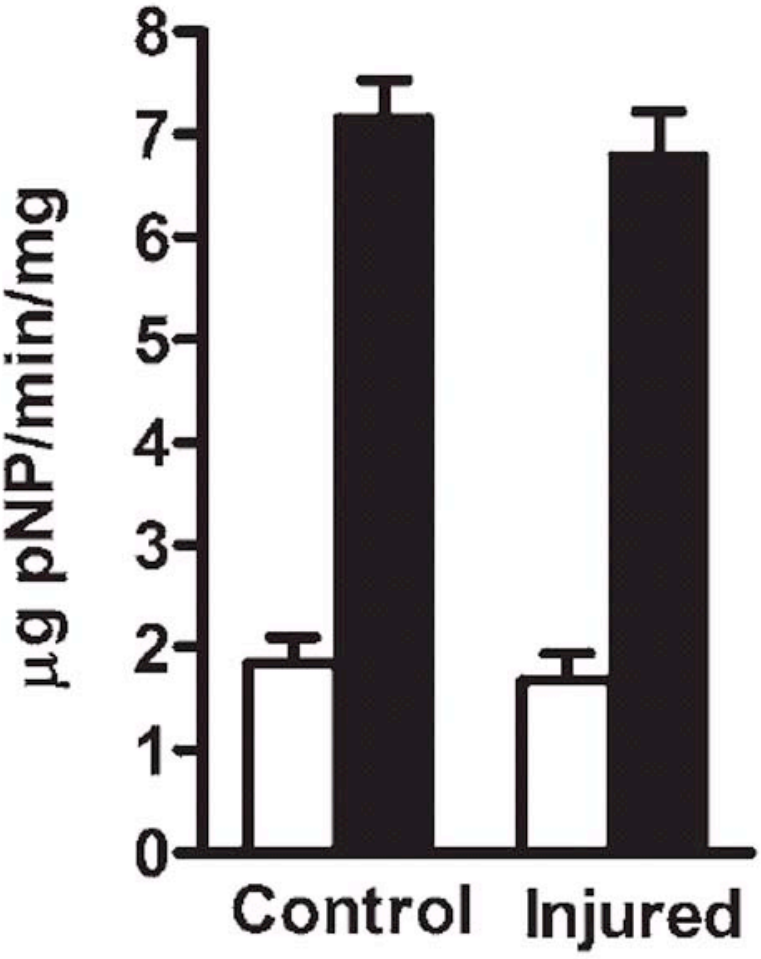

Figure 17. TBI did not affect CaN activity in the cerebellum.

Basal (white) and maximal (black) CaN activity was assayed in cerebellar homogenates 24 h post-TBI. Both basal and maximal activity appeared to decrease slightly; however values were not found to be significantly different from those observed in control homogenates ($p < 0.05$, $n = 10$, Student's *t*-test).

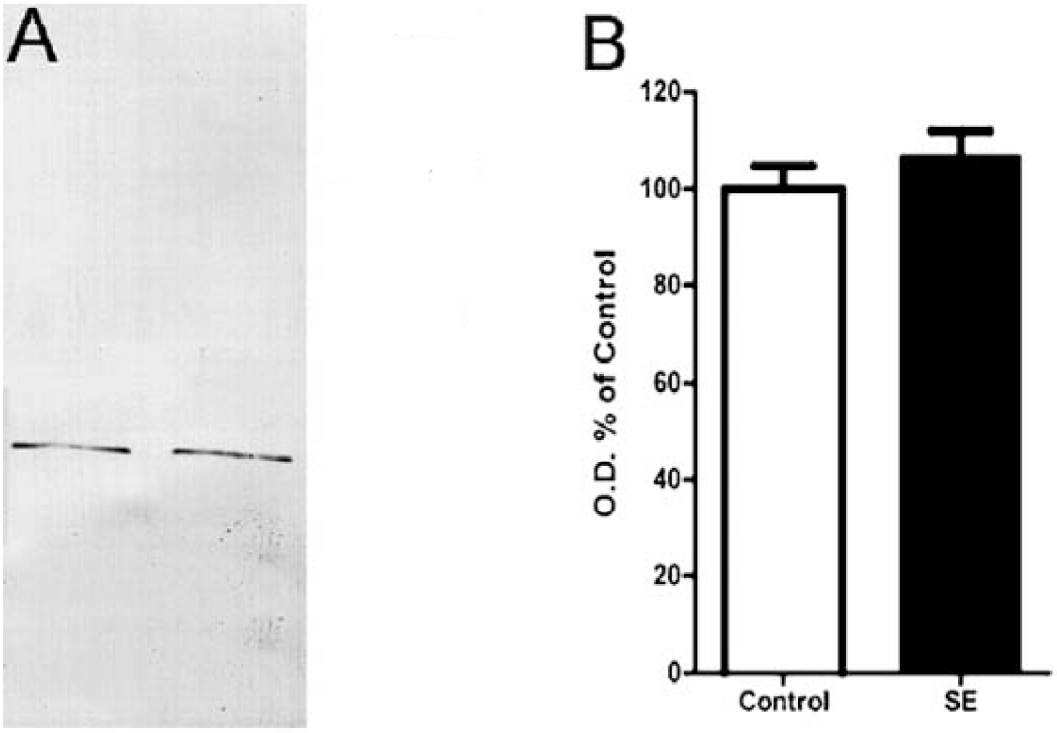

Figure 18. TBI did not induce significant neuronal loss in the cerebellum at the acute time-point.

(**A**) Western analysis for the neuron-specific protein β-tubulin was used to determine relative concentrations of neuronal tissue in TBI and control cerebellar homogenates. (**B**) Computer-assisted densitometry demonstrated that β-tubulin immunoreactivity was not significantly different between TBI homogenate and control, suggesting a roughly similar amount of neuronal tissue was present in the homogenate before and after injury. β-Tubulin immunoreactivity in TBI cerebellum was 106. ± 9.4% of control ($p > 0.05$, $n > 6$, Student's *t*-test).

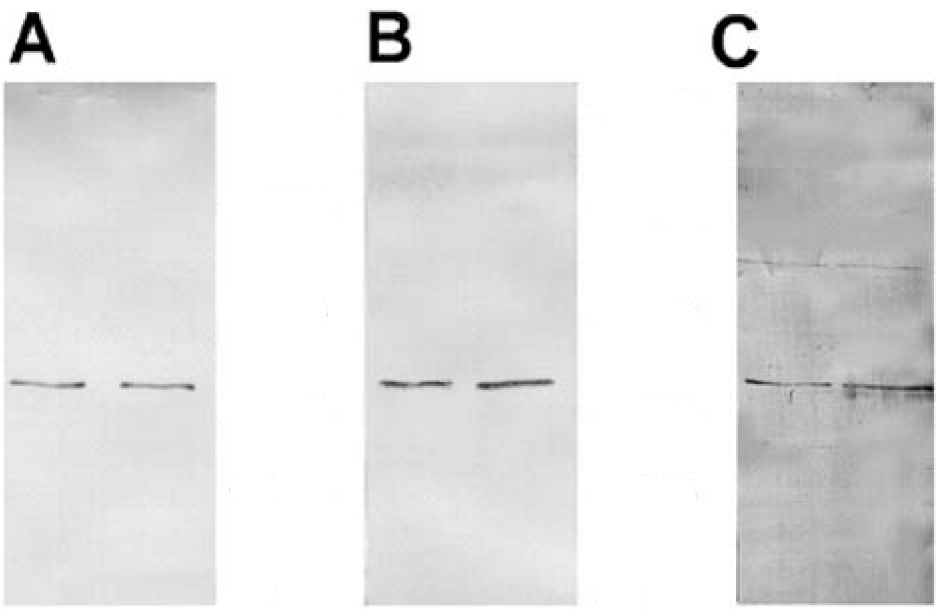

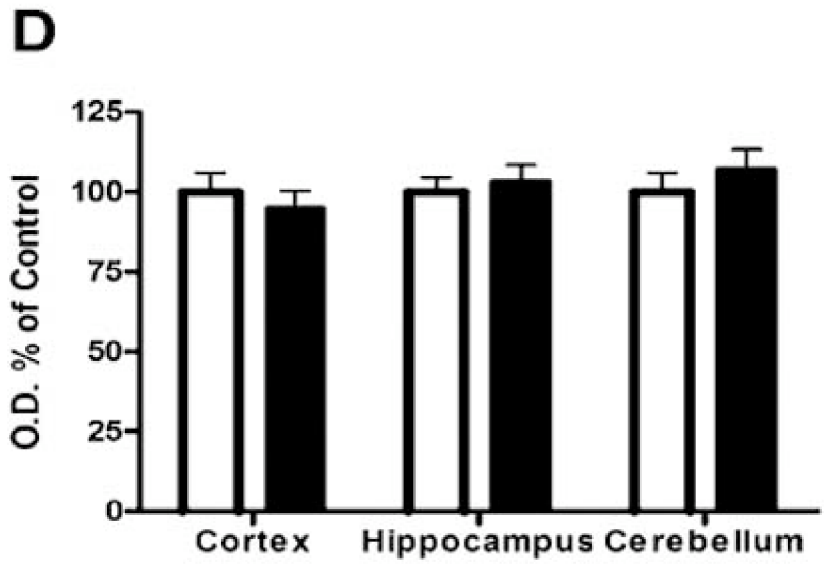

Figure 19. The post-TBI alteration in CaN activity was not due to a TBI-induced increase in CaN protein expression.

To determine if TBI resulted in increased CaN enzyme levels, homogenates from all brain regions were subjected to western analysis for the catalytic CaN A subunit. Immunoreactivity in the hippocampus (**A**), cortex (**B**), and cerebellum (**C**) was quantified with computer-assisted densitometry (**D**), and found not significantly different from control ($p < 0.05$, $n = 3$ for all brain regions, Student's *t*-test). Blots shown are representative from samples utilized for biochemical characterization.

CHAPTER IV

A PERSISTENT CHANGE IN SUBCELLULAR DISTRIBUTION OF CALCINEURIN FOLLOWING FLUID PERCUSSION INJURY IN THE RAT.

INTRODUCTION:

Traumatic brain injury (TBI) remains a major cause of death and disability in the United States today [183]. Although the initial injury often involves irreversible destruction of tissue, secondary, potentially preventable injury processes take place in the days and weeks after injury. This secondary damage causes pathological change in cells over a much greater area than the primary injury, and is often responsible for many of the lasting neurological deficits associated with TBI [183, 184] The delayed nature of this secondary injury offers a potential window for treatment, making it an exciting area for both basic research and clinical trials. Fluid percussion brain injury provides an excellent model for this type of secondary, generalized injury; moderate fluid percussion does very little immediate damage to the brain tissue, but animals are left with pathologically altered neuronal cells and lasting neurological deficits [212]. Central fluid percussion, in particular, is associated with reduced cell death when

compared with lateral fluid percussion [213].

Many of the mechanisms associated with secondary neuronal injury in TBI are associated with calcium and calcium-modulated systems [132]. A calcium-regulated enzyme of current interest is the neuronally enriched phosphatase, calcineurin (CaN). Expression of CaN mRNA is elevated after injury in at least one model [214]. Additionally, the CaN inhibitors cyclosporin A and FK-506 have both shown promise as neuroprotective agents in several models of TBI [93, 94, 215, 216], although only cyclosporin A has been evaluated in the specific model used in this study [94]. In the case of cyclosporin A, the neuroprotective effect may be due to CaN inhibition, but most studies suggest neuroprotection is due to the drug's effects on mitochondria. On the other hand, for FK-506, the neuroprotective action is more likely due to CaN inhibition [93, 216]. Finally, recent research has characterized a TBI-dependent increase in CaN activity in the fluid percussion model, further implicating CaN in brain trauma-induced pathology [217].

The present study expands on our previous study of CaN in TBI, further characterizing the effects of fluid percussion TBI on CaN in rat forebrain. CaN immunoreactivity was increased in synaptoplasmic membrane-enriched fractions from both the cortex and hippocampus. This elevation in CaN immunoreactivity persisted for 2 weeks in the cortex, and up to 4 weeks in the hippocampus. Additionally, immunohistochemical studies of the hippocampus demonstrated a TBI-dependent elevation in CaN immunoreactivity in dendritic processes of the CA1 region. The data suggest a long-lasting post-injury translocation of CaN to

the post-synaptic region of neurons, where it may play a role in pathologically altering synaptic activity.

METHODS:

Surgical preparation and fluid percussion injury:

All animal use procedures were in strict accordance with the *Guide for the Care and Use of Laboratory Animals* described by the National Institutes of Health and were approved by the Virginia Commonwealth University Institutional Animal Care and Use Committee. Adult male Sprague–Dawley rats weighing between 300 and 350 g were surgically prepared under sodium pentobarbital anesthesia (54 mg/kg intraperitoneally). Animals were placed in a stereotactic frame and the scalp was sagitally incised. A 4.8-mm hole was then trephined into the skull over the sagittal suture midway between bregma and lambda. A nickel-plated screw was placed 1 mm rostral to bregma, and a second screw was inserted 1 mm caudal to lambda. A modified female Luer-Loc syringe hub (2.6 mm inside diameter) was placed over the exposed dura and bonded in place with a cyanoacrylate adhesive. Dental acrylic was then poured around the syringe hub and screws. The scalp was then sutured, bacitracin was applied to the wound, and the animal was returned to its home cage.

Twenty-four hours following the surgical procedure, the rats were again anesthetized (4% isoflurane in a carrier gas mixture of 70% N_2O and 30% O_2). Rats in the sham-injury (control) group were anesthetized and connected to the

injury device, but the pendulum was not released. Rats in the injured group were anesthetized and subjected to a moderate (2.1 ± 0.1 atm) level of fluid percussion injury. The Luer-Loc fitting, screws, and dental cement were then removed from the skull. Following recovery, rats were returned to their home cages and allowed to survive for 24 h, 1 week, 2 weeks, 3 weeks, or 4 weeks prior to being sacrificed. Six injured and six sham-injured animals were obtained for each post-injury time point for Western analysis. An additional three injured and three sham-injured animals were obtained for immunohistochemical studies from the 24-h and 4-week time points.

Fluid percussion injury device:

The fluid percussion injury device used in these experiments is identical to that described by Dixon et al. [189]. Briefly, the device consisted of a Plexiglas cylinder reservoir 60 cm long and 4.5 cm in diameter. At one end of the cylinder was a rubber-covered Plexiglas piston mounted on O-rings. The opposite end of the cylinder had a metal housing 2 cm long, containing a transducer. A 5-mm-long tube with a 2-mm inner diameter was fitted at the end of the metal housing. The tube terminated with a male Luer-Loc fitting. This fitting was connected to a female Luer-Loc fitting that had been chronically implanted over the exposed dura of the rat. The entire system was filled with isotonic saline. The injury was produced by a metal pendulum that struck the piston of the injury device. The injury device injected a small volume of saline into the closed cranial cavity and produced brief displacement of brain tissue. The magnitude of injury was

controlled by varying the height from which the pendulum was released. The resulting pressure pulse was measured externally by a pressure transducer (model EPN-0300A*-100A, Entran Devices, Fairfield, NJ) and recorded on a storage oscilloscope (model 5111, Tektronix, Beaverton, OR).

Isolation and homogenization of brain regions:

Rats were anesthetized and decapitated 24 h, 1 week, 2 weeks, 3 weeks, and 4 weeks after injury or sham-injury. No obvious contusion or gross signs of injury were noted. Brains were dissected on a petri dish on ice to reduce postmortem alteration of enzyme activity. Cortical and hippocampal brain regions were quickly isolated and immediately homogenized with 10 strokes (up and down) at 12,000 rpm using a motorized homogenizer (TRI-R Instruments, Inc., Rockville Center, NY). Brain regions were homogenized into ice-cold homogenization buffer containing 5 mM HEPES (pH 7.0), 7 mM EGTA, 5 mM EDTA, 1 mM dithiothreitol, 0.3 mM phenylmethylsulfonylfloride, and 300 mM sucrose. Cortical regions were homogenized into 7 ml of buffer and hippocampal regions into 3 ml of buffer. Cortical homogenates consisted of both left and right hemispheres, while hippocampal homogenates consisted of both the left and right hippocampus. Subcellular fractions were then isolated by a differential centrifugation procedure [168] with modifications described previously [217]. Brain region homogenate was first centrifuged at 5000 × *g* for 10 min to produce a crude nuclear pellet (P1) and a supernatant (S1). The P1 pellet was resuspended in homogenization buffer, separated into aliquots, and stored at −80

°C until used. The S1 was centrifuged for 30 min at 18,000 × *g* to produce the crude synaptoplasmic membrane/mitochondiral pellet (P2) and a supernatant (S2). The S2 was separated into aliquots and stored at −80 °C. The P2 pellet was resuspended in homogenization buffer (1 ml for cortex, 500 µl for hippocampus), then separated into aliquots and stored at −80 °C until used.

CaN immunoblotting procedure:

Western analysis was performed essentially as described previously [146]. Briefly, homogenate protein concentrations were measured and balanced. Homogenates were then resolved on SDS-PAGE (5 µg/lane, 5 well, 1.5 mm thick gels, Mini-Protean II system, Bio-Rad, Hercules, CA) and transferred to a nitrocellulose membrane using the Geni blot system (Idea Scientific, Minneapolis, MN). Anti-CaN A antibody (clone CN-A1, mouse monoclonal IgG, Sigma Chemical Co.) was diluted 1:10,000 for Western analysis, and stained using the Vectastain Elite anti-mouse IgG kit (Vector Laboratories Inc., Burlingame, CA). Blots were developed with a solution containing 10 ml PBS, 0.025% (v/v) H_2O_2, and 8 mg 4-chloro-1-napthol dissolved in 2 ml of methanol. Specific immunoreactive bands were quantified by computer-assisted densitometry (GS-800 Calibrated Densitometer, BioRad).

Immunohistochemical analysis:

Immunohistochemical studies were carried out as described previously [146, 217]. At 24 h and 4 weeks post-injury, rats were anesthetized with

halothane and transcardially perfused with a solution containing 4% paraformaldehyde and 0.1% glutaraldehyde. Brains were then removed and allowed to post-fix in the perfusion fixative for 24 h. Brains were then blocked to allow sectioning of the dorsal hippocampus, embedded in agar and coronally sectioned into serial 40-μm sections on a Leica VT1000S vibratome (Leica Microsystems, Bannockburn, IL). Sections were stored in 12-well culture plates until used.

For immunohistochemical staining, sections were incubated for 30 min in normal serum at 37 °C. Sections were then incubated overnight with a polyclonal anti-CaN A antibody at a dilution of 1:50,000. Following incubation with the primary antibody, sections were then washed 4× with phosphate-buffered saline (PBS, pH 7.4) for 15 min per wash. The tissue was then incubated in secondary antibody for 1 h at 37 °C. Sections were washed 3× in PBS, then placed in Vectastain ABC reagent for 2 h. The first hour of incubation in ABC was performed at 37 °C, the second hour at room temperature. Sections were then washed 2× in PBS for 10 min per wash, and 1× in Tris–Base (pH 7.6). The tissue was then stained with a glucose oxidase-DAB-nickel preparation.

RESULTS:

TBI resulted in a long-lasting increase of CaN immunoreactivity in both the cortex and hippocampus

Western analysis was performed for homogenate and subcellular fractions

for both cortex and hippocampus. No significant post-TBI difference in CaN immunoreactivity was found in homogenate from either cortical or hippocampal tissues, indicating that there was no overall increase in the amount of CaN present in this tissue (Fig 20). Additionally, no difference in CaN immunoreactivity was detected in the P1 (nuclear-enriched) or S2 fractions (data not shown).

Crude synaptoplasmic membrane (SPM) fractions were isolated from the cortex and hippocampus at several time points post-injury to assess the duration of the increase in CaN immunoreactivity. All SPM fractions were compared with fractions isolated from sham-operated controls at identical time points post-sham-injury. At 24 h post-injury, a significant increase in CaN immunoreactivity was observed (257.9 ± 32.0% of control, Fig. 21 and Fig. 22) in the P2 (crude SPM) fraction isolated from post-TBI cortical tissue. CaN immunoreactivity remained increased to 218.1 ± 25.4% of control 1 week post-TBI (Figs. 21 and 22), and 202.1 ± 23.1% of control 2 weeks post TBI (Fig. 21C). At 3 weeks post-injury, CaN immunoreactivity had returned to baseline, and was indistinguishable from that of sham-operated animals (Figs. 21 and 22).

Similarly, a TBI-dependent increase in CaN immunoreactivity to 261.3 ± 24.8% of control was observed 24 h post-injury in hippocampal crude SPM (Figs. 23 and 24). CaN immunoreactivity remained elevated to 261.6 ± 26.2% of control 1 week post-TBI (Figs. 23 and 24), 259.2 ± 20.1% of control 2 weeks post-TBI (Figs. 23 and 24), and 138.7 ± 10.3% of control 3 weeks post-TBI (Figs 23 and 24). At 4 weeks post-injury, CaN immunoreactivity in hippocampal SPM-enriched fractions was 130.4 ± 12.5% of control (Figs. 23

and 24). Although the elevation in CaN immunoreactivity decreased over time in the hippocampus, it remained significantly higher than that of sham-operated control animals for the entire 4 weeks of this study, suggesting a persistent alteration in the CaN content of the SPM fraction.

TBI resulted in a long-lasting increase in CaN A immunoreactivity in apical dendrites of hippocampal CA1 neurons

To further characterize the TBI-dependent increase in CaN immunoreactivity observed in the crude SPM fraction, immunohistochemical studies were performed on paraformaldehyde-fixed coronal sections from TBI and control animals, both at 24 h (Fig. 25A, B) and 4 weeks (Fig. 25C, D) post-injury. Hippocampal sections from sham-control animals demonstrated no noticeable histological differences between 24-h and 4-week post-sham treatment (Fig. 25A, C). Hippocampal sections from control animals demonstrated diffuse staining throughout the pyramidal cell layer, with the exception of the pyramidal cell nuclei. Faint CaN immunoreactivity was observed in the surrounding cortex (data not shown). This diffuse cortical staining remained unchanged following TBI. Therefore, the intensity of cortical staining was used as a background value to compare control and TBI images. Individual hippocampal pyramidal neurons could be visualized in sham animals; the cytoplasm of these cells demonstrated very diffuse CaN-reactive staining. The darkest staining was seen around the plasma membrane of these neurons. Occasional dendritic processes demonstrated CaN immunoreactivity; however,

many apical dendrites could not be individually visualized in control sections. These histological findings were in agreement with previous studies demonstrating the presence of CaN in the hippocampal formation, particularly in the plasma membrane and in neurites [217].

Hippocampal sections from TBI animals demonstrated several qualitative changes when compared to sham-control sections (Fig. 25B, D). Similar to the control sections, diffuse CaN-reactive staining was present throughout the hippocampus. However, this staining was noticeably more intense in the 24-h post-injury sections. Staining was still relatively poor in the surrounding cortex in the TBI sections. Intense staining was found to be present around the plasma membranes and throughout the apical dendrites of pyramidal neurons. Unlike the control sections, where few processes could be seen, many apical dendrites were easily visualized and intensely stained in the TBI sections. It was not possible to visualize any axonal processes leading from the pyramidal cells, nor were any darkly stained processes observed in axonal layers of the hippocampus, suggesting that the increased CaN immunoreactivity was post- rather than presynaptic. Finally, no interneurons were detected in control or SE sections, suggesting an absence of CaN in these neurons that is in agreement with previous research. Although these changes were most intense in the 24-h post-injury sections, they remained noticeably different from control in the 4-week post-injury samples, a finding which corresponds well with the subcellular fraction data presented above.

DISCUSSION:

The present study identified an increase in CaN immunoreactivity in the P2 fraction isolated from hippocampal and cortical tissue that lasted for a significant amount of time post-injury. This study did not identify any significant increase in CaN immunoreactivity in homogenate from these tissues. This suggests that the increase in CaN content in the crude SPM fraction was due to translocation, rather than new protein synthesis. Additionally, immunohistochemical staining of hippocampal tissue revealed increased CaN staining in the apical dendrites of the CA1 region that persisted at least 4 weeks post-injury. These data suggest a TBI-induced translocation of CaN into specific synaptic membrane-rich compartments, and also indicate that this translocation remains in effect during the critical weeks immediately following brain injury.

Recent studies have suggested that CaN participates in the biochemical mechanisms leading to neuronal pathology following traumatic brain injury. Additionally, inhibitors of CaN, including cyclosporin A and FK506, can be neuroprotective if administered within a short time of the injury event. However, it is important to note that FK506 has not been specifically studied in the fluid percussion model of TBI, and caution should be used when applying results from these inhibitor studies across injury models. A great deal remains to be understood about the exact physiological role played by CaN in these pathological processes, and a better understanding of CaN activity post-TBI may allow more effective targeting of these treatments. Previous studies in our

laboratory described an increase in CaN activity beginning acutely post-injury and persisting for several weeks post-injury [218]. Since CaN regulates a diverse group of neuronal processes, understanding how this increase in activity relates to specific subcellular compartments is important in determining the role of CaN in TBI-induced pathology.

The P2 fraction described in this study is highly enriched in both crude synaptoplasmic membrane and mitochondria [168]. Previous studies have not detected significant amounts of CaN in purified mitochondrial preparations [171]; however, it is possible that TBI induces a translocation of the enzyme to these organelles. CaN plays an essential role in several apoptotic pathways [91, 166], and movement of the enzyme to the mitochondria would likely facilitate these apoptotic mechanisms, resulting in increased cell death. While this is an intriguing hypothesis, the lack of significant amounts of CaN in mitochondrial preparations from other studies, coupled with the immunohistochemical data in this study, makes mitochondrial translocation of CaN an unlikely explanation for the data presented.

CaN has been detected in purified synaptoplasmic membranes by several researchers [171, 219]. The increased immunoreactivity of CaN in the P2 fraction observed in this experiment could be due to a translocation of enzyme to the synaptic membrane. Immunohistochemical data presented in this study described a significant increase in CaN immunoreactivity in the pyramidal cell layers of the hippocampus, especially in the CA1 region. The fact that this increase in immunoreactivity was confined primarily to the apical dendrites

supports the hypothesis that TBI leads to a translocation of the enzyme to the post-synaptic membrane. This would place double the control amount of CaN in a region rich in substrates highly relevant to the pathology of TBI. This translocation is an especially intriguing possibility when considered along with prior observations that TBI induces an increase in CaN activity.

The fluid percussion model of TBI used in this study has been shown to lead to numerous cognitive deficits in the animals studied, including poor performance in tasks known to rely on new memory formation and hippocampal processing [202, 220-222]. Interestingly, the duration of some of the major deficits in learning and memory in the fluid percussion model correlates well with the duration of increased CaN immunoreactivity [221-223]. CaN plays an important role in learning and memory through its regulation of LTP and LTD [41, 224]. Through its actions leading to dephosphorylation of NMDA receptors, CaN activity is generally thought to be associated with weakening synaptic strength, i.e., LTD [69, 180, 225]. The translocation of CaN noted in this study would greatly increase the amount of CaN in the vicinity of these receptors, possibly increasing LTD of neurons important in memory formation and decreasing overall cognitive function. Additionally, CaN has been shown to cause depotentiation of neurons that have undergone LTP, also weakening relative synaptic strength [226]. A recent study has shown that fluid percussion TBI leads to an inability to maintain LTP in hippocampal CA1 neurons [227]. Interestingly, both the post-TBI translocation of CaN and the increase in its activity are present long after the initial injury in the hippocampus, a structure essential for memory formation and

highly vulnerable to TBI-induced damage.

Conversely, CaN has also been shown to decrease GABAergic neurotransmission by dephosphorylating an essential phosphorylation site on the GABA receptor [66, 68]. Additionally, CaN-mediated dephosphorylation is the rate-limiting step in dynamin-mediated vesicle endocytosis [228] such as occurs in $GABA_A$ receptor internalization [229]. Thus, an increase of CaN concentration in the vicinity of $GABA_A$ receptors could decrease inhibitory neurotransmission both by decreasing receptor function and decreasing the number of available receptors. A decrease in inhibitory neurotransmission could lead to pathologically hyperexcitable neuronal tissue, such as occurs in the epileptic activity and hippocampal hyperexcitability associated with the fluid percussion injury model [230-232]. Understanding the exact physiological role of CaN in TBI clearly depends on discovering which elements of the post-synaptic membrane CaN associates with after the injury, providing an intriguing area for future research.

This study is the first to describe a TBI-dependent increase in CaN concentration in the post-synaptic region of neurons. This increase persists well after the acute injury, suggesting that it may play a role in the development of TBI-associated pathologies. Discovery of TBI-associated effects on this important enzyme is especially relevant in light of the recent interest in the neuroprotective effects of CaN inhibitors. Further research into the effects of TBI on CaN will help lead to a better understanding of the biochemical processes occurring in the days and weeks post-injury, and will hopefully lead to more effective treatment options for these devastating injuries.

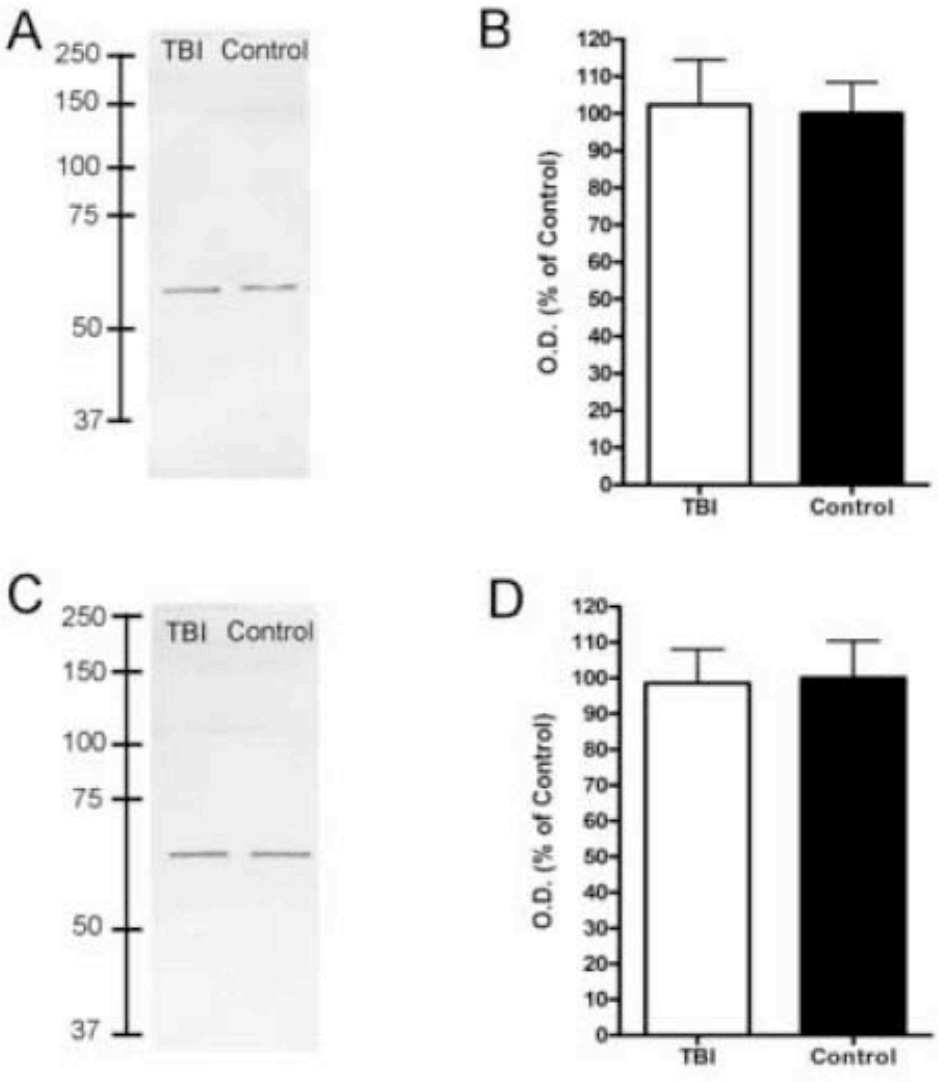

Figure 20: TBI did not alter total CaN A expression in hippocampal and cortical homogenates

Western analysis of cortical (A) and hippocampal (C) homogenates did not demonstrate a TBI-dependent change in CaN A immunoreactivity 24h post-injury when compared to sham animals. In cortical homogenates (B) from injured animals, CaN immunoreactivity was 98.7 % of control as determined by calibrated densitometry ($p > 0.05$, $n = 6$, Student's t-test). In hippocampal homogenates (D), CaN immunoreactivity was 103.2 % of control ($p > 0.05$, $n=6$).

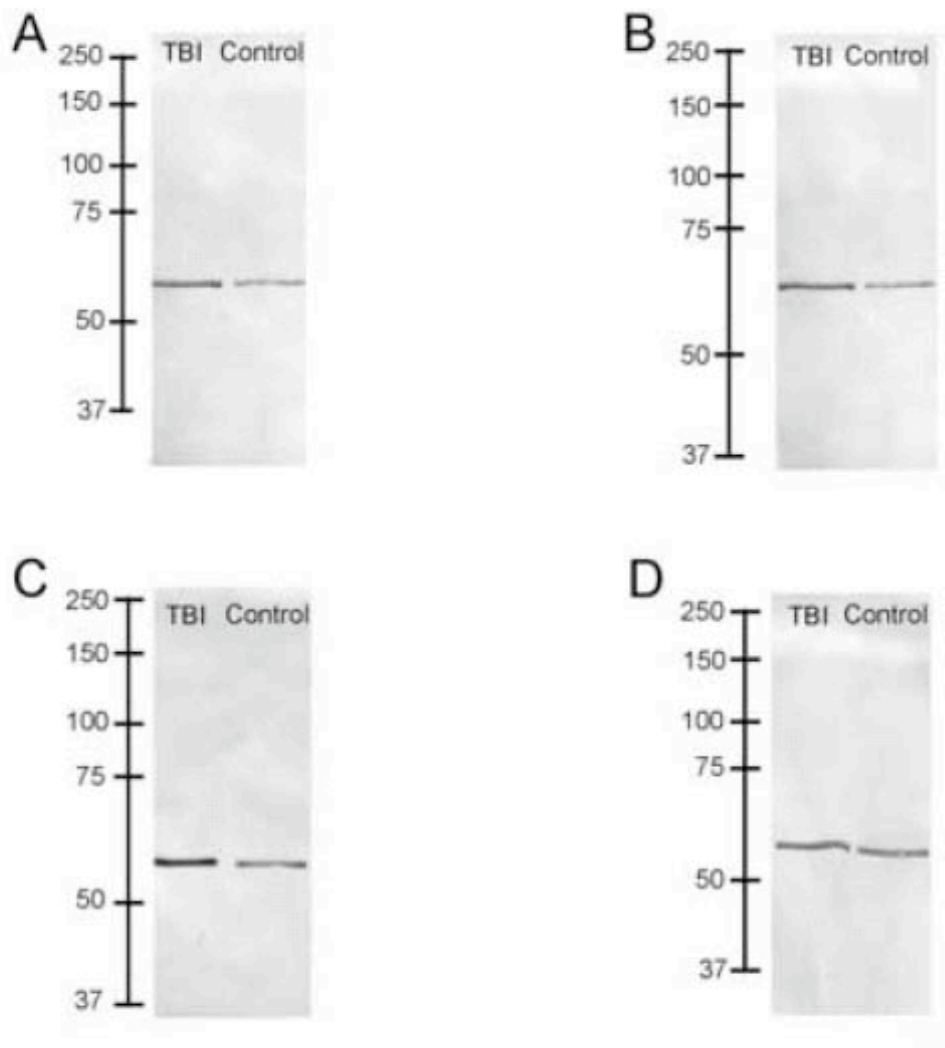

Figure 21: CaN immunoreactivity in crude SPM isolated from cortical tissue was elevated for 2 weeks post-TBI

In crude SPM isolated from the cortex of injured animals, a marked increase in CaN immunoreactivity was present 24h (A), one week (B), and two weeks post injury (C). CaN A immunoreactivity returned to baseline at three weeks postinjury (D) and remained similar to control values at four weeks post-injury (not shown).

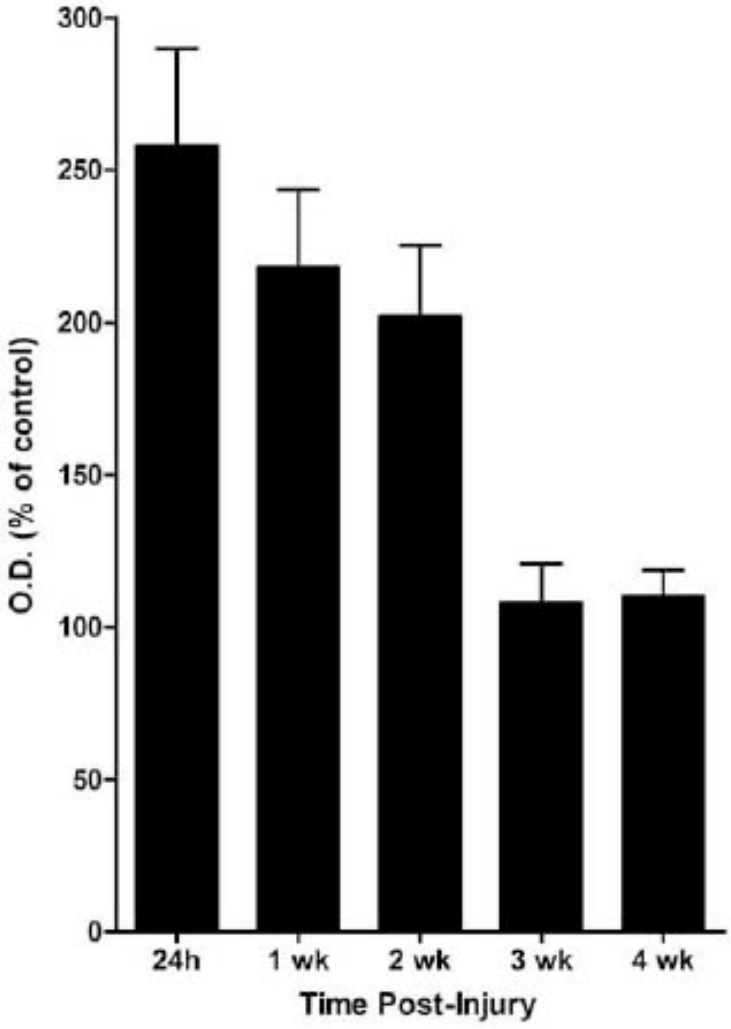

Figure 22: Calibrated densitometry of cortical crude SPM westerns reveals a significant increase in CaN A immunoreactivity

Optical density was calculated using a calibrated densitometer. CaN immunoreactivity was significantly increased over sham-control values at 24h ($p < 0.01$, n=6, Student's t-test), one week ($p < 0.01$, $n = 6$), and two weeks post-injury ($p < 0.01$, n=6). At both three and four weeks post-TBI, CaN immunoreactivity was indistinguishable from sham-control values ($p > 0.05$, n=6).

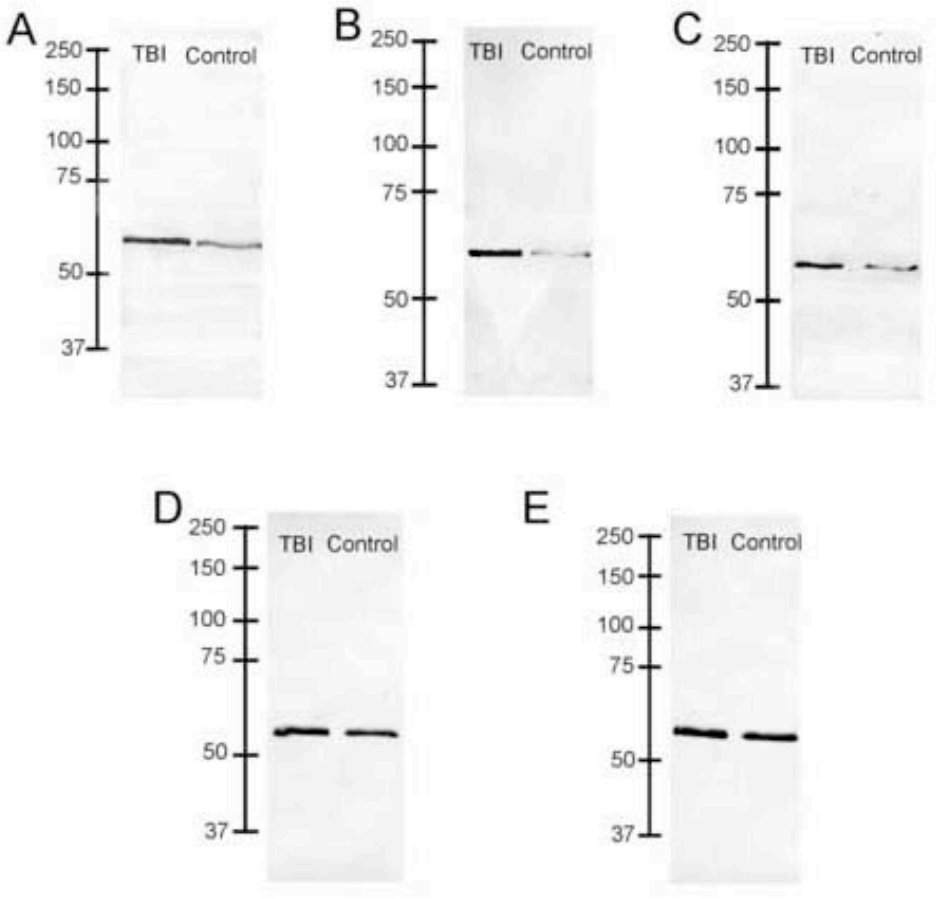

Figure 23: CaN immunoreactivity in crude SPM isolated from hippocampal tissue was elevated up to 4 weeks post-injury

In crude SPM isolated from hippocampal tissue, increased CaN A immunoreactivity was observed in injured animals 24h (A), one week (B), two weeks (C), three weeks (D) and four weeks (E) post-injury. Although the alteration in CaN A immunoreactivity decreased with time, CaN A levels in the hippocampus did not return to control values during the span of this study.

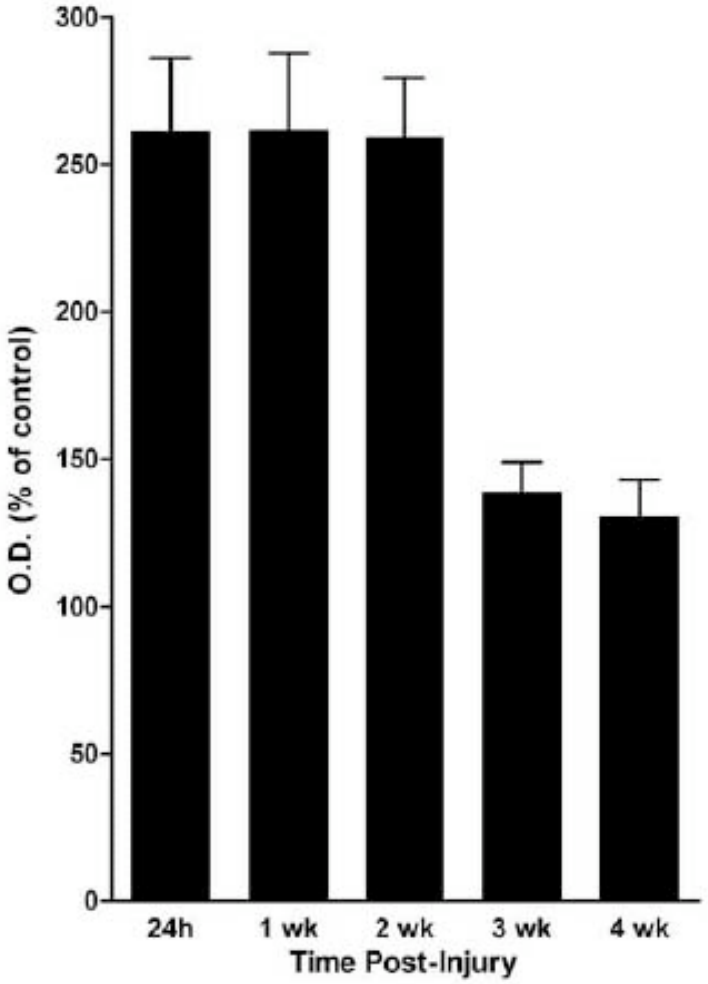

Figure 24: Calibrated densitometry of hippocampal crude SPM westerns demonstrates a significant increase in CaN A immunoreactivity

Optical density was calculated using a calibrated densitometer. CaN immunoreactivity was significantly increased over their respective sham-control values at 24h ($p < 0.001$, $n = 6$, Student's t-test), one week ($p < 0.01$, $n = 6$), two weeks ($p < 0.01$, $n=6$), three weeks ($p < 0.05$, $n = 6$), and four weeks post-injury ($p < 0.05$, $n = 6$). The increase in hippocampal CaN A immunoreactivity trended toward control values over time.

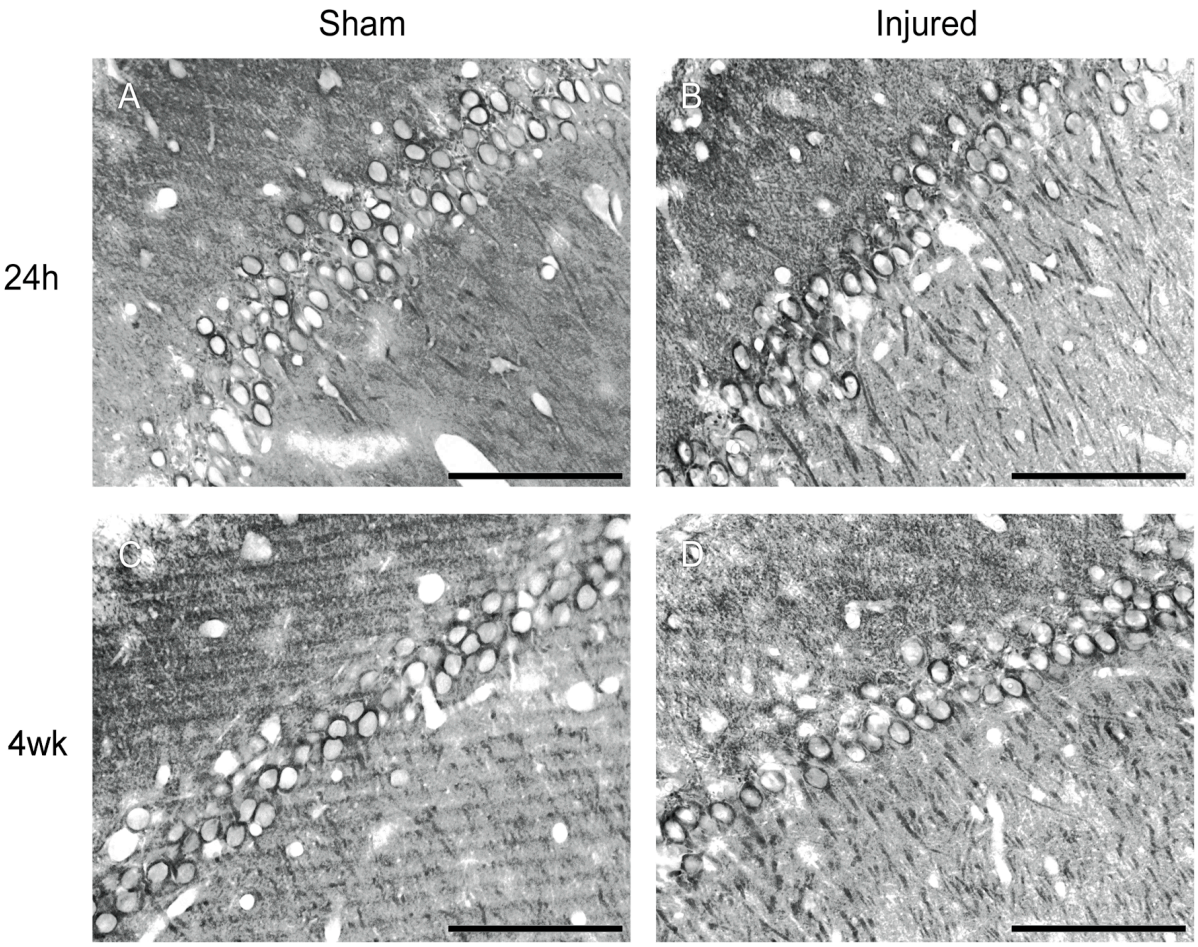

Figure 25: TBI induced an increase in CaN A immunoreactivity in apical dendrites of hippocampal CA1 neurons

Immunohistochemistry of sham-operated animals revealed diffuse CaN A immunoreactivity around the cell bodies of CA1 neurons at both 24h (A) and four weeks (C). In injured animals, CaN A immunoreactivity was far more intense than control in the apical dendrites of these neurons 24h post-injury, allowing numerous dendritic processes to be visualized (B). The injury-induced alteration in CaN A staining remained present four weeks post-injury, although qualitatively less intense (D). (representative slices shown, n=3).

CHAPTER V

A CELLULAR MECHANISM FOR DENDRITIC SPINE LOSS IN THE PILOCARPINE MODEL OF STATUS EPILEPTICUS

INTRODUCTION:

Status epilepticus (SE) is a severe neurological emergency characterized by persistent, continuous seizure activity [233]. In addition to an immediate risk of mortality, patients experiencing SE are at risk for a number of chronic neurological pathologies as a consequence of the seizure episode, including cognitive impairment, focal neurological deficits, and the development of chronic epilepsy [105, 116, 124]. A number of SE-induced biochemical and morphological changes in the brain have been investigated as possible causes of this long-term pathology. One recent finding that may have relevance to this subject is the SE-induced loss of dendritic spines [234].

Dendritic spines are small, dynamic protuberances from the dendritic shaft that are critical for synaptic transmission throughout the CNS, representing the primary location of excitatory glutamatergic neurotransmission [235]. The presence of dendritic spines is thought to aid neurotransmission in several ways, both by increasing the surface area for synaptic contact and by providing a specialized compartment for the excitatory postsynaptic machinery [236]. The

importance of these spines to excitatory neurotransmisson, and the apparent ability of neurons to alter spine density, size and shape in response to synaptic input, makes them an ideal location for regulation of synaptic strength. In fact, spine plasticity has been noted as a possible mechanism of long-term potentiation/depression [80] and has been implicated in several models of learning and memory [237-239].

Interestingly, profound decreases in dendritic spine density, as well as alterations in spine shape and size, have been detected in both SE and several models of chronic epilepsy [234, 240-242]. Although the precise physiological consequence of this pathological spine plasticity has not yet been elucidated, several possible theories have been proposed. SE and epilepsy have both been associated with long-term cognitive deficiencies [116], and a widespread and chronic loss of dendritic spine density could certainly play a major role in this pathology, especially considering the importance of spines in learning and memory models [237]. On the other hand, SE-induced spine plasticity may also represent a potential mechanism of epileptogenesis, in which the loss of dendritic spines is part of a pathological reorganization of synaptic networks leading to an overall increase in neuronal excitability [243]. In spite of the uncertainty about the pathological consequences of SE-induced spine plasticity, such a widespread alteration in the structure of excitatory synapses remains an important and highly interesting consequence of SE and certainly merits continued investigation.

Unfortunately, the biological mechanisms responsible for this SE-induced spine plasticity remain poorly understood as well. One potential mechanism

involves the calcium-regulated phosphatase, calcineurin (CaN). The cytoskeleton of spines is composed primarily of actin filaments, and CaN has been shown to regulate actin stability in a number of neuronal settings, including axonal growth cones and dendrites. Additionally, activation of CaN by NMDA-receptor associated calcium influx has been shown to destabilize F-actin in dendritic spines, and CaN and F-actin are co-localized in dendritic spines under these conditions [79]. Finally, recent research has demonstrated an SE-induced increase in CaN activity and enzyme concentration in post-synaptic regions of neurons [167, 217]. Thus an enzyme capable of regulating the structure of dendritic spines is both activated and localized into the vicinity of the spines in SE, placing CaN in an ideal position to play a role in SE-induced spine plasticity.

The present study investigated the CaN-dependent regulation of actin stability in the context of SE-induced dendritic spine loss. We demonstrate an SE-dependent dephosphorylation of cofilin, an actin-depolymerizing factor that is activated by dephosphorylation. We also show a subsequent increase in cofilin-actin binding and actin depolymerization. All of these SE-induced cytoskeletal events are shown to be blocked by pre-administration of the CaN inhibitors, FK506 (tacrolimus) and cyclosporin A, strongly suggesting a CaN-dependent mechanism. Finally, SE-induced dendritic spine loss was demonstrated histologically in several brain regions, this spine loss was also blocked by the administration of CaN inhibitors. These findings implicate CaN in a widespread, SE-induced alteration in the structure of synaptic contacts, potentially furthering

our understanding of the cellular mechanisms underlying chronic SE-induced neurological pathology.

METHODS:

Pilocarpine model of status epilepticus:

All animal-use procedures were in strict accordance with the National Institutes of Health Guide for the Care and Use of Laboratory Animals and were approved by the Virginia Commonwealth University Institutional Animal Care and Use Committee. Adult Sprague-Dawley rats were handled after arrival from Harlan Laboratories, for acclimation to handling before drug treatment. One week before the induction of SE, four surface electrodes were implanted into the skulls of rats under ketamine anesthesia, as described previously [244]. Two frontal electrodes were implanted over frontal cortex [3.5 mm anterior to bregma, ±2.5 mm L/R (F1/F2)]. Two posterior electrodes were implanted over parietal cortex and hippocampus [2.0 mm posterior to bregma, ±2.5 mm L/R (P1/P2)]. A fifth electrode was fixed onto the surface of the skull as a ground. The electrodes were secured in place with dental acrylate, and the animals were allowed ≥5 days to recover from surgery before experiments were performed.

Twenty minutes before the injection of pilocarpine, methylscopolamine, a muscarinic antagonist, was administered i.p. (1 mg/kg) to reduce adverse peripheral affects of the pilocarpine. Where appropriate, 10 mg/kg cyclosporin A

(Sigma) or 5 mg/kg FK506 (Fujisawa) was administered i.v. (tail vein) 3 hours prior to the induction of SE. Control and sham-surgery animals were attached to video-EEG machines (BMSI 5000; Nicolet**,** Madison, WI), and baseline EEG recordings were obtained for ≥10 min after scopolamine injection. SE was induced in experimental animals by i.p. injection of 375 mg/kg pilocarpine HCl, a muscarinic agonist. Behavioral and encephalographic activities were recorded throughout the procedure [244]. Once initial seizure activity was observed, the time was noted, and rats were allowed to seize for specific amounts of time before the animals were processed. These time points consisted of 10, 15, 20, 30, 40, 50, 60, and 70 min after the first discrete seizure. Since our laboratory has previously characterized SE onset as being 10 min after the first discrete seizure [244], these times approximate 0, 5, 10, 20, 30, 40, 50, and 60 min of SE, respectively. Behavioral seizures were assessed according to the scale of Racine [142].

Brain region isolation and subcellular fractionation:

Rats were rapidly decapitated after specific durations of SE. Brains were rapidly dissected on a petri dish on ice to preserve postmortem enzyme activity. Cortical and hippocampal brain regions were quickly isolated and immediately homogenized with 10 strokes (up and down) at 12,000 rpm, using a motorized homogenizer (TRI-R Instruments, Inc., Rockville Center, NY). Brain regions were homogenized into an ice-cold isotonic homogenization buffer containing 10 mM Tris-HCl (pH 7.0), 7 mM EGTA, 5 mM EDTA, 1 mM dithiothreitol (DTT), 0.3 mM

PMSF, and 187 mM sucrose. Cortical regions were homogenized into 7 ml of buffer and hippocampal regions into 3 ml. All brain homogenates were then subjected to the differential centrifugation procedure described below.

Isolation of crude synaptoplasmic membrane fractions was achieved using a differential centrifugation procedure [168] modified as described previously [217, 245]. Briefly, brain region homogenates were centrifuged at 5000*g* for 10 min to produce a crude nuclear pellet (P1) and a supernatant (S1). The P1 pellet was resuspended in homogenization buffer, separated into aliquots, and stored at -80°C. The S1 was centrifuged for 30 min at 18,000*g* to produce the crude synaptoplasmic membrane/ mitochondrial pellet (P2) and a supernatant (S2). The P2 pellet was resuspended in 1/10 the original volume of the homogenate (700 μl for cortex, 300 μl for hippocampus), separated into aliquots, and stored at -80°C until used.

Western analysis:

Western analysis was performed in a manner similar to that described previously [217]. Briefly, fractions were balanced for protein using the Bradford method [144], resolved on SDS-PAGE, and transferred to a nitrocellulose membrane using the Trans-blot system with the plates in the high-intensity field configuration (BioRad, Richmond, CA). Nitrocellulose was then immersed for 1 h in blocking solution, containing phosphate buffered saline (PBS, pH 7.4), 0.05% (v/v) polyoxyethylene sorbitan monolaurate (Tween 20), and 2.5% Bio-Rad blotting grade dry milk. The nitrocellulose membrane was then incubated with the

appropriate primary antibody in blocking solution for 1 h. Anti-CaN A antibody (clone CN-A1, mouse monoclonal IgG, Sigma Chemical Co.) was diluted 1:10,000, anti-actin antibody was diluted 1:5000, DARRP-32 antibody was diluted 1:1000, and anti-cofilin (Chemicon) and anti-phosphocofilin (Chemicon) were diluted 1:500 for western analysis. Membranes were then washed three times in a wash solution containing PBS, Tween 20, and dry milk. Next, nitrocellulose was reacted with the appropriate HRP-conjugated secondary antibody in blocking solution for 30 min, then washed 3X in PBS/Tween for 10 minutes each wash. Finally, blots were reacted with a luminol reagent for 5 minutes (Pierce Pico-sensitive reagent for CaN A and actin studies, Pierce Femto-sensitive reagent for cofilin and phospho-cofilin staining). Blots were immediately exposed to x-ray film (Kodak X-OMAT). Films were developed using a Kodak X-OMAT developer. Specific immunoreactive bands were quantified by computer-assisted densitometry (GS-800 calibrated densitometer and Quantity One software, BioRad) and compared to a linear concentration curve as described previously [146].

Immunoprecipitation:

Homogenates were spun at 5000 x g for 5 min to clear large insoluble material. All samples were balanced to ensure equivalent protein content, 500 μg of protein was incubated on a rotating rack with anti-cofilin antibody diluted 1:50 (Chemicon) overnight at 4º C. 30 μL of protein-A agarose beads were then added to the sample and incubated (rotating) for 3h at 4º C. The beads were then

precipitated by spinning the samples at 2000 x g for 2 minutes. The resulting pellet was washed 3X in phosphate buffered saline with 1% triton X-100. The pellet was then suspended in SDS sample buffer, placed in a boiling water bath for 5 minutes, and subjected to SDS-PAGE.

Actin polymerization assay:

Actin polymerization was assayed using the differential solubility of F-actin and G-actin in 1% triton. Samples were incubated in 1% triton for 1h at 4° C, then subjected to a 1h centrifugation at 100,000 x g. The resulting supernatant and pellet were balanced for protein concentration, then run on a 10% SDS-PAGE gel and subjected to western analysis as described previously. The ratio of the amounts of actin present in these two fractions was used to provide an estimate of the actin polymerization state in different brain region isolates.

Rapid Golgi impregnation:

Visualization of dendritic spines was accomplished via a modification of the single-section rapid Golgi procedure described previously [246]. After 1h of SE, animals were anesthetized with an overdose of sodium pentobarbital and transcardially perfused with 10% neutral buffered formalin. Brains were removed and postfixed overnight in 10% neutral buffered formalin, then sectioned into deionized water at 100 μm on a vibratome (Leica VT-1000S). Sections were then incubated 30 min at room temperature in a solution containing 0.5% osmium tetroxide, followed by a 2h incubation in a solution of 3.5% potassium

dichromate. Sections were removed from the dichromate solution and placed on a glass slide with a few drops of dichromate surrounding the section. A second slide was placed on top of the section, and the two slides were spaced apart from one another by a glass coverslip. The entire assembly was held together with cyanoacrylate-based glue. This assembly was placed in a solution of 1% silver nitrate and kept in the dark on a shaker for 6-12h. The slide/coverslip assembly was then disassembled and the slides rinsed in deionized water. Sections were then dehydrated through a series of increasing ethanol concentrations, cleared with xylene, and mounted on slides with glass coverslips using Permount. Slides were examined under 40X and 100X oil immersion objectives (400X and 1000X final magnification). A minimum of 3 neurons were studied per slide, and at least 3 slides were examined per animal. Photographic images were obtained with an Olympus Q-fire camera and processed with Adobe Photoshop CS.

Statistical analysis:

EEG review and analysis was performed using Insight II software (Persyst, Prescott, AZ). All statistical analysis was performed using GraphPad Prism 4.0 (GraphPad Software, San Diego, CA). For multiple group comparisons, ANOVA with Tukey post-hoc analysis was used with a minimum significance level of $p < 0.05$. All data is presented as mean ± SEM unless otherwise noted.

RESULTS:

SE induces a rapid increase in CaN activity and concentration in post-synaptic regions:

Previous studies in our laboratory described a dramatic increase in CaN immunoreactivity in post-synaptic neuronal regions after 1 hour of SE [217]. This places highly elevated amounts of CaN in an ideal location to regulate synaptic transmission through a number of post-synaptic mechanisms, including alteration of the dendritic cytoskeleton. The present study expands upon these results through the use of video-EEG monitoring, which allowed us to obtain tissue at highly precise time-points during SE, thus providing a temporal profile of SE-induced alterations in CaN activity and distribution.

Crude SPM fractions were isolated at specific times after the first discrete seizure as described previously [244], and western analysis for CaN was carried out to determine the CaN content of SPM isolated from both control and SE animals at several time-points. Fractions were analyzed from both cortical and hippocampal tissues, as these were the brain regions previously shown to demonstrate an increase in SPM CaN immunoreactivity. In both cortical and hippocampal samples, SPM CaN immunoreactivity was not significantly different from control at 10 minutes post-first discrete seizure (a time-point corresponding to the onset of status epilepticus). However, at 15 minutes post-first discrete seizure and all subsequent time points, CaN immunoreactivity was significantly increased over control values in both cortical and hippocampal SPM (Fig 26).

Using a pNPP-based phosphatase assay as described previously [167], we also examined CaN phosphatase activity at the above time-points in cortical and hippocampal crude SPM fractions (Fig 27). Similar to the increase in CaN concentration, CaN activity approximately doubled shortly after the onset of continuous seizure activity in both cortical and hippocampal crude SPM. This increase in activity is of roughly the same magnitude as the increase in CaN concentration described above, and is likely due to the increased quantity of the enzyme present in this fraction after the onset of SE. Interestingly, an additional increase in CaN activity – beyond the 2-fold increase observed at 10 minutes – was observed in cortical and hippocampal SPM fractions 30 minutes after the first discrete seizure. This increase in activity did not correspond to a further increase in CaN immunoreactivity in the crude SPM fraction. A similar increase in CaN activity is also observed in homogenates at this later time point [247]; we have previously hypothesized that this further increase in CaN activity represents a post-translational modification of the enzyme brought on by SE [167].

To further characterize the SE-induced increase in synaptic CaN concentration and activity, we examined the phosphorylation state of a known neuronal CaN substrate, DARRP-32 (Fig 28). In both cortical and hippocampal fractions, SE induced a profound dephosphorylation of DARRP-32. This dephosphorylation could be blocked by administration of FK506 or cyclosporin A prior to the induction of SE, indicating that SE-induced dephosphorylation of these substrates was CaN-dependent. In cortical SPM, phospho-DARRP-32 immunoreactivity was 12.3 ± 10.2% of control after SE, while immunoreactivity

was 62.1 ± 7.3% of control in animals that were treated with FK506 and 45.8 ± 9.1% of control in animals that were treated with cyclosporin A. Similar results were achieved in hippocampal tissue (data not shown). The CaN-dependent, SE-induced dephosphorylation of this substrate further demonstrates the dramatic increase in synaptic CaN activity that is present in SE, and confirms the efficacy of the CaN inhibitors used in this study.

Finally, the SE-induced increase in CaN enzyme activity in crude SPM was examined using an RII phosphopeptide-based assay. This assay allows the detection of phosphate released from a CaN-specific peptide substrate. Increases in CaN activity similar to those described with the pNPP assay were present in this assay as well. CaN activity increased after 1 hour of SE in both cortical (Fig 29A) and hippocampal (Fig 29B) crude SPM fractions.

The above results, taken together with our previous studies, demonstrate a significant increase in CaN activity and concentration in the post-synaptic regions of neurons shortly after the onset of continuous seizure activity.

CaN-dependent cofilin dephosphorylation in SE:

To determine the cellular consequences of the SE-induced increase in post-synaptic CaN activity, we examined the effect of SE on the stability of the dendritic cytoskeleton, and consequently on dendritic spine plasticity. CaN may regulate the stability of dendritc actin via cofilin, a CaN-regulated actin depolymerization factor. Through the use of a phospho-specific cofilin antibody we were able to assess the phosphorylation state of cofilin after SE, both with

and without the administration of CaN inhibitors. In both homogenates and crude SPM fractions isolated from SE animals, we found a significant dephosphorylation of cofilin in cortical and hippocampal samples. In cortical SPM, phospho-cofilin immunoreactivity was decreased 54.2 ± 12.3 % from control after 1h of SE (Fig 30A), while in hippocampal SPM phospho-cofilin levels decreased 74.1 ± 13.2 % from control (Fig 30B). A similar SE-induced decrease in cofilin phosphorylation was observed in homogenates from these brain regions, indicating that the effect was not an artifact of the SPM isolation procedure (data not shown). Overall cofilin immunoreactivity was not significantly affected by SE in any fraction tested (Fig 30 C, D), indicating that the observed decrease in phospho-cofilin was likely due to dephosphorylation of the protein rather than a decrease in the amount of cofilin present in the neuron.

To determine if the SE-induced dephosphorylation of cofilin was CaN-dependent, we administered CaN inhibitors, FK506 or cyclosporin A, to animals prior to induction of SE. In FK506-treated animals, SE decreased phospho-cofilin immunoreactivity by 18.2 ± 13.0% in cortical SPM (Fig 30A), and 37.1 ± 14.6% in hippocampal SPM (Fig 30B). While SE still induced some cofilin dephosphorylation in these FK506-treated animals, phospho-cofilin immunoreactivity was significantly greater in SPM samples from FK506-treated animals than in untreated SE animals, indicating that SE-induced cofilin dephosphorylation was at least partially CaN-dependent. Similar results were achieved by treating animals with cyclosporin A prior to SE. Phosphocofilin immunoreactivity was decreased 32.9 ± 9.7% in cortical SPM and 38.6 ± 11.7%

in hippocampal SPM isolated from cyclosporin A animals when compared to control (Fig 30 A, B). These values were significantly greater than the cofilin phosphorylation levels in untreated SE animals. The fact that two different CaN inhibitors (with different mechanisms of action) were effective in preventing SE-induced cofilin dephosphorylation provides a strong argument that CaN inhibition was indeed the important factor in preventing cofilin dephosphorylation, rather than some side-effect of the inhibitors. This data suggests that increased dendritic CaN activity leads to cofilin dephosphorylation after SE. While this study is the first to present such a finding, the data corresponds well with previous research detailing CaN's effects on cofilin and actin stability.

Time-course of cofilin dephosphorylation:

Western blot analysis was used to determine the phosphocofilin immunoreactivity by western blot at specific time-points post-first discrete seizure. Both cortical and hippocampal crude SPM isolates were examined, using control and pilocarpine-treated animals. In both cortical and hippocampal samples, cofilin phosphorylation levels decreased significantly from control levels after just 10 minutes of seizures, a time point which generally corresponded with the onset of continuous seizure activity. At 10 minutes post-first discrete seizure, phosphocofilin immunoreactivity was decreased 40.2 ± 6.7% from control in cortical samples (Fig 31A) and 60.1 ± 8.3% in hippocampal samples (Fig 31B). At the 20 and 40 minute time points, phosphocofilin immunoreactivity was indistinguishable from the 70 minute time point presented earlier. It is interesting

to note the speed with which cofilin phosphorylation responds to seizure activity, suggesting that even a few minutes of continuous seizure activity may be sufficient to induce widespread activation of this protein. We also noted that the temporal profile of cofilin dephosphorylation correlates with the timing of the increase in dendritic CaN activity, providing further support for the idea that CaN is partially responsible for SE-induced cofilin activation.

SE increases cofilin-actin binding:

Upon activation by dephosphorylation, cofilin binds tightly to F-actin at specific sites, leading to actin depolymerization. To study this binding, we utilized a co-immunoprecipitation protocol. Cofilin-associated actin was then measured via western analysis of the precipitate.

After one hour of SE, there was a profound increase in cofilin-actin co-immunoprecipitation. In cortical samples, actin immunoreactivity was 167.0 ± 20.1% of control values in the precipitate (Fig 32A, B), suggesting an approximately 1.5-fold increase in cofilin-actin binding. Similar results were achieved in hippocampal samples, with actin immunoreactivity increased by 201.3 ±17.6% in cofilin immunoprecipitates from SE animals (Fig 32C, D). When the precipitation procedure was carried out in the absence of anti-cofilin antibody, a minimal amount of actin was present in the precipitate, indicating that the primary source of actin immunoreactivity was actin that was bound to cofilin and co-precipitated with it.

Both FK506 and cyclosporin A significantly reduced cofilin-actin co-immunoprecipitation. Pretreatment of animals with FK506 resulted in a SE-induced cofilin-actin co-immunoprecipitation that was 102.9 ± 3% of control in cortical samples (Fig 32A, B) and 121.3 ± 8.2% of control in hippocampal samples (Fig 32C, D). Both of these values are significantly lower than those of untreated SE animals, suggesting that CaN inhibition prevents cofilin-actin binding. Similar results were achieved with cyclosporin A. This data complements our finding that CaN inhibition prevents SE-induced cofilin dephosphorylation, since dephosphorylation of cofilin is required for the protein to bind to actin.

SE induced actin depolymerization is CaN-dependent:

Following dephosphorylation and actin binding, cofilin induces depolymerization of F-actin to G-actin. To study this next step in our hypothesized pathway of SE-induced, CaN-mediated spine loss, we quantified the relative amounts of F and G-actin present in cortical and hippocampal SPM after SE. To accomplish this, we made use of the fact that F-actin is insoluble in 1% Triton X-100, while G-actin remains soluble. SPM fractions were treated with Triton and centrifuged to precipitate insoluble material, thus separating F-actin from G-actin. Both the pellet and supernatant were subjected to SDS-PAGE and western analysis to quantify the amount of actin present.

In crude SPM isolated from SE cortex, Triton-soluble actin immunoreactivity was 123.2 ± 8.1 % of control (Fig 33A), while Triton-insoluble actin immunoreactivity was 79.3 ± 6.7 % of control (Fig 33B), indicating an SE-

induced shift from F-actin to G-actin in the crude SPM. A similar change was noted in hippocampal samples, with Triton-soluble actin immunoreactivity 121.9 ± 7.4% of control (Fig 33C), while insoluble actin immunoreactivity was 71.3 ± 5.4% of control (Fig 33D), again demonstrating a decrease in F-actin and an increase in G-actin. Overall actin immunoreactivity in this fraction was unchanged by SE. In both cortical and hippocampal homogenates, FK506 significantly reduced this actin depolymerization, partially preventing the SE-induced increases in Triton-soluble actin immunoreactivity (G-actin) and the decreases in Triton-insoluble actin immunoreactivity (F-actin). Thus, by blocking the first step in this pathway – the CaN-induced dephosphorylation of cofilin – we prevented the final biochemical step of actin depolymerization.

CaN inhibitors prevent dendritic spine loss in SE:

The preceding results demonstrate that CaN-mediated cofilin dephosphorylation leads to actin depolymerization in SE. Actin is the primary component of the dendritic spine cytoskeleton, and spine morphogenesis and retraction require actin depolymerization. CaN-mediated actin depolymerization, therefore, may likely lead to dendritic spine loss in SE. We studied dendritic spine density in SE via a modification of the rapid Golgi impregnation procedure (Fig 34). This procedure has the advantage of staining neuronal processes in their entirety, allowing excellent visualization of dendritic arbors and spines. We examined neurons in frontal cortex, parietal cortex, and several hippocampal

subfields, including CA1, CA3 and dentate gyrus in sections from control animals, SE animals, and FK506-treated SE animals.

Previous studies have demonstrated a significant SE-induced loss of dendritic spines in the granule cells of the dentate gyrus. These results were confirmed in the present study with the Golgi technique. In control animals, numerous spines could be observed on all dendritic branches of the DG granule cells (Fig 34B). Following SE, spine density decreased remarkably, with few spines observed on any dendrites in the DG, a result consistent with previous studies (Fig 34C). Administration of the CaN inhibitor FK506 prevented SE-induced spine loss (Fig 34D). In dentate gyrus granule cells, FK506-treated animals had an observed spine density that was qualitatively far greater than that of untreated SE animals, and appeared similar to control. This data strongly suggests a CaN-dependent mechanism of spine loss in SE, such as the CaN-dependent activation of cofilin described above.

DISCUSSION:

The results presented in this study demonstrate a CaN-dependent mechanism of dendritic spine loss in the pilocarpine model of SE. A dramatic increase in CaN activity and concentration occurs in the crude SPM fraction of hippocampal and cortical tissues at or near the onset of continuous seizure activity. Coupled with our previous histochemical results [217], this demonstrates an increase in the effective amount of CaN phosphatase activity in dendritic regions of neurons. This study elucidated one pathological consequence of this

increased post-synaptic CaN activity by examining CaN's effects on dendritic actin stability. First, we have shown a CaN-dependent dephosphorylation of the actin-depolymerizing factor, cofilin. Like the increase in CaN concentration and activity, this dephosphorylation develops shortly after the onset of SE. The expected biochemical consequences of an SE-induced activation of cofilin were also found to occur in a CaN-mediated manner, with a SE-dependent increase in cofilin-actin binding and a subsequent SE-induced depolymerization of dendritic actin. Finally, the CaN-dependent depolymerization of dendritic actin led to SE-induced dendritic spine loss, which was demonstrated histologically in several brain regions and was blocked with the CaN inhibitor FK506. These findings implicate CaN in a widespread, SE-induced alteration in the structure of synaptic contacts, proving our hypothesis that SE-induced dendritic spine loss is CaN-dependent via cofilin. These findings also potentially further our understanding of the cellular mechanisms underlying chronic SE-induced neurological pathology.

SE, Epilepsy and Spine Loss:

The observed SE-induced reduction in dendritic spine density may be part of the long-term neurological pathology that is associated with SE. As the primary site of excitatory neuronal synapses, and given their importance in models of learning and memory, spines appear to be critical for normal cognition. Studies in animal models have documented cognitive difficulties associated with SE, both in adult and developing animals [116]. While SE-induced neuronal death undoubtedly accounts for some of this loss of cognitive function, other, more

subtle, mechanisms – such as spine loss – are likely responsible as well. Depending on the duration of the SE-induced decrease in dendritic spine density, the mechanism described in this study could be a mechanism underlying SE-induced cognitive dysfunction. In one previous study, dendritic spine density rebounded in the weeks following SE, although with significant alterations in spine morphology and location. Spine density then decreased again – possibly through a different mechanism – once chronic seizure activity ensued (spontaneous recurrent seizures are a common consequence of the pilocarpine model of SE) [240]. These findings tend to argue against the acute mechanism of spine loss described in this study as the cause of long-term cognitive dysfunction (although it may cause short-term deficits); however, they do suggest that it may be part of another chronic SE-associated pathology, epileptogenesis.

In the pilocarpine model of SE, spontaneous recurrent seizures typically begin approximately 2 weeks after the prolonged seizure episode. No epileptic activity is seen during this quiescent period, but there is a great deal happening on a cellular level. It is thought that the biochemical and structural changes that lead to recurrent seizure activity are being completed during this time. While the exact mechanisms responsible for epileptogenesis remain the subject of intense study and debate, dendritic spine plasticity certainly is a promising candidate for this role. The loss and subsequent regrowth of dendritic spines could represent a pathological reorganization of synaptic networks leading to the formation of epileptic foci in the brain. It is especially interesting that spine loss has been documented in the dentate gyrus of the hippocampus. Network reorganization

and neuronal hyperexcitability in this region are frequently proposed as possible mechanisms of epileptogenesis. Furthermore, after the SE-associated loss of spines, it has been shown that their regrowth in this region is colocalized with sites of mossy fiber sprouting [242]. Thus an outgrowth of axonal structures that has been previously implicated in epileptogenesis seems to coincide with a reorganization of post-synaptic structures, all of which is occurring in a region that seems to be critical in the development of temporal lobe epilepsy. Considered in the context of epileptogenesis, the CaN-mediated mechanism of spine loss presented in this paper may help explain the results of several other studies. FK506 ameliorated spine loss in the present study, while other researchers have documented that CaN inhibitors can prevent epileptogenesis in both a kainic acid model of SE [121] and a kindling model of epilepsy [122, 248]. Further research may determine if these two effects are related.

Cellular Mechanism of Spine Plasticity

Spine plasticity has long been observed in both chronic epilepsy and acute SE models [234], although the mechanisms that underlie this spine loss have not yet been determined. Like the increase in SPM CaN observed in this study, dendritic spine loss does not seem to occur with isolated, discrete seizure activity. Instead, spine loss only occurs in models that involve continuous seizure activity or chronic recurrent seizures, a characteristic that certainly fits with the observed behavior of CaN. Additionally, a great deal of research suggests that CaN modulates neuronal spine density and morphology under normal conditions,

with the enzyme having been previously shown to cause calcium-stimulated spine plasticity in several non-pathological model systems. Halpain et al. demonstrated a loss of spines in cultured hippocampal neurons in response to NMDA application. CaN was shown to co-localize with F-actin at synapses, and CaN inhibitors blocked NMDA-mediated spine loss in these neurons, strongly suggesting a CaN-mediated spine loss [79]. Simlarly, Zhou et al. described an LTD-associated spine shrinkage that required both NMDA and CaN to occur [80]. Under physiological conditions, it is highly probable that CaN-mediated spine plasticity is part of a learning and memory mechanism, considering the importance of both CaN and spines to learning models. However, with the profound increase in CaN levels at the synapse that we have observed in SE, this regulation of spine plasticity may become pathologically active, resulting in a detrimental reorganization of synaptic contacts.

The present study documented a profound increase in CaN concentration and activity in the crude SPM fraction of neuronal tissue of animals that had undergone as little as 5-10 minutes of continuous seizure activity. As we have described previously, continuous seizure activity typically began approximately 10 minutes after the first discrete seizure in this model [244]. No detectable increase was seen, however, in animals that experienced discrete, but not continuous, seizure activity, indicating that the onset of SE was essential for significant changes in CaN to occur. Such a translocation of CaN to the synapse may initially be a physiological defense mechanism for the neuron in the face of excessive excitation, as CaN is known to negatively modulate neurotransmission

through the AMPA and NMDA subtypes of glutamate receptor. Perhaps such a mechanism, occurring near the onset of continuous seizures, represents a pathway by which seizure activity can be terminated in brains that are not prone to SE. However, as SE progresses and worsens, this sustained increase in synaptic CaN activity also could play a pathological role in neurons. A number of recent studies support such a hypothesis. For example, it has long been known that administration of CaN inhibitors prior to SE prevents chronic SE-related behavioral pathologies, such as a SE-induced loss of cognitive abilities and the development of spontaneous continuous seizures [121]. Several mechanisms have been proposed as pathological roles for CaN in seizure disorders, including negative modulation of the GABA receptor [123, 249] and – the focus of the current study – modulation of dendritic spines.

CaN may perform this pathological modulation of spine morphology via its regulation of the actin-depolymerizing factor, cofilin. Cofilin is a small peptide that, when dephosphorylated, binds to F-actin and causes its depolymerization [250, 251]. Cofilin has been shown to regulate the structure of dendritic spines by inducing the depolymerization of their actin cytoskeleton [80, 82, 252]. Recent studies have shown that CaN induces cofilin dephosphorylation (and thus subsequent actin depolymerization) either directly [253], or, more likely, indirectly via an intermediary phosphatase known as slingshot [81], thus making a mechanism involving CaN activation of cofilin and subsequent spine loss quite plausible. In fact, one recent study has already shown spine loss in long-term depression through a mechanism dependent on both CaN and cofilin [80].

The data described in this study clearly indicate a CaN-dependent regulation of cofilin in SE. First, the SE-induced dephosphorylation of cofilin required the onset of continuous seizure activity, a requirement shared with the increase in SPM CaN and SE-induced dendritic spine loss. In fact, the timing of this loss of SPM cofilin phosphorylation coincides perfectly with the increase in SPM CaN concentration and activity. Furthermore, both of the CaN inhibitors cyclosporin A and FK506 blocked SE-induced cofilin dephosphorylation. The fact that two different CaN inhibitors blocked SE-induced cofilin dephosphorylation strongly argues in favor of a CaN-dependent mechanism, although some modest SE-induced dephosphorylation did occur in the presence of effective doses of each inhibitor. This is not in itself surprising, as a number of other mechanisms exist for the regulation of cofilin phosphorylation. Activation of these pathways in SE is certainly possible, and merits future study. However, CaN-mediated dephosphorylation represented a major portion of the observed decrease in phosphocofilin immunoreactivity. This CaN-dependent dephosphorylation of cofilin did indeed activate the molecule, as SE was also shown to lead to a CaN-dependent increase in cofilin-actin binding and a CaN-dependent depolymerization of actin. While the observed change in the F/G actin ratio was relatively modest, when one considers the prevalence of actin in all cell types and cellular structures in the brain, even a 20% difference in the relative amounts of F- and G- actually represents a quite profound structural change. This structural change manifested itself in a CaN-dependent loss of dendritic spines. As other researchers have previously, we observed a SE-dependent loss of

dendritic spines after 1 hour of SE. Considering the timing of the CaN-induced cofilin dephosphorylation, this loss of spines may, in fact, have occurred even earlier in SE, and future studies should certainly explore synaptic changes at these earlier time-points.

The novel findings presented in this study describe a cellular mechanism for actin depolymerization and dendritic spine loss in the pilocarpine model of SE. This spine loss is widespread throughout the forebrain after SE, and is CaN-dependent, involving the actin depolymerizing factor, cofilin. Further research in this area may help elucidate the role of dendritic spine plasticity in SE-associated neuronal pathologies, potentially provide insight into some of the mechanisms underlying epileptogenesis and providing the basis for future treatment options.

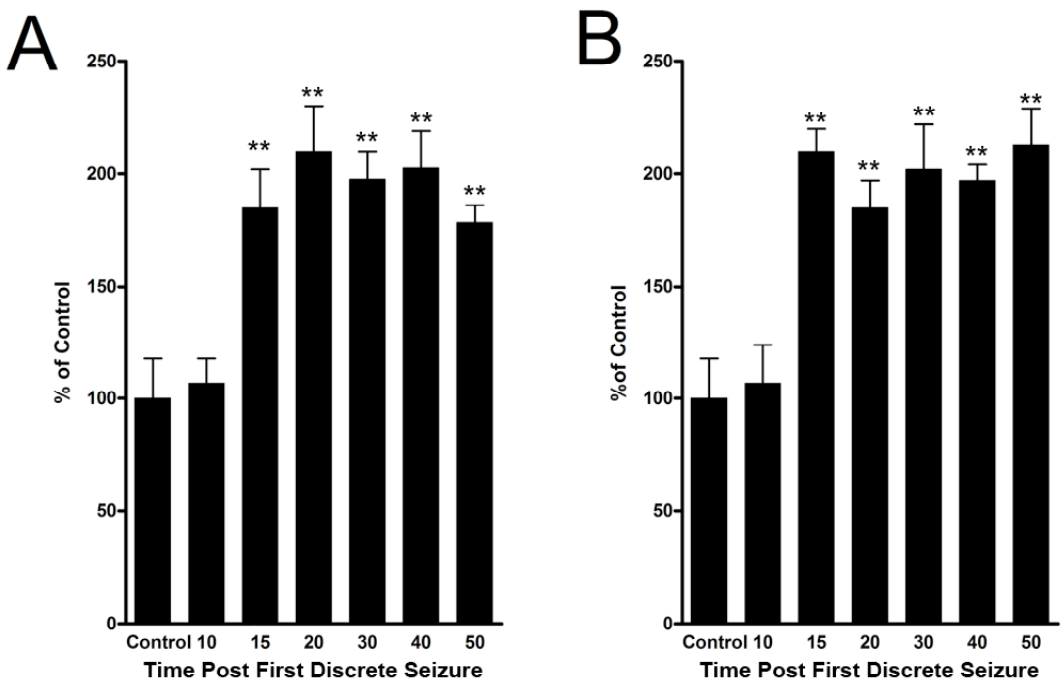

Figure 26: The seizure-induced increase in crude SPM CaN immunoreactivity occurs near the onset of SE. CaN immunoreactivity was measured in crude SPM fractions isolated from cortex (A) and hippocampus (B). In both fractions, CaN immunoreactivity was found to be increased significantly above control values at 15 minutes post-first discrete seizure, or approximately 5 minutes after the onset of continuous seizure activity. CaN immunoreactivity doubled at this time-point in both cortical and hippocampal SPM, and remained similarly elevated at all subsequent time-points. (** $p < 0.01$, $n = 3$ per time-point, student's t-test).

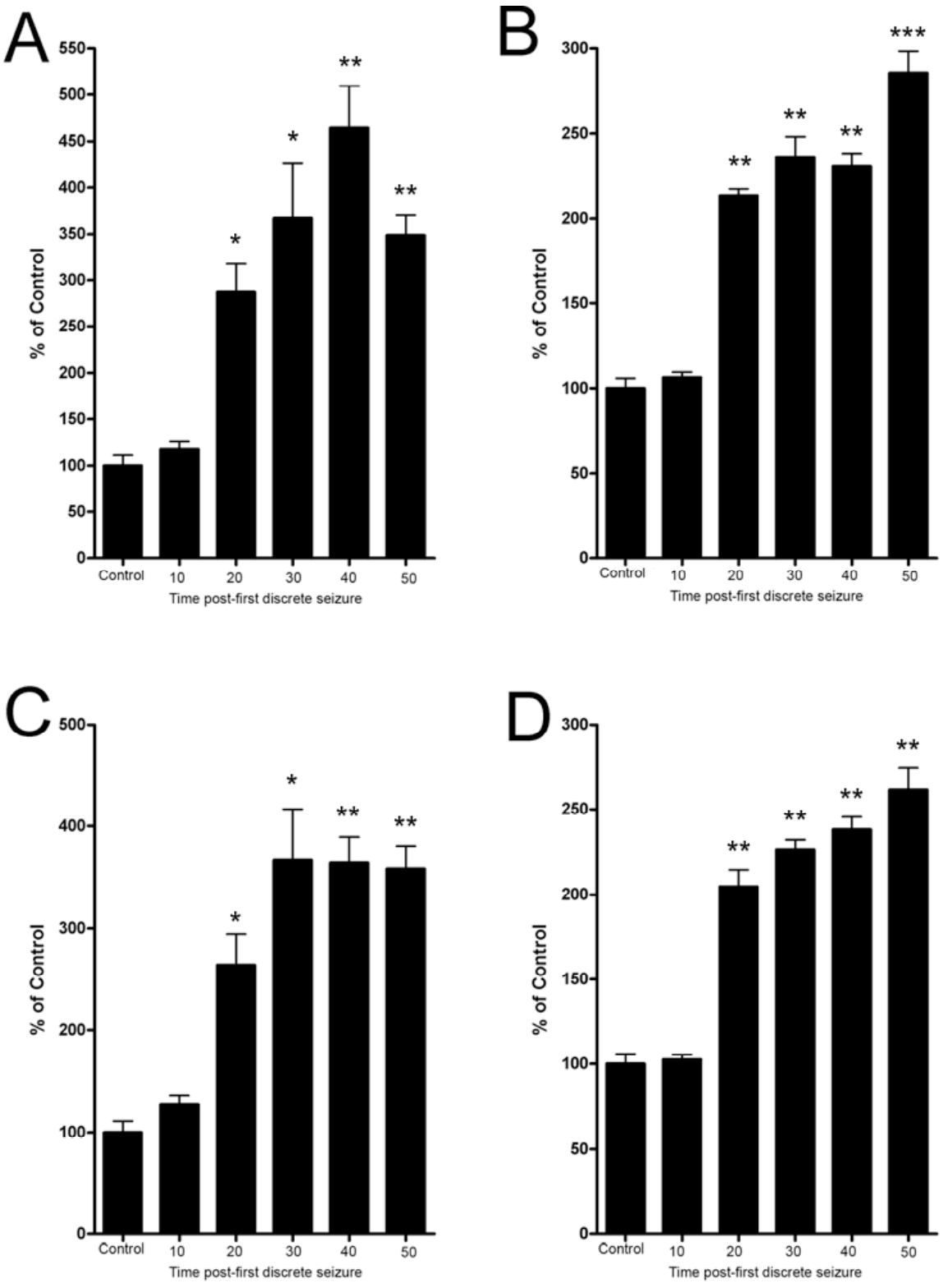

Figure 27: Temporal profile of basal and cation-stimulated CaN activity in cortical and hippocampal crude SPM. In both cortex (A, B) and hippocampus (C, D) CaN activity (as measured by the pNPP assay) in the SPM increased with a temporal profile similar to the SE-induced increase in CaN immunoreactivity noted above. Both basal (A, C) and cation-stimulated (B, D) activity increased significantly by 20 minutes post-first discrete seizure, with the magnitude of the increase being roughly similar to the magnitude of the increase in CaN immunoreactivity via western blot. As SE continued, a further increase in CaN activity was observed in all fractions and in all reaction conditions (although this increase is most noticeable in under the basal reaction conditions). The timing of this later increase corresponds to an increase in CaN activity that is observed in the overall homogenate and is discussed previously (* $p < 0.05$, ** $p < 0.01$, *** $p < 0.001$).

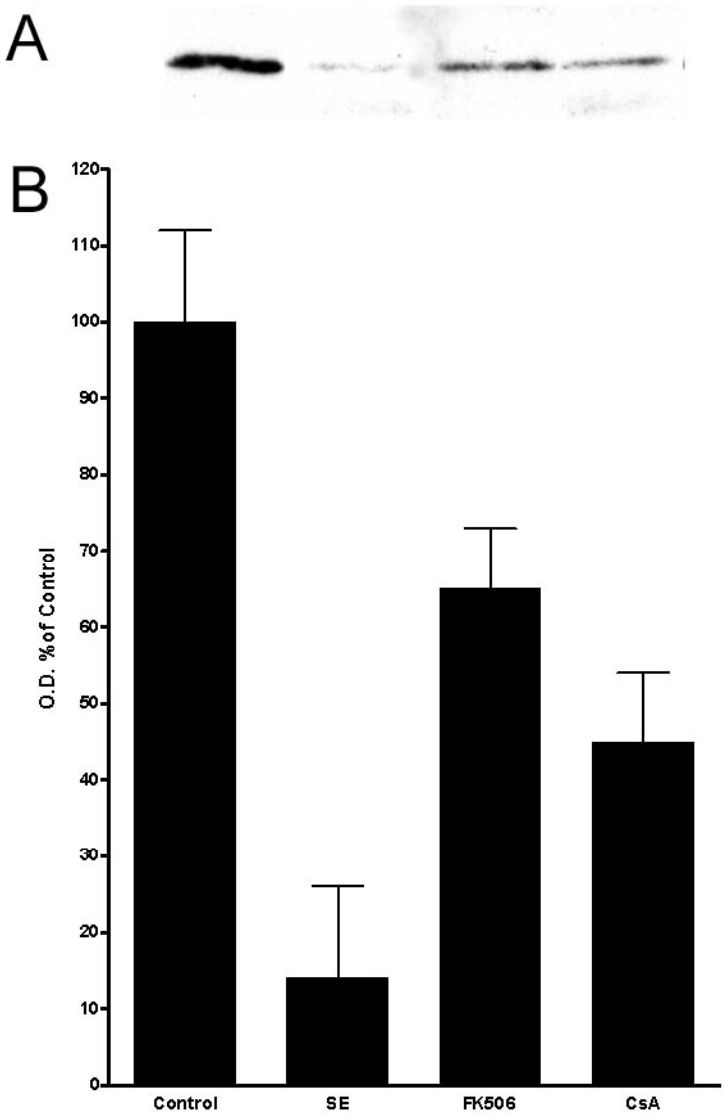

Figure 28: SE leads to increased CaN-dependent dephosphorylation of DARRP-32. Phospho-DARRP-32 immunoreactivity was determined via western analysis. SE was found to induce a significant dephosphorylation of the protein ($p < 0.05$, $n=3$), a finding that is consistent with increased CaN activity. Pretreatment of animals with either CaN inhibitor reduced DARRP dephosphorylation significantly ($p < 0.05$ compared to SE, $n=3$), indicating that the inhibitors were reaching the brain in sufficient concentrations to inhibit CaN activity.

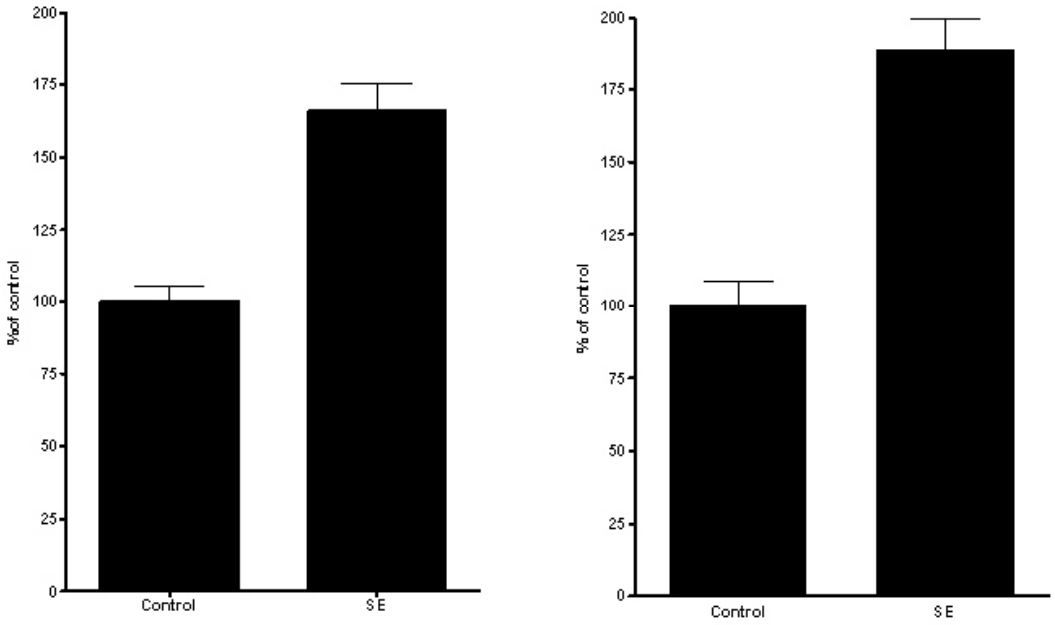

Figure 29: RII phosphopeptide assay for CaN activity. To further expand upon our previous results, we examined CaN activity in the crude SPM of cortex and hippocampus using an additional enzyme assay procedure. Phosphate released from RII phosphopeptide, a specific CaN substrate, was assayed using a malachite-green based reaction and read in a spectrophotometer at 620nm. In both cortex (A) and hippocampus (B) a significant increase in CaN activity was observed after 1h of SE. This increase was of similar magnitude to that observed with the pNPP assay. ($p < 0.05$, n=3).

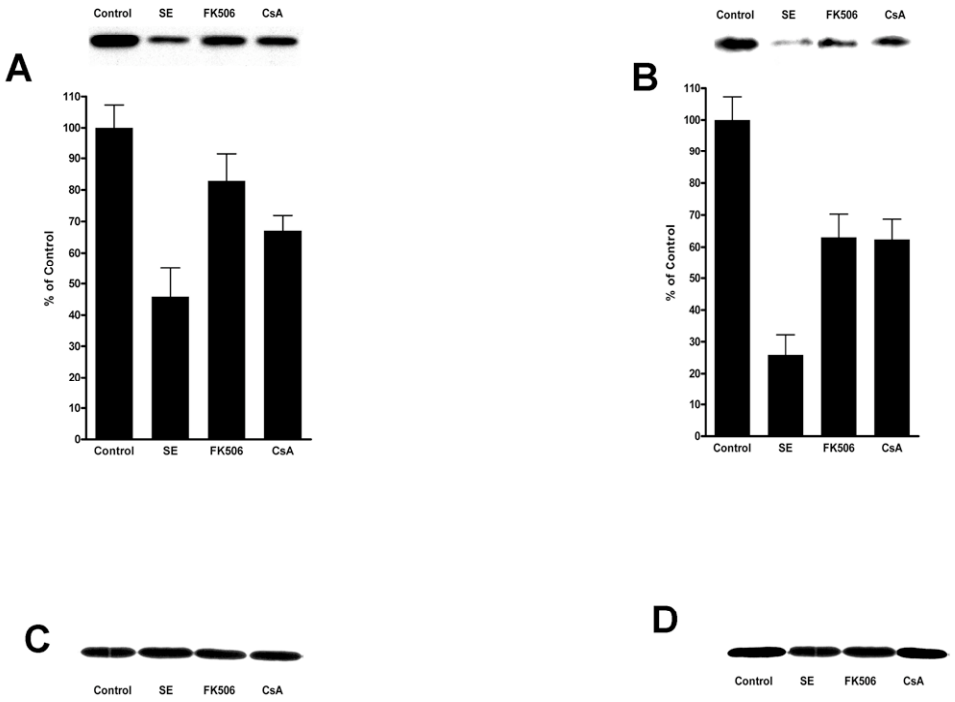

Figure 30: SE induces a CaN-dependent dephosphorylation of cofilin. In both cortical (A) and hippocampal (B) crude SPM, SE induced a significant ($p < 0.01$, n=10 in both regions) dephosphorylation of cofilin, as measured by immunoreactivity on western analysis using a phosphocofilin antibody. Administration of one of the immunosuppressant CaN inhibitors (FK506 or cyclosporin A) prior to SE partially blocked this dephosphorylation ($p < 0.05$ when compared to SE, n = 6 in both cortex and hippocampus). Changes in phosphocofilin immunoreactivity were not due to changes in overall cofilin concentration, as western analysis with a cofilin antibody revealed no change in overall levels of the protein in either cortical (C) or hippocampal (D) SPM.

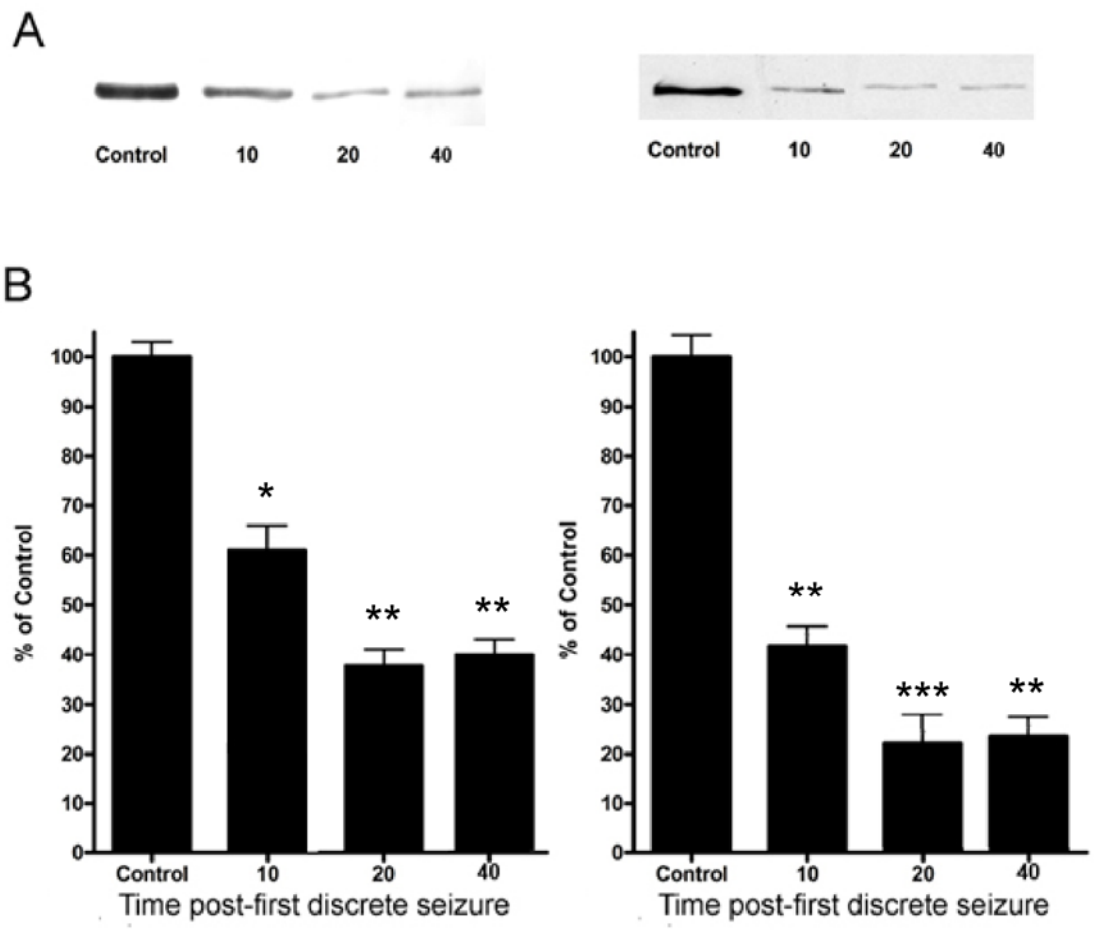

Figure 31: Temporal profile of cofilin dephosphorylation in the pilocarpine model of SE. (A) Western analysis for phosphocofilin in cortical (left) and hippocampal (right) crude SPM at 10, 20 and 40 minutes post-first discrete seizure. Cofilin phosphorylation was detected as early as 10 minutes post-first discrete seizure in both brain regions. This time point corresponds approximately to the onset of continuous seizure activity in this model. (B) Calibrated densitometry of phosphocofilin western blots in cortical (left) and hippocampal (right) crude SPM fractions. Cofilin phosphorylation was significantly decreased at 10 minutes and all subsequent time points (* $p < 0.05$, ** $p < 0.01$, *** $p < 0.001$)

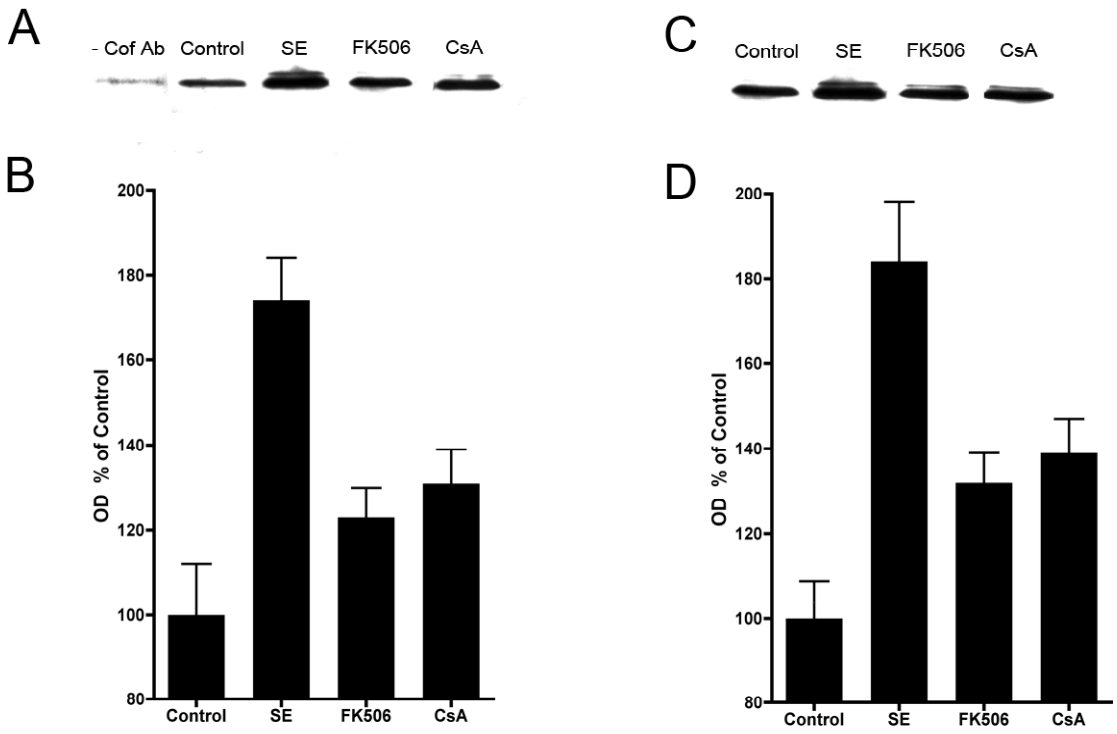

Figure 32: SE induces a CaN-dependent binding of cofilin to actin as detected by coimmunoprecipitation. Cofilin was immunoprecipitated from cortical (A, B) and hippocampal (C,D) homogenates, then the actin content of the precipitate was determined by western analysis. Very little actin was precipitated in the absence of cofilin primary antibody (A, far left), confirming the specificity of the assay procedure. In both cortical (A, B) and hippocampal (C,D) samples, SE led to a significant ($p < 0.05$) increase in cofilin-actin coprecipitation. This association of the two proteins was significantly blocked by calcineurin inhibitors ($p < 0.05$ when compared to SE value).

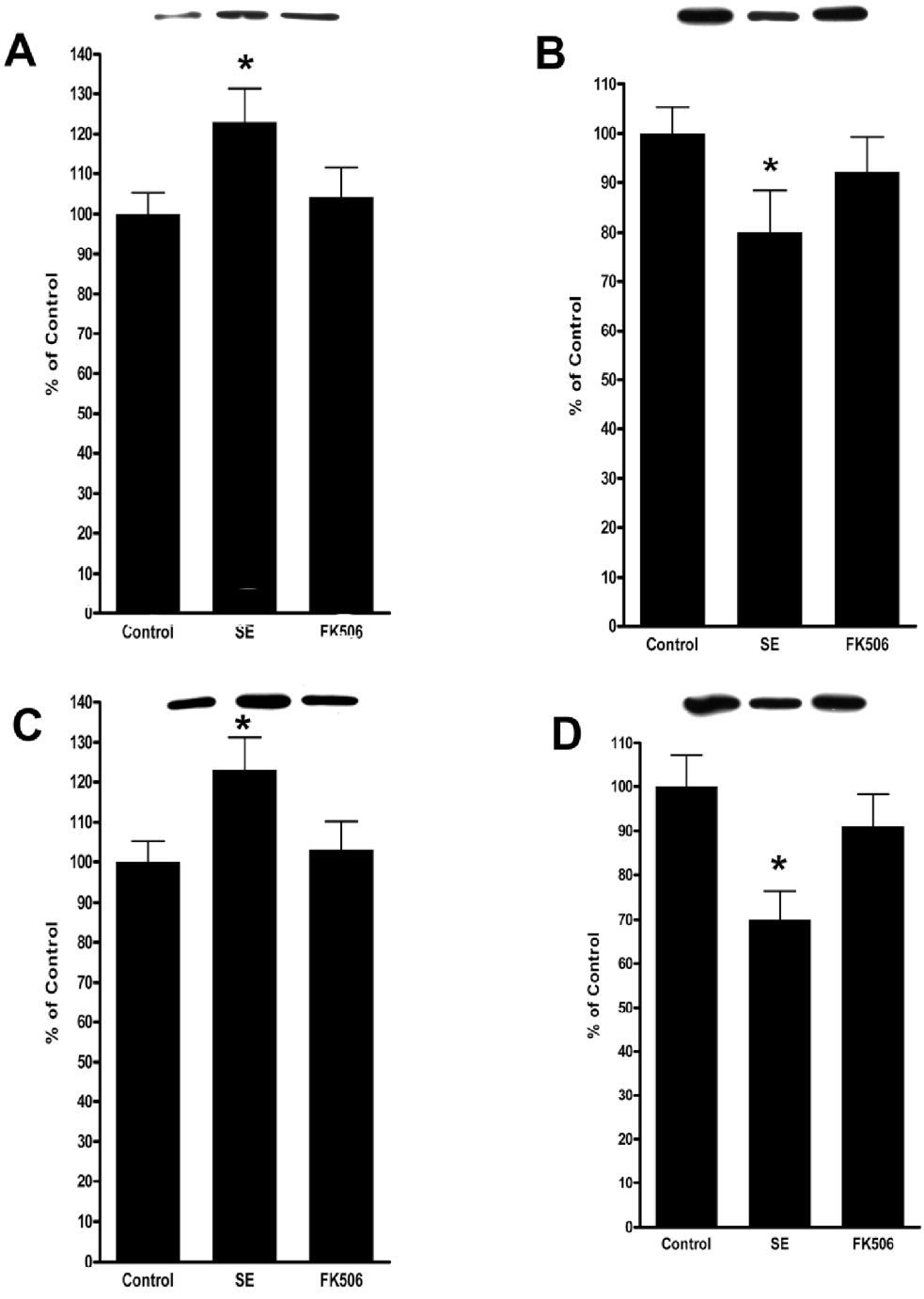

Figure 33: SE induces CaN dependent actin depolymerization. F-actin and G-actin were separated by solubility in 1% triton, then assayed by western analysis in cortical (A, B) and hippocampal (C,D) crude SPM. In cortical SPM, SE caused a significant ($p < 0.05$) increase in the amount of actin present in the triton-soluble fraction (A). G-actin is soluble in triton while F-actin is not, and thus this increase in soluble actin likely represents an SE-induced depolymerization of actin. A similar decrease in triton-insoluble actin (F-actin) was observed in cortical homogenates following SE (B). The CaN inhibitor FK506 blocked the shift of actin from the soluble to insoluble fraction, suggesting that the observed actin depolymerization was CaN-dependent. Similar effects were observed in hippocampal triton-soluble (C) and triton-insoluble (D) fractions isolated from crude SPM (n = 3 for all groups).

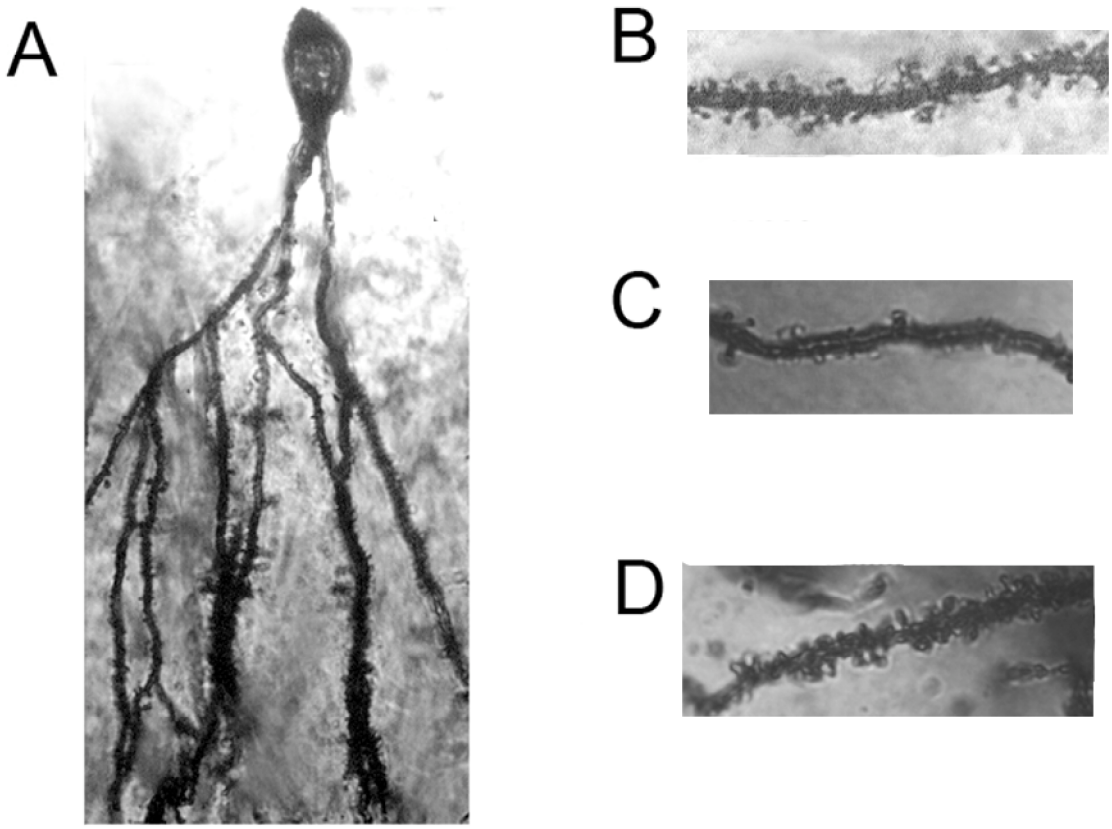

Figure 34: FK506 blocks SE-induced dendritic spine loss in granule cells of the dentate gyrus. Coronal sections were blocked for dorsal hippocampus and sectioned at 150 microns on a vibratome, then stained using a single-section variant of the rapid Golgi method. Granule cells with numerous processes were easily visualized in control sections (A). Under higher magnification, numerous dendritic spines were visualized in control dendrites (B), while relatively few spines were observed in dendrites of SE animals (C). In SE animals pre-treated with FK506, spine density appeared qualitatively to be preserved. (representative sections shown, n = 3 animals per group)

DISCUSSION

The present study examined the effects of two different models of neuronal injury on the activity and distribution of CaN. In chapter one, we demonstrated an SE-dependent increase in both basal and maximal CaN activity and a corresponding change in CaN substrate kinetics. This change was dependent on NMDA-mediated calcium influx, and not due to an increase in the overall amount of CaN present in the cell after SE. In chapter two, through the use of western and immunohistochemical analysis, we showed an SE-dependent increase in the amount of CaN present in the post-synaptic region of neurons. This SE-induced increase in synaptoplasmic CaN concentration was accompanied by a dramatic increase in CaN activity in this fraction. We suspect that the SE-induced increase in synaptic CaN is due to a translocation of the enzyme, as the results of chapter one indicated that no new CaN synthesis had taken place. Taken together, the results presented in the first two chapters of this study describe a profound increase in post-synaptic CaN concentration and activity after one hour of SE, changes that could have major implications in the pathology of SE. In chapters three and four we demonstrated a similar increase in CaN activity and post-synaptic increase in CaN concentration in the moderate fluid percussion model of traumatic brain injury. These changes in CaN activity

and subcellular distribution persisted for several weeks post-injury, a time-course which corresponds to a number of TBI-associated pathologies Finally, in chapter five, we examined one potential physiological consequence of SE-induced increases in post-synaptic CaN activity and concentration. CaN was shown to be part of a cellular mechanism of SE-induced dendritic spine loss, possibly implicating the enzyme in SE-induced chronic neurological pathology. Altogether, the results presented in this study provide compelling evidence that CaN is involved in neuronal damage in two disparate models of injury, and provide at least one cellular mechanism for this damage in the pilocarpine model of SE. Ideally, further research in this topic will provide a basis for future neuroprotective and therapeutic treatments.

The presence of injury-dependent changes in CaN activity in both models may be explained by the importance of glutamate-mediated excitotoxic mechanisms to the pathology of both conditions. In fact, this alteration in CaN activity and distribution would not be the first pathologic mechanism shared between TBI and SE. For example, MK801, a non-competitive NMDA channel blocker, is neuroprotective in animal models of both conditions [254, 255]. Both TBI and SE lead to neuronal hyperexcitability, particularly in the hippocampus. Additionally, both TBI and SE are epileptogenic in animal models and clinical studies (in fact, TBI represents one of the major causes of epilepsy in the United States). Thus, while TBI and SE are clearly different types of neuronal injury, it is just as clear that they share some pathological mechanisms and long-term consequences. The identification of these common pathological pathways, such

as CaN activation and redistribution, may allow for the development of multi-use treatment modalities.

Increased forebrain homogenate CaN activity in SE and TBI:

In both SE and TBI, a significant increase in basal and Mn-stimulated CaN activity was observed. Western analysis in homogenates from both models revealed no significant increase in CaN concentration, suggesting that this increase in activity was not due to injury-stimulated synthesis of new enzyme. A number of other possibilities exist to explain this increase in activity. First of all, glutamate-induced calcium influx could directly stimulate the enzyme, resulting in the observed increase in activity. This explanation is unlikely for several reasons. First, the levels of free calcium achieved inside neurons during toxic glutamate stimulation are well above the concentration range commonly associated with CaN activation. In fact, high calcium concentrations have actually been shown to *inactivate* the enzyme, rather than activating it. Second, the timing of the increase in CaN activity in homogenate correlates poorly with calcium entry as a mechanism. In SE, homogenate CaN activity increased after approximately 30 minutes of continuous seizure activity, although cellular free calcium levels rise much sooner. Finally, addition of excess chelator to the reaction mix did not eliminate the observed increase in activity. On the other hand, local calcium concentrations in some portions of the neuron could certainly be within the appropriate range, due to the separation of specialized compartments within the cell. When CaN activity is considered on a finer scale than that provided by

tissue homogenization, direct activation by glutamate-induced calcium influx is certainly possible, however we belive it is not likely to explain the wholesale increase in activity observed in the homogenates after both injuries.

While direct activation of the enzyme by glutamate-induced calcium influx does not seem to explain the increase in CaN activity, NMDA-receptor associated calcium influx still was essential for the enzyme activation to occur. This tends to implicate other calcium-regulated systems in the activation of the enzyme in homogenate. Phosphorylation of the enzyme by a calcium-stimulated kinase is one such explanation, although significant regulation of the enzyme through such a mechanism has not been conclusively demonstrated. Another possible mechanism involves partial proteolysis of the enzyme by calcium stimulated proteases. Such proteolysis has been shown to activate the enzyme via removal of the autoinhibitory domain. Interestingly, the calcium stimulated protease, calpain, has been shown to be activated in both SE and TBI, and this mechanism of CaN activation has been demonstrated in an *in vitro* model of glutamate excitotoxicity. Further research is needed to determine if calpain-mediated activation of CaN is responsible for the delayed increase in CaN activity observed in SE, and the similar increase in homogenate CaN activity observed in TBI. Interestingly, the increase in CaN activity persisted for several weeks in TBI, and it is possible that this sustained increase is due to some combination of post-translational modification and increased resting calcium levels.

Increased synaptoplasmic CaN concentration in SE and TBI:

In both model systems, a profound increase in the amount of CaN present in the crude synaptoplasmic membrane fraction was noted in hippocampal and cortical isolates. Additionally, immunohistochemistry confirmed this increase in post-synaptic CaN immunoreactivity in hippocampal slices from both SE and TBI animals. Two possible explanations exist for this increased CaN immunoreactivity in SPM fractions and on IHC; either new CaN has been synthesized or existing CaN has been translocated to the membrane.

Regardless of the cause of the increased CaN immunoreactivity, the result is functionally the same. Both injury processes result in a dramatic increase in the amount of CaN present at the synapse. In SE, this increase was determined to be very rapid, occurring shortly after the onset of continuous seizure activity (in contrast to the increase in homogenate activity, which was delayed until 20-30 minutes of continuous seizures had occurred). A proportional increase in activity accompanied this increase in CaN concentration in both models. At least in the SE model, this increase in activity was determined to be mechanistically distinct from the increase in homogenate activity discussed above. A careful analysis of the temporal profile of SE-induced CaN activity changes in SPM reveals an immediate increase in CaN activity that corresponds in timing and magnitude with the increase in SPM CaN concentration, and a separate, later increase in activity that corresponds temporally with the increase in homogenate activity. Thus two events appear to be taking place: increased CaN concentration post-

synaptically shortly after the onset of continuous seizure activity, and a later increase in CaN activity caused by post-translational modification of the enzyme.

There are numerous possible implications of this increased post-synaptic CaN activity and concentration for the observed pathologies of both models. As described previously, CaN regulates a number of neurotransmitter receptors. Disregulation of the $GABA_A$ receptor has been observed as a pathological mechanism in both TBI and SE [161, 256-258]. A number of studies have demonstrated negative modulation of $GABA_A$ function by CaN [66, 67], and at least one study has shown a direct CaN-mediated dephosphorylation of a $GABA_A$ subunit [69]. Additionally, an injury-induced modulation of the receptor by CaN has already been observed in a model of hypoxic injury in immature rats [123]. The dramatically increased SPM CaN activity observed in the two model systems in this study could result in increased $GABA_A$ receptor dephosphorylation (or increased receptor internalization), decreased GABAergic neurotransmission, and increased neuronal excitability. Post-injury hyperexcitability and eventual epileptogenesis are hallmarks of both TBI and SE [230], pathologies that could be explained by a negative modulation of $GABA_A$ receptors by the increased post-synaptic CaN. Futhermore, one study has demonstrated a loss of GABAergic inhibition that was NMDA-dependent, like the increase in CaN activity described in this study [259]. This mechanism of neuronal disinhibition merits future research in both of these conditions.

CaN and cognitive function:

A second potential implication of increased post-synaptic CaN is decreased cognitive function. This is of particular interest in TBI, where cognitive deficits are a common and unfortunate consequence of the injury. A great deal of evidence suggests that CaN exerts a negative modulation on learning and memory. Studies in rats have revealed that CaN inhibition increases performance in associative memory-related tasks. For example, Ikegami et al. demonstrated an increase in conditioned fear memory in rats treated with CaN antisense oligonucleotides or FK506 [260]. Similarly Lin et al. demonstrated that application of CaN inhibitors to the amygdala *in vivo* prevented the extinction of fear memory [261, 262]. A number of studies have examined the effects of genetically reduced CaN activity on learning and memory, either via overexpression of a calcineurin autoinhibitory peptide or by CaN knockout. Conditional (doxycycline-dependent) overexpression of the CaN autoinhibitory peptide in adult mouse brain resulted in enhanced short- and long-term memory in an object recognition task [5]. Additionally, overexpression of the autoinhibitory peptide enhanced performance in the Morris water maze (MWM) task. Mutant mice treated with doxycycline learned the position of the platform in the maze more rapidly and retained this information longer (the platform was removed and the number of times the mouse crossed the prior location on successive days measured), indicating a positive effect of CaN inhibition on learning and memory [5]. Finally, several studies have investigated the effects of conditional overexpression of calcineurin, often using a doxycycline-sensitive mutant mouse that overexpresses a

truncated, active form of calcineurin (see calpain proteolysis, above). Mansuy and colleagues demonstrated that calcineurin overexpressing mice had deficient long-term memory and deficient spatial learning as tested by the Barnes maze task, but normal short term memory. These deficits could be entirely rescued by "turning off" the calcineurin overexpression. Additionally, the mice in this study had difficulty with an object-recognition task when tested at long (but not short) intervals [224]. The researchers theorized that CaN was essential for the transition from short-term to long term memory; on a cellular level, they hypothesized that this was due to CaN's negative effects on an intermediate-length form of LTP [224, 263, 264]. In a later study by the same laboratory, the mutant mice also exhibited impaired spatial learning on the MWM task. When conditional mutants were allowed to train on the MWM task with CaN overexpression suppressed (normal CaN levels) their performance was the same as control mice; however, if CaN overexpression was then induced after the training phase, the performance of the mice declined and they could no longer remember the position of the platform. This seems to indicate that CaN overexpression also interferes with memory retrieval. Interestingly, if CaN levels were subsequently restored to normal, memory of platform position was recovered [264]. The results of these CaN overexpression studies correspond well with the inhibitor and autoinhibitory peptide-based studies, suggesting that within a certain range, CaN activity generally acts to prevent memory formation and retrieval while promoting memory extinction. Thus a dramatic increase in post-synaptic CaN, such as that observed in SE and TBI in this study, could be

responsible for decreased cognition after the injury event. Interestingly, the duration of increased CaN activity and post-synaptic concentration correlates with previous results documenting the duration of cognitive deficits after TBI. Future research into this cellular mechanism may provide clinical options for preserving cognitive abilities after brain injury.

SE, epilepsy and spine loss:

Finally, injury-induced increases in post-synaptic CaN may lead to negative modulation of dendritic spines. Decreased spine density has been previously observed in SE [240], and is postulated to be involved in chronic post-seizure pathology. As discussed above, CaN negatively modulates spine density in several model systems [79, 80]. Thus, an SE (or TBI)-mediated increase in CaN activity and concentration in the immediate vicinity of dendritic spines could account for decreased spine density in these conditions. We investigated this intriguing cellular mechanism in the pilocarpine model of SE, and discovered a profound CaN-dependent loss of dendritic spines.

There are several potential physiological roles of the CaN-dependent loss of spines described in this study. In the pilocarpine model of SE, spontaneous recurrent seizures typically begin approximately 2 weeks after the prolonged seizure episode [265]. No epileptic activity is seen during this quiescent period, but there is a great deal happening on a cellular level. It is thought that the biochemical and structural changes that lead to recurrent seizure activity are being completed during this time. While the exact mechanisms responsible for

epileptogenesis remain the subject of intense study and debate, dendritic spine plasticity certainly is a promising candidate for this role. The loss and subsequent regrowth of dendritic spines could represent a pathological reorganization of synaptic networks leading to the formation of epileptic foci in the brain. It is especially interesting that spine loss has been documented in the dentate gyrus of the hippocampus [242]. Network reorganization and neuronal hyperexcitability in this region are frequently proposed as possible mechanisms of epileptogenesis. Furthermore, after the SE-associated loss of spines, it has been shown that their regrowth in this region is colocalized with sites of mossy fiber sprouting [242]. Thus an outgrowth of axonal structures that has been previously implicated in epileptogenesis seems to coincide with a reorganization of post-synaptic structures, all of which is occurring in a region that seems to be critical in the development of temporal lobe epilepsy.

Conclusion:

These studies describe a novel increase in CaN activity after both TBI and SE, and demonstrate an increase in CaN in crude SPM fractions after both conditions. In TBI, these changes were shown to persist for 2 weeks in cortical samples and up to 4 weeks in hippocampal samples. Immunohistochemical studies confirmed that this increase in SPM CaN represented an increase in the amount of enzyme in hippocampal dendrites. The pathological implications of these changes include potential mechanisms for decreased cognitive function and epileptogenesis. Finally, we presented one physiological consequence of

increased dendritic CaN in SE: dendritic spine loss. We demonstrated a CaN-dependent cellular mechanism for this decrease in spine density involving the actin-depolymerizing factor, cofilin. These results help further our understanding of the pathologies set in motion by these two models of neuronal injury, and may provide the basis for future clinical treatments, ideally decreasing the impact of neuronal injury on patient's quality of life.

LIST OF REFERENCES

LIST OF REFERENCES:

1. DeLorenzo, R.J. and D.A. Sun, *Basic mechanisms in status epilepticus: role of calcium in neuronal injury and the induction of epileptogenesis.* Adv Neurol, 2006. **97**: p. 187-97.
2. Klee, C.B., T.H. Crouch, and M.H. Krinks, *Calcineurin: a calcium- and calmodulin-binding protein of the nervous system.* Proc Natl Acad Sci U S A, 1979. **76**(12): p. 6270-3.
3. Stewart, A.A., et al., *Discovery of a Ca2+- and calmodulin-dependent protein phosphatase: probable identity with calcineurin (CaM-BP80).* FEBS Lett, 1982. **137**(1): p. 80-4.
4. Manalan, A.S., M.H. Krinks, and C.B. Klee, *Calcineurin: a member of a family of calmodulin-stimulated protein phosphatases.* Proc Soc Exp Biol Med, 1984. **177**(1): p. 12-6.
5. Malleret, G., et al., *Inducible and reversible enhancement of learning, memory, and long-term potentiation by genetic inhibition of calcineurin.* Cell, 2001. **104**(5): p. 675-86.
6. Clipstone, N.A. and G.R. Crabtree, *Identification of calcineurin as a key signalling enzyme in T-lymphocyte activation.* Nature, 1992. **357**(6380): p. 695-7.
7. Hubbard, M.J. and C.B. Klee, *Functional domain structure of calcineurin A: mapping by limited proteolysis.* Biochemistry, 1989. **28**(4): p. 1868-74.
8. Klee, C.B., H. Ren, and X. Wang, *Regulation of the calmodulin-stimulated protein phosphatase, calcineurin.* J Biol Chem, 1998. **273**(22): p. 13367-70.
9. Stemmer, P.M. and C.B. Klee, *Dual calcium ion regulation of calcineurin by calmodulin and calcineurin B.* Biochemistry, 1994. **33**(22): p. 6859-66.
10. Klee, C.B., G.F. Draetta, and M.J. Hubbard, *Calcineurin.* Adv Enzymol Relat Areas Mol Biol, 1988. **61**: p. 149-200.
11. Crivici, A. and M. Ikura, *Molecular and structural basis of target recognition by calmodulin.* Annu Rev Biophys Biomol Struct, 1995. **24**: p. 85-116.
12. Tallant, E.A., L.M. Brumley, and R.W. Wallace, *Activation of a calmodulin-dependent phosphatase by a Ca2+-dependent protease.* Biochemistry, 1988. **27**(6): p. 2205-11.
13. Wang, K.K., A. Villalobo, and B.D. Roufogalis, *Activation of the Ca2+-ATPase of human erythrocyte membrane by an endogenous Ca2+-dependent neutral protease.* Arch Biochem Biophys, 1988. **260**(2): p. 696-704.

14. Wang, K.K., B.D. Roufogalis, and A. Villalobo, *Characterization of the fragmented forms of calcineurin produced by calpain I.* Biochem Cell Biol, 1989. **67**(10): p. 703-11.
15. Manalan, A.S. and C.B. Klee, *Activation of calcineurin by limited proteolysis.* Proc Natl Acad Sci U S A, 1983. **80**(14): p. 4291-5.
16. Kuno, T., et al., *Distinct cellular expression of calcineurin A alpha and A beta in rat brain.* J Neurochem, 1992. **58**(5): p. 1643-51.
17. Nishio, H., et al., *The evidence for post-meiotic expression of a testis-specific isoform of a regulatory subunit of calcineurin using a monoclonal antibody.* Biochem Biophys Res Commun, 1992. **187**(2): p. 828-31.
18. Rusnak, F. and P. Mertz, *Calcineurin: form and function.* Physiol Rev, 2000. **80**(4): p. 1483-521.
19. Yang, S.A. and C.B. Klee, *Low affinity Ca2+-binding sites of calcineurin B mediate conformational changes in calcineurin A.* Biochemistry, 2000. **39**(51): p. 16147-54.
20. Zhu, D., M.E. Cardenas, and J. Heitman, *Myristoylation of calcineurin B is not required for function or interaction with immunophilin-immunosuppressant complexes in the yeast Saccharomyces cerevisiae.* J Biol Chem, 1995. **270**(42): p. 24831-8.
21. Pallen, C.J. and J.H. Wang, *Regulation of calcineurin by metal ions. Mechanism of activation by Ni2+ and an enhanced response to Ca2+/calmodulin.* J Biol Chem, 1984. **259**(10): p. 6134-41.
22. Gupta, R.C., R.L. Khandelwal, and P.V. Sulakhe, *Intrinsic phosphatase activity of bovine brain calcineurin requires a tightly bound trace metal.* FEBS Lett, 1984. **169**(2): p. 251-5.
23. Rao, J. and J.H. Wang, *Calcineurin immunoprecipitated from bovine brain extract contains no detectable Ni2+ or Mn2+.* J Biol Chem, 1989. **264**(2): p. 1058-61.
24. Stemmer, P.M., et al., *Factors responsible for the Ca(2+)-dependent inactivation of calcineurin in brain.* FEBS Lett, 1995. **374**(2): p. 237-40.
25. Lai, M.M., et al., *Cain, a novel physiologic protein inhibitor of calcineurin.* J Biol Chem, 1998. **273**(29): p. 18325-31.
26. Lai, M.M., et al., *The calcineurin-binding protein cain is a negative regulator of synaptic vesicle endocytosis.* J Biol Chem, 2000. **275**(44): p. 34017-20.
27. Gutierrez-Ford, C., et al., *Characterization of tescalcin, a novel EF-hand protein with a single Ca2+-binding site: metal-binding properties, localization in tissues and cells, and effect on calcineurin.* Biochemistry, 2003. **42**(49): p. 14553-65.
28. Lin, X., et al., *Inhibition of calcineurin phosphatase activity by a calcineurin B homologous protein.* J Biol Chem, 1999. **274**(51): p. 36125-31.
29. Rahmani, Z., et al., *Critical role of the D21S55 region on chromosome 21 in the pathogenesis of Down syndrome.* Proc Natl Acad Sci U S A, 1989. **86**(15): p. 5958-62.

30. Harris, C.D., G. Ermak, and K.J. Davies, *Multiple roles of the DSCR1 (Adapt78 or RCAN1) gene and its protein product Calcipressin 1 (or RCAN1) in disease.* Cell Mol Life Sci, 2005.
31. Ermak, G., C.D. Harris, and K.J. Davies, *The DSCR1 (Adapt78) isoform 1 protein calcipressin 1 inhibits calcineurin and protects against acute calcium-mediated stress damage, including transient oxidative stress.* Faseb J, 2002. **16**(8): p. 814-24.
32. Vega, R.B., et al., *Multiple domains of MCIP1 contribute to inhibition of calcineurin activity.* J Biol Chem, 2002. **277**(33): p. 30401-7.
33. Leal, R.B., et al., *S100B protein stimulates calcineurin activity.* Neuroreport, 2004. **15**(2): p. 317-20.
34. Calalb, M.B., R.L. Kincaid, and T.R. Soderling, *Phosphorylation of calcineurin: effect on calmodulin binding.* Biochem Biophys Res Commun, 1990. **172**(2): p. 551-6.
35. Hashimoto, Y. and T.R. Soderling, *Regulation of calcineurin by phosphorylation. Identification of the regulatory site phosphorylated by Ca2+/calmodulin-dependent protein kinase II and protein kinase C.* J Biol Chem, 1989. **264**(28): p. 16524-9.
36. Hashimoto, Y., M.M. King, and T.R. Soderling, *Regulatory interactions of calmodulin-binding proteins: phosphorylation of calcineurin by autophosphorylated Ca2+/calmodulin-dependent protein kinase II.* Proc Natl Acad Sci U S A, 1988. **85**(18): p. 7001-5.
37. Martensen, T.M., B.M. Martin, and R.L. Kincaid, *Identification of the site on calcineurin phosphorylated by Ca2+/CaM-dependent kinase II: modification of the CaM-binding domain.* Biochemistry, 1989. **28**(24): p. 9243-7.
38. Brautigan, D.L., *Flicking the switches: phosphorylation of serine/threonine protein phosphatases.* Semin Cancer Biol, 1995. **6**(4): p. 211-7.
39. Singh, T.J. and J.H. Wang, *Phosphorylation of calcineurin by glycogen synthase (casein) kinase-1.* Biochem Cell Biol, 1987. **65**(10): p. 917-21.
40. Kashishian, A., et al., *AKAP79 inhibits calcineurin through a site distinct from the immunophilin-binding region.* J Biol Chem, 1998. **273**(42): p. 27412-9.
41. Mansuy, I.M., *Calcineurin in memory and bidirectional plasticity.* Biochem Biophys Res Commun, 2003. **311**(4): p. 1195-208.
42. Burley, J.R. and T.S. Sihra, *A modulatory role for protein phosphatase 2B (calcineurin) in the regulation of Ca2+ entry.* Eur J Neurosci, 2000. **12**(8): p. 2881-91.
43. Armstrong, D.L., *Calcium channel regulation by calcineurin, a Ca2+-activated phosphatase in mammalian brain.* Trends Neurosci, 1989. **12**(3): p. 117-22.
44. Lukyanetz, E.A., *Evidence for colocalization of calcineurin and calcium channels in dorsal root ganglion neurons.* Neuroscience, 1997. **78**(3): p. 625-8.

45. Zhu, Y. and J.L. Yakel, *Calcineurin modulates G protein-mediated inhibition of N-type calcium channels in rat sympathetic neurons.* J Neurophysiol, 1997. **78**(2): p. 1161-5.
46. Schuhmann, K., et al., *Intracellular Ca2+ inhibits smooth muscle L-type Ca2+ channels by activation of protein phosphatase type 2B and by direct interaction with the channel.* J Gen Physiol, 1997. **110**(5): p. 503-13.
47. Norris, C.M., et al., *Calcineurin enhances L-type Ca(2+) channel activity in hippocampal neurons: increased effect with age in culture.* Neuroscience, 2002. **110**(2): p. 213-25.
48. Wang, J.H. and P.T. Kelly, *Postsynaptic calcineurin activity downregulates synaptic transmission by weakening intracellular Ca2+ signaling mechanisms in hippocampal CA1 neurons.* J Neurosci, 1997. **17**(12): p. 4600-11.
49. Cameron, A.M., et al., *Calcineurin associated with the inositol 1,4,5-trisphosphate receptor-FKBP12 complex modulates Ca2+ flux.* Cell, 1995. **83**(3): p. 463-72.
50. Groth, R.D. and P.G. Mermelstein, *Brain-derived neurotrophic factor activation of NFAT (nuclear factor of activated T-cells)-dependent transcription: a role for the transcription factor NFATc4 in neurotrophin-mediated gene expression.* J Neurosci, 2003. **23**(22): p. 8125-34.
51. Genazzani, A.A., E. Carafoli, and D. Guerini, *Calcineurin controls inositol 1,4,5-trisphosphate type 1 receptor expression in neurons.* Proc Natl Acad Sci U S A, 1999. **96**(10): p. 5797-801.
52. Guerini, D., et al., *Calcineurin controls the expression of isoform 4CII of the plasma membrane Ca(2+) pump in neurons.* J Biol Chem, 2000. **275**(5): p. 3706-12.
53. Carafoli, E., A. Genazzani, and D. Guerini, *Calcium controls the transcription of its own transporters and channels in developing neurons.* Biochem Biophys Res Commun, 1999. **266**(3): p. 624-32.
54. Li, L., D. Guerini, and E. Carafoli, *Calcineurin controls the transcription of Na+/Ca2+ exchanger isoforms in developing cerebellar neurons.* J Biol Chem, 2000. **275**(27): p. 20903-10.
55. Dodge, K.L. and J.D. Scott, *Calcineurin anchoring and cell signaling.* Biochem Biophys Res Commun, 2003. **311**(4): p. 1111-5.
56. Coghlan, V.M., et al., *Association of protein kinase A and protein phosphatase 2B with a common anchoring protein.* Science, 1995. **267**(5194): p. 108-11.
57. Snyder, G.L., et al., *Regulation of AMPA receptor dephosphorylation by glutamate receptor agonists.* Neuropharmacology, 2003. **45**(6): p. 703-13.
58. Roche, K.W., et al., *Characterization of multiple phosphorylation sites on the AMPA receptor GluR1 subunit.* Neuron, 1996. **16**(6): p. 1179-88.
59. Wang, J.H. and M.J. Zhang, *Differential modulation of glutamatergic and cholinergic synapses by calcineurin in hippocampal CA1 fast-spiking interneurons.* Brain Res, 2004. **1004**(1-2): p. 125-35.

60. Beattie, E.C., et al., *Regulation of AMPA receptor endocytosis by a signaling mechanism shared with LTD.* Nat Neurosci, 2000. **3**(12): p. 1291-300.
61. Lieberman, D.N. and I. Mody, *Regulation of NMDA channel function by endogenous Ca(2+)-dependent phosphatase.* Nature, 1994. **369**(6477): p. 235-9.
62. Tong, G. and C.E. Jahr, *Regulation of glycine-insensitive desensitization of the NMDA receptor in outside-out patches.* J Neurophysiol, 1994. **72**(2): p. 754-61.
63. Krupp, J.J., et al., *Calcineurin acts via the C-terminus of NR2A to modulate desensitization of NMDA receptors.* Neuropharmacology, 2002. **42**(5): p. 593-602.
64. Tong, G., D. Shepherd, and C.E. Jahr, *Synaptic desensitization of NMDA receptors by calcineurin.* Science, 1995. **267**(5203): p. 1510-2.
65. Macdonald, R.L. and R.W. Olsen, *GABAA receptor channels.* Annu Rev Neurosci, 1994. **17**: p. 569-602.
66. Amico, C., et al., *Involvement of phosphatase activities in the run-down of GABA(A) receptor function in rat cerebellar granule cells in culture.* Neuroscience, 1998. **84**(2): p. 529-35.
67. Huang, R.Q. and G.H. Dillon, *Maintenance of recombinant type A gamma-aminobutyric acid receptor function: role of protein tyrosine phosphorylation and calcineurin.* J Pharmacol Exp Ther, 1998. **286**(1): p. 243-55.
68. Lu, Y.M., et al., *Calcineurin-mediated LTD of GABAergic inhibition underlies the increased excitability of CA1 neurons associated with LTP.* Neuron, 2000. **26**(1): p. 197-205.
69. Wang, J., et al., *Interaction of calcineurin and type-A GABA receptor gamma 2 subunits produces long-term depression at CA1 inhibitory synapses.* J Neurosci, 2003. **23**(3): p. 826-36.
70. Goto, S., et al., *Dephosphorylation of microtubule-associated protein 2, tau factor, and tubulin by calcineurin.* J Neurochem, 1985. **45**(1): p. 276-83.
71. Mandelkow, E.M., et al., *Tau domains, phosphorylation, and interactions with microtubules.* Neurobiol Aging, 1995. **16**(3): p. 355-62; discussion 362-3.
72. Drewes, G., et al., *Dephosphorylation of tau protein and Alzheimer paired helical filaments by calcineurin and phosphatase-2A.* FEBS Lett, 1993. **336**(3): p. 425-32.
73. Wei, Q., et al., *Dephosphorylation of tau protein by calcineurin triturated into neural living cells.* Cell Mol Neurobiol, 2002. **22**(1): p. 13-24.
74. Garver, T.D., et al., *Reduction of calcineurin activity in brain by antisense oligonucleotides leads to persistent phosphorylation of tau protein at Thr181 and Thr231.* Mol Pharmacol, 1999. **55**(4): p. 632-41.
75. Goedert, M., A. Klug, and R.A. Crowther, *Tau protein, the paired helical filament and Alzheimer's disease.* J Alzheimers Dis, 2006. **9**(3 Suppl): p. 195-207.

76. Ferreira, A., R. Kincaid, and K.S. Kosik, *Calcineurin is associated with the cytoskeleton of cultured neurons and has a role in the acquisition of polarity.* Mol Biol Cell, 1993. **4**(12): p. 1225-38.
77. Lautermilch, N.J. and N.C. Spitzer, *Regulation of calcineurin by growth cone calcium waves controls neurite extension.* J Neurosci, 2000. **20**(1): p. 315-25.
78. Chang, H.Y., et al., *Asymmetric retraction of growth cone filopodia following focal inactivation of calcineurin.* Nature, 1995. **376**(6542): p. 686-90.
79. Halpain, S., A. Hipolito, and L. Saffer, *Regulation of F-actin stability in dendritic spines by glutamate receptors and calcineurin.* J Neurosci, 1998. **18**(23): p. 9835-44.
80. Zhou, Q., K.J. Homma, and M.M. Poo, *Shrinkage of dendritic spines associated with long-term depression of hippocampal synapses.* Neuron, 2004. **44**(5): p. 749-57.
81. Wang, Y., F. Shibasaki, and K. Mizuno, *Calcium signal-induced cofilin dephosphorylation is mediated by Slingshot via calcineurin.* J Biol Chem, 2005. **280**(13): p. 12683-9.
82. Sarmiere, P.D. and J.R. Bamburg, *Regulation of the neuronal actin cytoskeleton by ADF/cofilin.* J Neurobiol, 2004. **58**(1): p. 103-17.
83. Meng, Y., et al., *Regulation of spine morphology and synaptic function by LIMK and the actin cytoskeleton.* Rev Neurosci, 2003. **14**(3): p. 233-40.
84. Bruns, J., Jr. and W.A. Hauser, *The epidemiology of traumatic brain injury: a review.* Epilepsia, 2003. **44 Suppl 10**: p. 2-10.
85. Agrawal, A., et al., *Post-traumatic epilepsy: an overview.* Clin Neurol Neurosurg, 2006. **108**(5): p. 433-9.
86. Katayama, Y., et al., *Massive increases in extracellular potassium and the indiscriminate release of glutamate following concussive brain injury.* J Neurosurg, 1990. **73**(6): p. 889-900.
87. Persson, L. and L. Hillered, *Chemical monitoring of neurosurgical intensive care patients using intracerebral microdialysis.* J Neurosurg, 1992. **76**(1): p. 72-80.
88. Zauner, A. and R. Bullock, *The role of excitatory amino acids in severe brain trauma: opportunities for therapy: a review.* J Neurotrauma, 1995. **12**(4): p. 547-54.
89. Faden, A.I., et al., *The role of excitatory amino acids and NMDA receptors in traumatic brain injury.* Science, 1989. **244**(4906): p. 798-800.
90. Bullock, M.R., B.G. Lyeth, and J.P. Muizelaar, *Current status of neuroprotection trials for traumatic brain injury: lessons from animal models and clinical studies.* Neurosurgery, 1999. **45**(2): p. 207-17; discussion 217-20.
91. Ankarcrona, M., et al., *Calcineurin and mitochondrial function in glutamate-induced neuronal cell death.* FEBS Lett, 1996. **394**(3): p. 321-4.
92. Felipo, V., et al., *Neurotoxicity of ammonia and glutamate: molecular mechanisms and prevention.* Neurotoxicology, 1998. **19**(4-5): p. 675-81.

93. Singleton, R.H., et al., *The immunophilin ligand FK506 attenuates axonal injury in an impact-acceleration model of traumatic brain injury.* J Neurotrauma, 2001. **18**(6): p. 607-14.
94. Scheff, S.W. and P.G. Sullivan, *Cyclosporin A significantly ameliorates cortical damage following experimental traumatic brain injury in rodents.* J Neurotrauma, 1999. **16**(9): p. 783-92.
95. Leppik, I.E., *Quality of life of people with epilepsy in the United States.* Clin Ther, 1998. **20 Suppl A**: p. A13-8; discussion A58-60.
96. Barnard, C. and E. Wirrell, *Does status epilepticus in children cause developmental deterioration and exacerbation of epilepsy?* J Child Neurol, 1999. **14**(12): p. 787-94.
97. Yagi, K., *Epilepsy: comprehensive care, quality of life, and factors preventing people with epilepsy from being employed.* Clin Ther, 1998. **20 Suppl A**: p. A19-29.
98. Aldenkamp, A.P., M. De Krom, and R. Reijs, *Newer antiepileptic drugs and cognitive issues.* Epilepsia, 2003. **44 Suppl 4**: p. 21-9.
99. Aldenkamp, A.P., *Effect of seizures and epileptiform discharges on cognitive function.* Epilepsia, 1997. **38 Suppl 1**: p. S52-5.
100. DeLorenzo, R.J., et al., *Epidemiology of status epilepticus.* J Clin Neurophysiol, 1995. **12**(4): p. 316-25.
101. Kaplan, P.W., *The clinical features, diagnosis, and prognosis of nonconvulsive status epilepticus.* Neurologist, 2005. **11**(6): p. 348-61.
102. Logroscino, G., et al., *Long-term mortality after a first episode of status epilepticus.* Neurology, 2002. **58**(4): p. 537-41.
103. DeLorenzo, R.J., et al., *A prospective, population-based epidemiologic study of status epilepticus in Richmond, Virginia.* Neurology, 1996. **46**(4): p. 1029-35.
104. Waterhouse, E.J. and R.J. DeLorenzo, *Status epilepticus in older patients: epidemiology and treatment options.* Drugs Aging, 2001. **18**(2): p. 133-42.
105. Fountain, N.B., *Status epilepticus: risk factors and complications.* Epilepsia, 2000. **41 Suppl 2**: p. S23-30.
106. De Santis, A., E. Cappricci, and G. Granata, *Early post traumatic seizures in adults. Study of 84 cases.* J Neurosurg Sci, 1979. **23**(3): p. 207-10.
107. Vespa, P.M., et al., *Increased incidence and impact of nonconvulsive and convulsive seizures after traumatic brain injury as detected by continuous electroencephalographic monitoring.* J Neurosurg, 1999. **91**(5): p. 750-60.
108. Segatore, M. and M. Jacobs, *Posttraumatic seizures: consensus and controversies.* Axone, 1993. **15**(2): p. 34-9.
109. Mayer, S.A., et al., *Refractory status epilepticus: frequency, risk factors, and impact on outcome.* Arch Neurol, 2002. **59**(2): p. 205-10.
110. Chen, J.W. and C.G. Wasterlain, *Status epilepticus: pathophysiology and management in adults.* Lancet Neurol, 2006. **5**(3): p. 246-56.
111. Lothman, E.W. and E.H. Bertram, 3rd, *Epileptogenic effects of status epilepticus.* Epilepsia, 1993. **34 Suppl 1**: p. S59-70.

112. Smolders, I., et al., *NMDA receptor-mediated pilocarpine-induced seizures: characterization in freely moving rats by microdialysis.* Br J Pharmacol, 1997. **121**(6): p. 1171-9.
113. Rice, A.C. and R.J. DeLorenzo, *N-methyl-D-aspartate receptor activation regulates refractoriness of status epilepticus to diazepam.* Neuroscience, 1999. **93**(1): p. 117-23.
114. Delorenzo, R.J., D.A. Sun, and L.S. Deshpande, *Cellular mechanisms underlying acquired epilepsy: the calcium hypothesis of the induction and maintainance of epilepsy.* Pharmacol Ther, 2005. **105**(3): p. 229-66.
115. Rice, A.C. and R.J. DeLorenzo, *NMDA receptor activation during status epilepticus is required for the development of epilepsy.* Brain Res, 1998. **782**(1-2): p. 240-7.
116. Rice, A.C., et al., *Status epilepticus causes long-term NMDA receptor-dependent behavioral changes and cognitive deficits.* Epilepsia, 1998. **39**(11): p. 1148-57.
117. Raza, M., et al., *Long-term alteration of calcium homeostatic mechanisms in the pilocarpine model of temporal lobe epilepsy.* Brain Res, 2001. **903**(1-2): p. 1-12.
118. Pal, S., et al., *In vitro status epilepticus causes sustained elevation of intracellular calcium levels in hippocampal neurons.* Brain Res, 1999. **851**(1-2): p. 20-31.
119. Pal, S., et al., *Induction of spontaneous recurrent epileptiform discharges causes long-term changes in intracellular calcium homeostatic mechanisms.* Cell Calcium, 2000. **28**(3): p. 181-93.
120. Parsons, J.T., et al., *Pilocarpine-induced status epilepticus causes N-methyl-D-aspartate receptor-dependent inhibition of microsomal Mg(2+)/Ca(2+) ATPase-mediated Ca(2+) uptake.* J Neurochem, 2000. **75**(3): p. 1209-18.
121. Moriwaki, A., et al., *An immunosuppressant, FK506, protects against neuronal dysfunction and death but has no effect on electrographic and behavioral activities induced by systemic kainate.* Neuroscience, 1998. **86**(3): p. 855-65.
122. Moia, L.J., et al., *Immunosuppressants and calcineurin inhibitors, cyclosporin A and FK506, reversibly inhibit epileptogenesis in amygdaloid kindled rat.* Brain Res, 1994. **648**(2): p. 337-41.
123. Sanchez, R.M., et al., *AMPA/kainate receptor-mediated downregulation of GABAergic synaptic transmission by calcineurin after seizures in the developing rat brain.* J Neurosci, 2005. **25**(13): p. 3442-51.
124. Bleck, T.P., *Convulsive disorders: status epilepticus.* Clin Neuropharmacol, 1991. **14**(3): p. 191-8.
125. Rice, A., et al., *Long-lasting reduction of inhibitory function and gamma-aminobutyric acid type A receptor subunit mRNA expression in a model of temporal lobe epilepsy.* Proc Natl Acad Sci U S A, 1996. **93**(18): p. 9665-9.
126. Wasterlain, C.G., et al., *Pathophysiological mechanisms of brain damage from status epilepticus.* Epilepsia, 1993. **34 Suppl 1**: p. S37-53.

127. Churn, S.B., et al., *Excitotoxic activation of the NMDA receptor results in inhibition of calcium/calmodulin kinase II activity in cultured hippocampal neurons.* J Neurosci, 1995. **15**(4): p. 3200-14.
128. Chittajallu, R., S. Alford, and G.L. Collingridge, *Ca2+ and synaptic plasticity.* Cell Calcium, 1998. **24**(5-6): p. 377-85.
129. Choi, D.W., *Ionic dependence of glutamate neurotoxicity.* J Neurosci, 1987. **7**(2): p. 369-79.
130. Parsons, J.T., S.B. Churn, and R.J. DeLorenzo, *Ischemia-induced inhibition of calcium uptake into rat brain microsomes mediated by Mg2+/Ca2+ ATPase.* J Neurochem, 1997. **68**(3): p. 1124-34.
131. Parsons, J.T., S.B. Churn, and R.J. DeLorenzo, *Global ischemia-induced inhibition of the coupling ratio of calcium uptake and ATP hydrolysis by rat whole brain microsomal Mg(2+)/Ca(2+) ATPase.* Brain Res, 1999. **834**(1-2): p. 32-41.
132. Tymianski, M. and C.H. Tator, *Normal and abnormal calcium homeostasis in neurons: a basis for the pathophysiology of traumatic and ischemic central nervous system injury.* Neurosurgery, 1996. **38**(6): p. 1176-95.
133. Rzigalinski, B.A., et al., *Intracellular free calcium dynamics in stretch-injured astrocytes.* J Neurochem, 1998. **70**(6): p. 2377-85.
134. Kochan, L.D., et al., *Status epilepticus results in an N-methyl-D-aspartate receptor-dependent inhibition of Ca2+/calmodulin-dependent kinase II activity in the rat.* Neuroscience, 2000. **95**(3): p. 735-43.
135. del Cerro, S., et al., *Stimulation of NMDA receptors activates calpain in cultured hippocampal slices.* Neurosci Lett, 1994. **167**(1-2): p. 149-52.
136. Montoro, R.J., et al., *N-methyl-D-aspartate stimulates the dephosphorylation of the microtubule-associated protein 2 and potentiates excitatory synaptic pathways in the rat hippocampus.* Neuroscience, 1993. **54**(4): p. 859-71.
137. Pallen, C.J. and J.H. Wang, *A multifunctional calmodulin-stimulated phosphatase.* Arch Biochem Biophys, 1985. **237**(2): p. 281-91.
138. Riedel, G., *If phosphatases go up, memory goes down.* Cell Mol Life Sci, 1999. **55**(4): p. 549-53.
139. Wang, J.H. and A. Stelzer, *Inhibition of phosphatase 2B prevents expression of hippocampal long-term potentiation.* Neuroreport, 1994. **5**(17): p. 2377-80.
140. Springer, J.E., et al., *Calcineurin-mediated BAD dephosphorylation activates the caspase-3 apoptotic cascade in traumatic spinal cord injury.* J Neurosci, 2000. **20**(19): p. 7246-51.
141. Mello, L.E., et al., *Circuit mechanisms of seizures in the pilocarpine model of chronic epilepsy: cell loss and mossy fiber sprouting.* Epilepsia, 1993. **34**(6): p. 985-95.
142. Racine, R.J., *Modification of seizure activity by electrical stimulation. II. Motor seizure.* Electroencephalogr Clin Neurophysiol, 1972. **32**(3): p. 281-94.

143. Pallen, C.J. and J.H. Wang, *Calmodulin-stimulated dephosphorylation of p-nitrophenyl phosphate and free phosphotyrosine by calcineurin.* J Biol Chem, 1983. **258**(14): p. 8550-3.
144. Bradford, M.M., *A rapid and sensitive method for the quantitation of microgram quantities of protein utilizing the principle of protein-dye binding.* Anal Biochem, 1976. **72**: p. 248-54.
145. Churn, S.B., *Multifunctional calcium and calmodulin-dependent kinase II in neuronal function and disease.* Adv Neuroimmunol, 1995. **5**(3): p. 241-59.
146. Churn, S.B., et al., *Global forebrain ischemia induces a posttranslational modification of multifunctional calcium- and calmodulin-dependent kinase II.* J Neurochem, 1992. **59**(4): p. 1221-32.
147. Thompson, R.Q., et al., *Comparison of methods for following alkaline phosphatase catalysis: spectrophotometric versus amperometric detection.* Anal Biochem, 1991. **192**(1): p. 90-5.
148. Swarup, G., S. Cohen, and D.L. Garbers, *Inhibition of membrane phosphotyrosyl-protein phosphatase activity by vanadate.* Biochem Biophys Res Commun, 1982. **107**(3): p. 1104-9.
149. Morioka, M., et al., *Serine/threonine phosphatase activity of calcineurin is inhibited by sodium orthovanadate and dithiothreitol reverses the inhibitory effect.* Biochem Biophys Res Commun, 1998. **253**(2): p. 342-5.
150. Bialojan, C. and A. Takai, *Inhibitory effect of a marine-sponge toxin, okadaic acid, on protein phosphatases. Specificity and kinetics.* Biochem J, 1988. **256**(1): p. 283-90.
151. Miller, R.J., *The control of neuronal Ca2+ homeostasis.* Prog Neurobiol, 1991. **37**(3): p. 255-85.
152. Carafoli, E., *Intracellular calcium homeostasis.* Annu Rev Biochem, 1987. **56**: p. 395-433.
153. White, B.C., et al., *Brain ischemia and reperfusion: molecular mechanisms of neuronal injury.* J Neurol Sci, 2000. **179**(S 1-2): p. 1-33.
154. Buki, A., et al., *The role of calpain-mediated spectrin proteolysis in traumatically induced axonal injury.* J Neuropathol Exp Neurol, 1999. **58**(4): p. 365-75.
155. Hashimoto, Y., B.A. Perrino, and T.R. Soderling, *Identification of an autoinhibitory domain in calcineurin.* J Biol Chem, 1990. **265**(4): p. 1924-7.
156. Sola, C., J.M. Tusell, and J. Serratosa, *Comparative study of the distribution of calmodulin kinase II and calcineurin in the mouse brain.* J Neurosci Res, 1999. **57**(5): p. 651-62.
157. Bronstein, J., D. Farber, and C. Wasterlain, *Decreased calmodulin kinase activity after status epilepticus.* Neurochem Res, 1988. **13**(1): p. 83-6.
158. Churn, S.B., L.D. Kochan, and R.J. DeLorenzo, *Chronic inhibition of Ca(2+)/calmodulin kinase II activity in the pilocarpine model of epilepsy.* Brain Res, 2000. **875**(1-2): p. 66-77.
159. Chen, Q.X., et al., *GABAA receptor function is regulated by phosphorylation in acutely dissociated guinea-pig hippocampal neurones.* J Physiol, 1990. **420**: p. 207-21.

160. Chen, Q.X. and R.K. Wong, *Suppression of GABAA receptor responses by NMDA application in hippocampal neurones acutely isolated from the adult guinea-pig.* J Physiol, 1995. **482 (Pt 2)**: p. 353-62.
161. Kapur, J. and D.A. Coulter, *Experimental status epilepticus alters gamma-aminobutyric acid type A receptor function in CA1 pyramidal neurons.* Ann Neurol, 1995. **38**(6): p. 893-900.
162. Jain, J., et al., *The T-cell transcription factor NFATp is a substrate for calcineurin and interacts with Fos and Jun.* Nature, 1993. **365**(6444): p. 352-5.
163. Shi, J., M. Townsend, and M. Constantine-Paton, *Activity-dependent induction of tonic calcineurin activity mediates a rapid developmental downregulation of NMDA receptor currents.* Neuron, 2000. **28**(1): p. 103-14.
164. Umemiya, M., et al., *A calcium-dependent feedback mechanism participates in shaping single NMDA miniature EPSCs.* J Neurosci, 2001. **21**(1): p. 1-9.
165. Cordeiro, J.M., et al., *Ca(2+) regulation of the carrier-mediated gamma-aminobutyric acid release from isolated synaptic plasma membrane vesicles.* Neurosci Res, 2000. **38**(4): p. 385-95.
166. Shibasaki, F. and F. McKeon, *Calcineurin functions in Ca(2+)-activated cell death in mammalian cells.* J Cell Biol, 1995. **131**(3): p. 735-43.
167. Kurz, J.E., et al., *A significant increase in both basal and maximal calcineurin activity in the rat pilocarpine model of status epilepticus.* J Neurochem, 2001. **78**(2): p. 304-15.
168. Edelman, A.M., et al., *Subcellular distribution of calcium- and calmodulin-dependent myosin light chain phosphorylating activity in rat cerebral cortex.* J Neurosci, 1985. **5**(10): p. 2609-17.
169. Baumgrass, R., et al., *Reversible inhibition of calcineurin by the polyphenolic aldehyde gossypol.* J Biol Chem, 2001. **276**(51): p. 47914-21.
170. Goto, S., et al., *The distribution of calcineurin in rat brain by light and electron microscopic immunohistochemistry and enzyme-immunoassay.* Brain Res, 1986. **397**(1): p. 161-72.
171. Anthony, F.A., et al., *Quantitative subcellular localization of calmodulin-dependent phosphatase in chick forebrain.* J Neurosci, 1988. **8**(4): p. 1245-53.
172. Sik, A., et al., *The absence of a major Ca2+ signaling pathway in GABAergic neurons of the hippocampus.* Proc Natl Acad Sci U S A, 1998. **95**(6): p. 3245-50.
173. Ho, S., et al., *Cloning and characterization of NF-ATc and NF-ATp: the cytoplasmic components of NF-AT.* Adv Exp Med Biol, 1994. **365**: p. 167-73.
174. Plyte, S., et al., *Identification and characterization of a novel nuclear factor of activated T-cells-1 isoform expressed in mouse brain.* J Biol Chem, 2001. **276**(17): p. 14350-8.

175. Williams, M.B. and R.S. Jope, *Distinctive rat brain immediate early gene responses to seizures induced by lithium plus pilocarpine.* Brain Res Mol Brain Res, 1994. **25**(1-2): p. 80-9.
176. Jankowsky, J.L. and P.H. Patterson, *Differential regulation of cytokine expression following pilocarpine-induced seizure.* Exp Neurol, 1999. **159**(2): p. 333-46.
177. Hendriksen, H., et al., *Altered hippocampal gene expression prior to the onset of spontaneous seizures in the rat post-status epilepticus model.* Eur J Neurosci, 2001. **14**(9): p. 1475-84.
178. Halpain, S., J.A. Girault, and P. Greengard, *Activation of NMDA receptors induces dephosphorylation of DARPP-32 in rat striatal slices.* Nature, 1990. **343**(6256): p. 369-72.
179. Sim, A.T., et al., *Modulation of synaptosomal protein phosphorylation/dephosphorylation by calcium is antagonised by inhibition of protein phosphatases with okadaic acid.* Neurosci Lett, 1991. **126**(2): p. 203-6.
180. Mulkey, R.M., et al., *Involvement of a calcineurin/inhibitor-1 phosphatase cascade in hippocampal long-term depression.* Nature, 1994. **369**(6480): p. 486-8.
181. Kayyali, U.S., et al., *Cytoskeletal changes in the brains of mice lacking calcineurin A alpha.* J Neurochem, 1997. **68**(4): p. 1668-78.
182. Sola, C., J.M. Tusell, and J. Serratosa, *Decreased expression of calmodulin kinase II and calcineurin messenger RNAs in the mouse hippocampus after kainic acid-induced seizures.* J Neurochem, 1998. **70**(4): p. 1600-8.
183. Ghajar, J., *Traumatic brain injury.* Lancet, 2000. **356**(9233): p. 923-9.
184. Siesjo, B.K. and P. Siesjo, *Mechanisms of secondary brain injury.* Eur J Anaesthesiol, 1996. **13**(3): p. 247-68.
185. Jayaraman, T. and A.R. Marks, *Calcineurin is downstream of the inositol 1,4,5-trisphosphate receptor in the apoptotic and cell growth pathways.* J Biol Chem, 2000. **275**(9): p. 6417-20.
186. Dawson, T.M., et al., *Immunosuppressant FK506 enhances phosphorylation of nitric oxide synthase and protects against glutamate neurotoxicity.* Proc Natl Acad Sci U S A, 1993. **90**(21): p. 9808-12.
187. Matsuda, T., et al., *Involvement of calcineurin in Ca2+ paradox-like injury of cultured rat astrocytes.* J Neurochem, 1998. **70**(5): p. 2004-11.
188. Pyrzynska, B., et al., *Cyclosporin A-sensitive signaling pathway involving calcineurin regulates survival of reactive astrocytes.* Neurochem Int, 2001. **38**(5): p. 409-15.
189. Dixon, C.E., et al., *A fluid percussion model of experimental brain injury in the rat.* J Neurosurg, 1987. **67**(1): p. 110-9.
190. Lee, M.K., et al., *The expression and posttranslational modification of a neuron-specific beta-tubulin isotype during chick embryogenesis.* Cell Motil Cytoskeleton, 1990. **17**(2): p. 118-32.
191. Easter, S.S., Jr., L.S. Ross, and A. Frankfurter, *Initial tract formation in the mouse brain.* J Neurosci, 1993. **13**(1): p. 285-99.

192. Cortez, S.C., T.K. McIntosh, and L.J. Noble, *Experimental fluid percussion brain injury: vascular disruption and neuronal and glial alterations.* Brain Res, 1989. **482**(2): p. 271-82.
193. Fineman, I., et al., *Concussive brain injury is associated with a prolonged accumulation of calcium: a 45Ca autoradiographic study.* Brain Res, 1993. **624**(1-2): p. 94-102.
194. Weber, J.T., et al., *Alterations in calcium-mediated signal transduction after traumatic injury of cortical neurons.* Cell Calcium, 1999. **26**(6): p. 289-99.
195. Weber, J.T., B.A. Rzigalinski, and E.F. Ellis, *Traumatic injury of cortical neurons causes changes in intracellular calcium stores and capacitative calcium influx.* J Biol Chem, 2001. **276**(3): p. 1800-7.
196. Kampfl, A., et al., *Mechanisms of calpain proteolysis following traumatic brain injury: implications for pathology and therapy: implications for pathology and therapy: a review and update.* J Neurotrauma, 1997. **14**(3): p. 121-34.
197. Hashimoto, Y., R.K. Sharma, and T.R. Soderling, *Regulation of Ca2+/calmodulin-dependent cyclic nucleotide phosphodiesterase by the autophosphorylated form of Ca2+/calmodulin-dependent protein kinase II.* J Biol Chem, 1989. **264**(18): p. 10884-7.
198. Shima, K. and A. Marmarou, *Evaluation of brain-stem dysfunction following severe fluid-percussion head injury to the cat.* J Neurosurg, 1991. **74**(2): p. 270-7.
199. Mautes, A.E., K. Fukuda, and L.J. Noble, *Cellular response in the cerebellum after midline traumatic brain injury in the rat.* Neurosci Lett, 1996. **214**(2-3): p. 95-8.
200. Smith, D.H., et al., *Evaluation of memory dysfunction following experimental brain injury using the Morris water maze.* J Neurotrauma, 1991. **8**(4): p. 259-69.
201. Bramlett, H.M., E.J. Green, and W.D. Dietrich, *Hippocampally dependent and independent chronic spatial navigational deficits following parasagittal fluid percussion brain injury in the rat.* Brain Res, 1997. **762**(1-2): p. 195-202.
202. Wiley, J.L., et al., *Reduced sensorimotor reactivity following traumatic brain injury in rats.* Brain Res, 1996. **716**(1-2): p. 47-52.
203. Riess, P., et al., *Effects of chronic, post-injury Cyclosporin A administration on motor and sensorimotor function following severe, experimental traumatic brain injury.* Restor Neurol Neurosci, 2001. **18**(1): p. 1-8.
204. Alessandri, B., et al., *Cyclosporin A improves brain tissue oxygen consumption and learning/memory performance after lateral fluid percussion injury in rats.* J Neurotrauma, 2002. **19**(7): p. 829-41.
205. Szabo, I. and M. Zoratti, *The giant channel of the inner mitochondrial membrane is inhibited by cyclosporin A.* J Biol Chem, 1991. **266**(6): p. 3376-9.

206. O'Dell, D.M., et al., *Positive and negative modulation of the GABA(A) receptor and outcome after traumatic brain injury in rats.* Brain Res, 2000. **861**(2): p. 325-32.
207. Asai, A., et al., *High level calcineurin activity predisposes neuronal cells to apoptosis.* J Biol Chem, 1999. **274**(48): p. 34450-8.
208. Rink, A., et al., *Evidence of apoptotic cell death after experimental traumatic brain injury in the rat.* Am J Pathol, 1995. **147**(6): p. 1575-83.
209. Zipfel, G.J., et al., *Neuronal apoptosis after CNS injury: the roles of glutamate and calcium.* J Neurotrauma, 2000. **17**(10): p. 857-69.
210. Raghupathi, R., et al., *Mild traumatic brain injury induces apoptotic cell death in the cortex that is preceded by decreases in cellular Bcl-2 immunoreactivity.* Neuroscience, 2002. **110**(4): p. 605-16.
211. Buki, A., D.O. Okonkwo, and J.T. Povlishock, *Postinjury cyclosporin A administration limits axonal damage and disconnection in traumatic brain injury.* J Neurotrauma, 1999. **16**(6): p. 511-21.
212. McIntosh, T.K., et al., *Traumatic brain injury in the rat: alterations in brain lactate and pH as characterized by 1H and 31P nuclear magnetic resonance.* J Neurochem, 1987. **49**(5): p. 1530-40.
213. Delahunty, T.M., et al., *Differential consequences of lateral and central fluid percussion brain injury on receptor coupling in rat hippocampus.* J Neurotrauma, 1995. **12**(6): p. 1045-57.
214. Price, M., et al., *Seven cDNAs enriched following hippocampal lesion: possible roles in neuronal responses to injury.* Brain Res Mol Brain Res, 2003. **117**(1): p. 58-67.
215. Okonkwo, D.O., et al., *Dose-response of cyclosporin A in attenuating traumatic axonal injury in rat.* Neuroreport, 2003. **14**(3): p. 463-6.
216. Suehiro, E., et al., *The immunophilin ligand FK506 attenuates the axonal damage associated with rapid rewarming following posttraumatic hypothermia.* Exp Neurol, 2001. **172**(1): p. 199-210.
217. Kurz, J.E., et al., *Status epilepticus-induced changes in the subcellular distribution and activity of calcineurin in rat forebrain.* Neurobiol Dis, 2003. **14**(3): p. 483-93.
218. Kurz, J.E., et al., *A significant increase in both basal and maximal calcineurin activity following fluid percussion injury in the rat.* J Neurotrauma, 2005. **22**(4): p. 476-90.
219. Husi, H., et al., *Proteomic analysis of NMDA receptor-adhesion protein signaling complexes.* Nat Neurosci, 2000. **3**(7): p. 661-9.
220. Hamm, R.J., et al., *Cognitive deficits following traumatic brain injury produced by controlled cortical impact.* J Neurotrauma, 1992. **9**(1): p. 11-20.
221. Hamm, R.J., et al., *Selective cognitive impairment following traumatic brain injury in rats.* Behav Brain Res, 1993. **59**(1-2): p. 169-73.
222. Hamm, R.J., et al., *Working memory deficits following traumatic brain injury in the rat.* J Neurotrauma, 1996. **13**(6): p. 317-23.

223. Sun, D.A., et al., *Long-lasting alterations in neuronal calcium homeostasis in an in vitro model of stroke-induced epilepsy.* Cell Calcium, 2004. **35**(2): p. 155-63.
224. Mansuy, I.M., et al., *Restricted and regulated overexpression reveals calcineurin as a key component in the transition from short-term to long-term memory.* Cell, 1998. **92**(1): p. 39-49.
225. Hodgkiss, J.P. and J.S. Kelly, *Only 'de novo' long-term depression (LTD) in the rat hippocampus in vitro is blocked by the same low concentration of FK506 that blocks LTD in the visual cortex.* Brain Res, 1995. **705**(1-2): p. 241-46.
226. Jovanovic, J.N., et al., *Opposing changes in phosphorylation of specific sites in synapsin I during Ca2+-dependent glutamate release in isolated nerve terminals.* J Neurosci, 2001. **21**(20): p. 7944-53.
227. Scorza, F.A., et al., *Glucose utilization during interictal intervals in an epilepsy model induced by pilocarpine: a qualitative study.* Epilepsia, 1998. **39**(10): p. 1041-5.
228. Lai, M.M., et al., *The calcineurin-dynamin 1 complex as a calcium sensor for synaptic vesicle endocytosis.* J Biol Chem, 1999. **274**(37): p. 25963-6.
229. Higashima, M., et al., *Activation of GABAergic function necessary for afterdischarge generation in rat hippocampal slices.* Neurosci Lett, 1996. **207**(2): p. 101-4.
230. Akasu, T., N. Muraoka, and H. Hasuo, *Hyperexcitability of hippocampal CA1 neurons after fluid percussion injury of the rat cerebral cortex.* Neurosci Lett, 2002. **329**(3): p. 305-8.
231. D'Ambrosio, R., et al., *Post-traumatic epilepsy following fluid percussion injury in the rat.* Brain, 2004. **127**(Pt 2): p. 304-14.
232. Santhakumar, V., et al., *Long-term hyperexcitability in the hippocampus after experimental head trauma.* Ann Neurol, 2001. **50**(6): p. 708-17.
233. Lowenstein, D.H. and B.K. Alldredge, *Status epilepticus.* N Engl J Med, 1998. **338**(14): p. 970-6.
234. Wong, M., *Modulation of dendritic spines in epilepsy: cellular mechanisms and functional implications.* Epilepsy Behav, 2005. **7**(4): p. 569-77.
235. Gray, E.G., *Electron microscopy of synaptic contacts on dendrite spines of the cerebral cortex.* Nature, 1959. **183**(4675): p. 1592-3.
236. Hayashi, Y. and A.K. Majewska, *Dendritic spine geometry: functional implication and regulation.* Neuron, 2005. **46**(4): p. 529-32.
237. Leuner, B. and T.J. Shors, *New spines, new memories.* Mol Neurobiol, 2004. **29**(2): p. 117-30.
238. Leuner, B., J. Falduto, and T.J. Shors, *Associative memory formation increases the observation of dendritic spines in the hippocampus.* J Neurosci, 2003. **23**(2): p. 659-65.
239. O'Malley, A., et al., *Transient spine density increases in the mid-molecular layer of hippocampal dentate gyrus accompany consolidation of a spatial learning task in the rodent.* Neuroscience, 2000. **99**(2): p. 229-32.
240. Isokawa, M., *Remodeling dendritic spines in the rat pilocarpine model of temporal lobe epilepsy.* Neurosci Lett, 1998. **258**(2): p. 73-6.

241. Ferhat, L., et al., *Increased levels of acidic calponin during dendritic spine plasticity after pilocarpine-induced seizures.* Hippocampus, 2003. **13**(7): p. 845-58.
242. Isokawa, M., *Remodeling dendritic spines of dentate granule cells in temporal lobe epilepsy patients and the rat pilocarpine model.* Epilepsia, 2000. **41 Suppl 6**: p. S14-7.
243. Sierra-Paredes, G., et al., *Seizures induced by in vivo latrunculin a and jasplakinolide microperfusion in the rat hippocampus.* J Mol Neurosci, 2006. **28**(2): p. 151-60.
244. Singleton, M.W., et al., *Modulation of CaM kinase II activity is coincident with induction of status epilepticus in the rat pilocarpine model.* Epilepsia, 2005. **46**(9): p. 1389-400.
245. Kurz, J.E., et al., *A persistent change in subcellular distribution of calcineurin following fluid percussion injury in the rat.* Brain Res, 2005. **1048**(1-2): p. 153-60.
246. Gabbott, P.L. and J. Somogyi, *The 'single' section Golgi-impregnation procedure: methodological description.* J Neurosci Methods, 1984. **11**(4): p. 221-30.
247. Kurz, J.E., M.W. Singleton, and S.B. Churn, *Temporally disparate effects on CaN activity and subcellular distribution in the rat pilocarpine model (Abstract 2.063).* Epilepsia, 2005. **46 S8**(Suppl. 8): p. 112
248. Moriwaki, A., et al., *Immunosuppressant FK506 prevents mossy fiber sprouting induced by kindling stimulation.* Neurosci Res, 1996. **25**(2): p. 191-4.
249. McNamara, J.O., Y.Z. Huang, and A.S. Leonard, *Molecular signaling mechanisms underlying epileptogenesis.* Sci STKE, 2006. **2006**(356): p. re12.
250. Bamburg, J.R., *Proteins of the ADF/cofilin family: essential regulators of actin dynamics.* Annu Rev Cell Dev Biol, 1999. **15**: p. 185-230.
251. Agnew, B.J., L.S. Minamide, and J.R. Bamburg, *Reactivation of phosphorylated actin depolymerizing factor and identification of the regulatory site.* J Biol Chem, 1995. **270**(29): p. 17582-7.
252. Meng, Y., et al., *Regulation of ADF/cofilin phosphorylation and synaptic function by LIM-kinase.* Neuropharmacology, 2004. **47**(5): p. 746-54.
253. Meberg, P.J., et al., *Actin depolymerizing factor and cofilin phosphorylation dynamics: response to signals that regulate neurite extension.* Cell Motil Cytoskeleton, 1998. **39**(2): p. 172-90.
254. Lee, M.G., et al., *MK-801 augments pilocarpine-induced electrographic seizure but protects against brain damage in rats.* Prog Neuropsychopharmacol Biol Psychiatry, 1997. **21**(2): p. 331-44.
255. McIntosh, T.K., et al., *Effects of the N-methyl-D-aspartate receptor blocker MK-801 on neurologic function after experimental brain injury.* J Neurotrauma, 1989. **6**(4): p. 247-59.
256. Mangan, P.S. and E.H. Bertram, 3rd, *Shortened-duration GABA(A) receptor-mediated synaptic potentials underlie enhanced CA1 excitability*

in a chronic model of temporal lobe epilepsy. Neuroscience, 1997. **80**(4): p. 1101-11.
257. Kapur, J., *Hippocampal neurons express GABA A receptor insensitive to diazepam in hyperexcitable conditions.* Epilepsia, 2000. **41 Suppl 6**: p. S86-9.
258. Sihver, S., et al., *Changes in mACh, NMDA and GABA(A) receptor binding after lateral fluid-percussion injury: in vitro autoradiography of rat brain frozen sections.* J Neurochem, 2001. **78**(3): p. 417-23.
259. Kapur, J. and E.W. Lothman, *NMDA receptor activation mediates the loss of GABAergic inhibition induced by recurrent seizures.* Epilepsy Res, 1990. **5**(2): p. 103-11.
260. Ikegami, S. and K. Inokuchi, *Antisense DNA against calcineurin facilitates memory in contextual fear conditioning by lowering the threshold for hippocampal long-term potentiation induction.* Neuroscience, 2000. **98**(4): p. 637-46.
261. Lin, C.H., et al., *Identification of calcineurin as a key signal in the extinction of fear memory.* J Neurosci, 2003. **23**(5): p. 1574-9.
262. Lin, C.H., C.C. Lee, and P.W. Gean, *Involvement of a calcineurin cascade in amygdala depotentiation and quenching of fear memory.* Mol Pharmacol, 2003. **63**(1): p. 44-52.
263. Winder, D.G., et al., *Genetic and pharmacological evidence for a novel, intermediate phase of long-term potentiation suppressed by calcineurin.* Cell, 1998. **92**(1): p. 25-37.
264. Mansuy, I.M., et al., *Inducible and reversible gene expression with the rtTA system for the study of memory.* Neuron, 1998. **21**(2): p. 257-65.
265. Turski, L., et al., *Review: cholinergic mechanisms and epileptogenesis. The seizures induced by pilocarpine: a novel experimental model of intractable epilepsy.* Synapse, 1989. **3**(2): p. 154-71.

VITA

Jonathan Elledge Kurz was born on July 13, 1979, in Washington, D.C., and is an American citizen. He graduated from the Chesterfield County Mathematics and Science High School at Clover Hill in 1997, and received his Bachelor of Science in Biology (Magna Cum Laude) from Virginia Commonwealth University in 2001.

Awards:
VCU Undergraduate Research Grants, 2000 and 2001
Epilepsy Foundation of America Predoctoral Fellowship 2005-2006

Publications:
Kurz, J.E., Sheets, D., Parsons, J.T., Rana, A., DeLorenzo, R.J., Churn, S.B. A significant increase in both basal and maximal calcineurin activity in the rat pilocarpine model of status epilepticus. (2001) J. Neurochem. 78: 304-315

Kurz, J.E., Rana, A., Parsons, J.T., Churn, S.B. Status epilepticus-induced changes in the subcellular distribution and activity of calcineurin in rat forebrain. (2003) Neurobiol. Dis. 14:483-493

Singleton, M.W., Holbert, W.M., Ryan, M.L., Lee, A.T., Kurz, J.E., Churn, S.B. Age dependence of pilocarpine-induced status epilepticus and inhibition of CaM Kinase II activity in the rat. (2005) Brain Res. Dev. Brain Res. 156:67-77

Kurz, J.E., Parsons, J.T., Rana, A., Gibson, C.J., Hamm, R.J., Churn, S.B. A significant increase in both basal and maximal calcineurin activity following fluid percussion injury in the rat. (2005) J. Neurotrauma 22:476-490

Kurz, J.E., Hamm, R.J., Singleton, R.H., Povlishock, J.T., Churn, S.B. A persistent change in subcellular distribution of calcineurin following fluid percussion injury in the rat. (2005) Brain Res. 1048:153-160